UNIVERSITÀ DEGLI STUDI DI UDINE
hic sunt futura
www.uniud.it

Ph.D Course in

Food and Human Health

XXXV Cycle

Thesis Title

Hyperbaric Storage as an innovative technology to extend stability and improve functionality of food

Ph.D. Student
Federico Basso

Supervisors
Prof. Lara Manzocco
Prof. Maria Cristina Nicoli

Year (2023)

TABLE OF CONTENTS

SUMMARY

This Ph.D Thesis consisted of a multi-aspect investigation on hyperbaric storage, focusing the attention on: (i) the identification of packaging solutions feasible for pressurized storage applications; (ii) the capability of hyperbaric storage to obtain microbiological, enzymatic and chemical stabilization of food; (iii) the modification of the structure of proteins to improve the technological functionality of food.

Firstly, a preliminary investigation was carried out to explore the effects of hyperbaric storage on food packaging materials. The objective was to identify plastic films that were adequate for packaging of food intended for hyperbaric storage. To this aim, single and multilayer packaging materials, derived from petroleum or renewable sources, were tested. Among these materials, petroleum-based multi-layer solutions (poly-amide/poly-ethylene, poly-propylene/ethylene-vinyl-alcohol/poly-ethylene) were identified as appropriate for pressurized storage purposes, and were thus used in the subsequent experimental work.

Following, the capability of hyperbaric storage to guarantee microbiological, enzymatic and chemical stability of food was assessed. The attention was focused on the possibility to obtain: (i) pasteurization of raw skim milk; (ii) polyphenoloxidase inactivation in model systems and apple juice; (iii) inhibition of non-enzymatic browning in sugar-aminoacid solutions. Hyperbaric storage was shown to irreversibly inactivate 5 log units of inoculated *E. coli* and *S. aureus* in milk and to control the native milk microflora, demonstrating its suitability for pasteurization. Application of hyperbaric storage also allowed to irreversibly inactivate polyphenoloxidase in aqueous model systems and to inhibit enzymatic browning in apple juice. The rate of Maillard reaction in glucose-glycine model systems was significantly inhibited by pressure with kinetic parameters affected by solution pH and storage temperature. In this framework, a model based on the combination of Arrhenius and Eyring equations was developed to accurately predict reaction rate in different pressure and temperature conditions.

In the last part of the Thesis, the capability of hyperbaric storage to modify protein structure was further investigated with the aim of improving techno-functional properties in protein-rich food. Milk, egg white and egg yolk were considered based on the different native structure of their proteins. The effects of hyperbaric storage were found to depend on protein structure: (i) globular proteins either unfolded or underwent changes in particle size and electrostatic behavior, leading to an increase in foaming properties; (ii) casein micelles progressively destabilized, resulting in coagulation; (iii) pressure-modified micelles were more prone to enzymatic hydrolysis mediated by endogenous proteases, resulting in the production of highly foaming peptides; (iv) differently

organized proteins, concomitantly occurring in the food systems, easily interacted further modifying their structure; (v) proteins in protein-lipid complexes underwent sever unfolding, leading to the complete gelation.

The results achieved in this Thesis demonstrate the multi-tasking character of hyperbaric storage, which is concomitantly capable to stabilize and improve techno-functionality of food. The technology has thus the potential to evolve from storage technology solely, to non-conventional treatment to improve food quality in a number of different ways. However, several development gaps need to be filled in order to make hyperbaric storage viable for the industrial context, with particular reference to the development of economically sustainable working units. Overcoming these gaps would allow to fully exploit the wide potential of hyperbaric storage.

RIASSUNTO

L'obiettivo di questa Tesi di Dottorato è stato quello di condurre un'indagine multi-aspetto sulla conservazione iperbarica, focalizzando l'attenzione su: (i) identificazione di materiali di packaging adatti all'applicazione della tecnologia; (ii) capacità della conservazione iperbarica di garantire la stabilità microbiologica, enzimatica e chimica degli alimenti; (iii) modificazione strutturale delle proteine per migliorare la funzionalità tecnologica degli alimenti.

Innanzitutto, è stata effettuata un'indagine preliminare, con l'obiettivo di esplorare gli effetti della conservazione iperbarica su materiali tipicamente impiegati per il confezionamento degli alimenti. Sono stati testati materiali mono- e multi-strato, derivati sia dal petrolio che da fonti rinnovabili. Tra questi, i film multistrato costituiti da materiali plastici derivati dal petrolio (PA/PE, PP/EVOH/PE) sono stati identificati come appropriati per la conservazione iperbarica, e sono stati quindi utilizzati per le successive sperimentazioni.

In seguito, è stata valutata la capacità della conservazione iperbarica di garantire la stabilità microbiologica, enzimatica e chimica degli alimenti. L'attenzione è stata focalizzata sulla possibilità di ottenere: (i) la pastorizzazione di latte scremato crudo; (ii) l'inattivazione della polifenolossidasi in sistemi modello e succo di mela; (iii) l'inibizione dell'imbrunimento non-enzimatico in soluzioni modello di zuccheri e amminoacidi. L'applicazione della conservazione iperbarica al latte ha consentito di inattivare irreversibilmente 5 unità logaritmiche di *Escherichia coli* e *Staphylococcus aureus*, controllando allo stesso tempo la microflora nativa della matrice. Tali risultati hanno dimostrato la possibilità di pastorizzare il latte utilizzando questa tecnologia. Quest'ultima si è dimostrata in grado di inattivare non solo microorganismi patogeni nel latte, ma anche enzimi responsabili del decadimento qualitativo in derivati vegetali freschi (*e.g.*, succhi di frutta). In particolare, la conservazione iperbarica ha permesso di inattivare in modo irreversibile la polifenolossidasi nel succo di mela, consentendo di limitarne l'imbrunimento enzimatico. L'applicazione della tecnologia ha anche consentito di ridurre in modo significativo la velocità della reazione di Maillard in soluzioni modello di glucosio e glicina, con parametri cinetici influenzati sia dal pH del sistema che dalla temperatura. In questo contesto, è stato sviluppato un modello cinetico basato su una combinazione delle equazioni di Arrhenius ed Eyring, il quale è risultato capace di predire accuratamente la velocità di reazione in un ampio range di condizioni di temperatura e pressione.

Nella parte finale della Tesi, l'attenzione è stata focalizzata sulla capacità della conservazione iperbarica di modificare la struttura delle proteine e migliorare le proprietà tecno-funzionali di alimenti ad alto contenuto proteico. A questo scopo, il latte, l'albume d'uovo e il tuorlo d'uovo

sono stati selezionati come casi studio. Gli effetti della conservazione iperbarica si sono rivelati dipendenti dalla struttura nativa delle proteine delle matrici considerate. In particolare: (i) le proteine globulari sono andate incontro ad *unfolding* o compressione, portando in entrambi i casi ad un miglioramento delle proprietà schiumogene; (ii) le micelle caseiniche presenti nel latte sono state progressivamente destabilizzate dalla pressione, portando alla coagulazione del sistema; (iii) le micelle destabilizzate sono risultate più prone all'idrolisi enzimatica da parte di proteasi endogene, risultando nella produzione di peptidi ad alta attività schiumogena; (iv) nel caso di co-presenza di proteine con diversa organizzazione strutturale, sono state osservate delle interazioni in grado di causare ulteriori modifiche strutturali; (v) le proteine facenti parte di complessi lipidici sono andate incontro ad evidente *unfolding*, portando alla completa gelificazione del sistema.

I risultati ottenuti in questa Tesi dimostrano il carattere *multi-tasking* della conservazione iperbarica, la quale è contemporaneamente in grado di stabilizzare e migliorare la funzionalità tecnologica degli alimenti. Questa tecnologia ha il potenziale per evolversi da semplice approccio per la conservazione degli alimenti, ad un trattamento non-convenzionale per migliorarne la qualità sotto diversi aspetti. Va tuttavia sottolineata la necessità di colmare diverse lacune tecniche per rendere la conservazione iperbarica applicabile nel contesto industriale, con particolare riferimento allo sviluppo di unità operative economicamente sostenibili. Colmare tali lacune consentirebbe di sfruttare pienamente l'ampio potenziale della tecnologia.

Chapter I: State of the art and Thesis outline

In this first Chapter of the Thesis, the state of the art about hyperbaric storage is described. An historical and technical overview of the technology is presented, as well as an explanation of its working principles. Literature evidence reporting the effect of pressurized storage on microbiological, chemical, physical and sensory properties of foods is reviewed. This analysis is used as a foundation to pinpoint challenges of hyperbaric storage worthy of investigation, focusing on unaddressed technical issues and unexplored applications. The final output of this Chapter is represented by the Thesis outline, summarizing the organization of the experimental work.

I.I Hyperbaric storage

I.I.I Introduction

Hyperbaric storage (HS) is a developing food preservation technology, based on the application of pressure up to 250 MPa. The technology is mentioned as hyperbaric storage at room temperature (HS-RT) if pressure is applied at room temperature with no specific control, or hyperbaric storage at low temperature (HS-LT) when pressure is combined with low temperature to assist food refrigeration or freezing.

The first study investigating the possibility of storing foodstuff under pressure was performed in Japan in 1972 (Mitsuda et al., 1972). In this pioneering work, the Authors used high pressure naturally occurring underground and underwater to preserve biological activity and nutritional status of grain and pulse seeds. When recovered after three years of storage, the seeds presented unaltered germinative and enzymatic activity, with minor changes in nutrient content. Five years later, Charm et al. (1977) were able to control microbial growth and sensory changes in raw chicken and beef for up to 60 days by storing them in a steel tank pressurized at ~ 20 MPa. This study paved the way for subsequent research on the topic, defining the basic design of pressurized storage working units.

HS working units consist in pressure-holding steel tanks where hydrostatic pressure is applied by means of a pressurizing fluid (Fernandes et al., 2019). An example of a typical configuration of pilot-scale HS equipment is shown in Figure I, with particular reference to the plant available at the Department of Agricultural, Food, Environmental and Animal Sciences of the University of Udine.

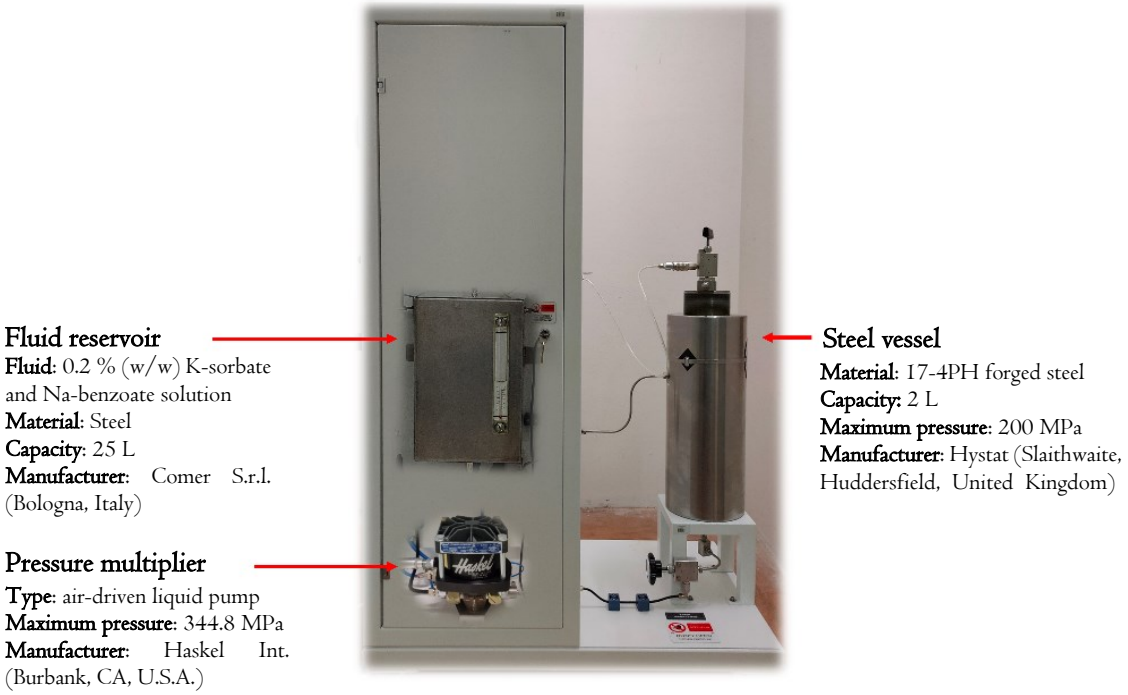

Figure 1: Hyperbaric storage working unit available at the Department of Agricultural, Food, Environmental and Animal Sciences of the University of Udine. Technical details are also indicated.

In most cases, the food (solid or liquid) is packaged inside flexible plastic pouches and immersed in a liquid medium (*i.e.* water or propylene glycol aqueous solution) (Figure 2 A).

When the goal is to control ripening and delay senescence in bulk fruit and vegetable, a lower storage pressure (up to 0.9 MPa) is generally applied by means of a gas (*i.e.* air) (Figure 2 B) (Goyette et al., 2007, 2012). More recently, an evolution of HS working unit design was proposed with reference to bulk liquid foods (Bermejo-Prada et al., 2017; Otero, 2019) (Figure 2 C). The latter was suggested to be directly stored into the vessel. In this case, the pressurizing fluid is the liquid food itself.

From a technical point of view, HS is very similar to high hydrostatic pressure processing (HHP), since both technologies involve pressurization of food inside steel vessels. However, the technologies differ in their scope. In particular, while HS aims at storing food, HHP is generally employed as a non-thermal approach for pasteurization or to enhance food technological functionality (San Martín et al., 2002).

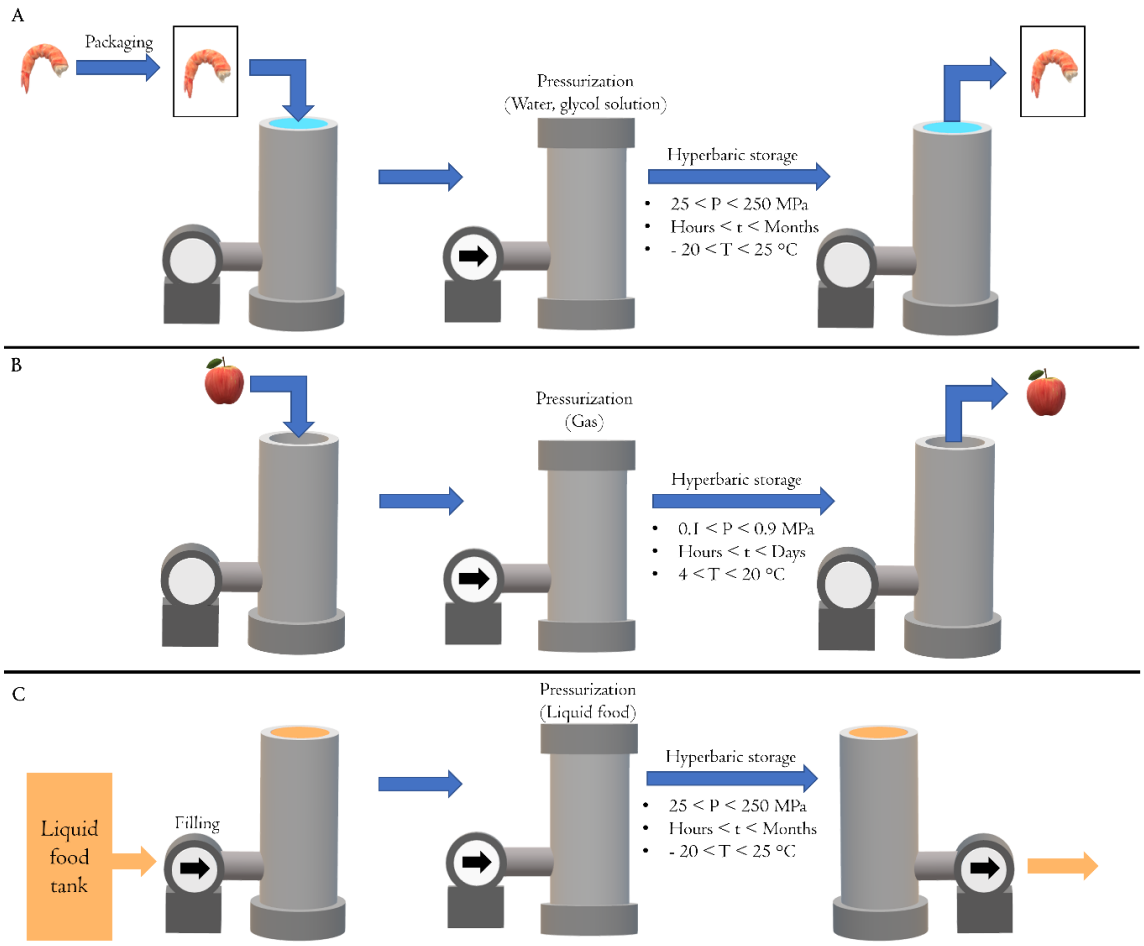

Figure 2: Schematization of hyperbaric storage application to packed foods (A), bulk fruit and vegetables (B), and bulk liquid foods (C). P: pressure, t: storage time, T: temperature.

1.1.2 Principle of the effect of pressure on food systems

Similar to HHP, HS is considered a non-thermal food technology approach. However, from a physical point of view, the increase in pressure (P) on any system is expected to cause a temperature (T) increase due to adiabatic heating, according to Eq. 1.

Eq. 1 $$\frac{dT}{dP} = \frac{\alpha T}{\rho C_p}$$

Where: α is compressibility, ρ is density and C_p is specific heat at constant pressure. When water is used as pressurizing fluid, $\alpha = 5.1 \cdot 10^{-10}$ Pa^{-1} (at 0 °C) (Fine & Millero, 1973), $\rho = 1000$ kg m^{-3} (Katyal & Morrison, 2007), and $C_p = 4.2$ kJ kg^{-1} °C^{-1} (Patazca et al. 2007). This means that, upon a pressure increase of several hundred MPa, water temperature only increases by few degrees. A similar consideration can be drawn for food matrices, which present α, ρ and C_p values in the same magnitude order of water ones (Cheftel & Culioli, 1997). Hydrostatic pressure treatments,

including HS, are based on Pascal and Le Chatelier principles, and on the Transition State Theory (Martinez-Monteagudo & Saldaña, 2014). The first states that, in a confined fluid, any pressure increase is instantaneously and isostatically transmitted to any point of the fluid. Pressure is thus uniformly applied and its effects on food are independent from product size and geometry (Wang et al., 2016). On the other hand, the latter two state that any chemical or physical phenomenon implying a negative activation volume ($\Delta V^{\neq}$; mL mol^{-1}) is boosted by a pressure increase and *vice-versa* (Evans & Polanyi, 1935; Laidler & King, 1983; Le Chatelier, 1891). The greater the absolute value of $\Delta V^{\neq}$, the higher the sensitivity of a phenomenon to pressure. Any increase of pressure will, consequently, limit the kinetic rate of biological, physical and chemical phenomena associated to a volume increase. In particular, the rate of these phenomena is known to exponentially depend on the applied pressure following the Eyring Equation (Eq. 2) (Evans & Polanyi, 1935; Eyring, 1935).

Eq. 2 $$ln(k_p) = ln\left(k_{P_{ref}}\right) - \frac{(\Delta V^{\neq})}{RT}\,P$$

Where k_p is the rate of a phenomenon at the pressure P (MPa), $k_{P_{ref}}$ is the rate of the same phenomenon at ambient pressure (0.1 MPa), R (J K^{-1} mol^{-1}) is the ideal gas constant and T (K) is the absolute temperature.

1.1.3 Effect of moderate hydrostatic pressure on the rate of chemical, physical and biological phenomena occurring in food

Most of the phenomena occurring in food are associated to significant values of activation volume, being thus affected by the application of pressure. Even though the value of $\Delta V^{\neq}$ might be rather small for some phenomena, the effect of pressure could become not negligible in a HS context. In fact, a minor increase in reaction rate upon pressure application could result into significant quality changes over prolonged storage time. Table 1 shows $\Delta V^{\neq}$ values of the main phenomena affecting food properties and cell functionality in the typical pressure range of HS (< 250 MPa). According to the literature, even moderate pressure is able to decrease the stability of electrostatic and hydrophobic interactions as well as ionic bonding, whilst covalent and hydrogen bonds, as well as molecule solvation, are generally favored (Rivalain et al., 2010). The consequences of such effects are multiple. For instance, the stabilization of hydrogen bonding hinders water freezing, resulting in the possibility of storing food at sub-zero temperatures (HS-LT) without ice formation. Oppositely, pressure strongly promotes the lipid solid state, which is considerably less voluminous than the liquid one (Hiramatsu et al., 1989).

Table 1: Activation volume ($\Delta V^{\neq}$) in the HS pressure (P < 250 MPa) and temperature range of the main phenomena affecting food properties and cell functionality.

Phenomenon	System	Environment	$\Delta V^{\neq}$ (mL mol^{-1})	Temperature (°C)	Pressure (MPa)	References
Bond cleavage	Electrostatic interactions		-21.0	n.r.	0/250	Marquis, 1976
	Hydrophobic interactions		-20.0/-10.0	n.r.	100/200	Rivalain et al., 2010
	Hydrogen bonding		-1.0/+3.0			
	Ionic bonds		-10.0			
Freezing	Water	Pure water	+0.1	-20	193	Kalichevsky et al., 1995
Melting	Oleic acid (β)	Pure oleic acid	+41.1	16.2	0.1/200	Hiramatsu et al., 1989
Crystallization	Phospholipids	Liposomes	+25.7	32	0.1/250	Macdonald, 1978
Weak acid dissociation	$H_2PO_4^-$	Aqueous solution	-25.3/-23.8	25	98.1	Neuman et al., 1973
Weak basis dissociation	NH_3	Aqueous solution	-28.8	25	200	Read, 1982
Gelation	Agarose	Aqueous dispersion	-3.1	25	150	Gekko & Fukamizu, 1991
	ι-carrageenan	Aqueous dispersion	+1.7/+3.4	25	0.1/250	Gekko & Kasuya, 1985
Gelation	β-Lactoglobulin	Vaccine milk	-24.8/-7.7	20	> 100	Mazri et al., 2012
Disruption	Actin	Rabbit muscle	-72.0/-67.0	20	250	Ikeuchi et al., 2002
Enzyme activity	Pectinmethylesterase	Carrot	-6.3	30	100/200	Sila et al., 2007
	α-amylase	Saliva	-28.0/-22.0	22	20/200	Laidler, 1951
	Trypsin	Bovine pancreas	-8.8	20	< 40	Gross, Auerbach, et al., 1993
	Polygalacturonase	Tomato	+12.6	25	100/250	Verlent et al., 2005
Oxidation	Hydroperoxide formation	Fresh salmon	-10.8	30	100/250	Aubourg et al., 2010
	Malonaldehyde formation	Raw beef meat	-12.4	20	0.1/250	Ma et al., 2007
Maillard reaction	Melanoidins formation	Amino acids-sugars solutions	+21.7/+27.0	95	200	Tamaoka et al., 1991
Cell functionality	Membrane fluidity	Liposomes	+25.7	32	0.1/250	Macdonald, 1978
	Motility inhibition	*Escherichia coli*	-66.9	24	>10	Meganathan & Marquis, 1973
	Amino-acids uptake	*Saccharomyces cerevisiae*	+50.8/+89.3	24	15/25	Abe & Iida, 2003
	DNA replication	*Escherichia coli*	+55.0	37	50	Yayanos & Pollard, 1969
	DNA transcription	*Escherichia coli*	+55.0/+65.0	35	50/100	Erijman & Clegg, 1998
	DNA translation	Bacterial ribosomes	+100.0	n.r.	60	Gross, Lehle, et al., 1993
Migration	Packaging polymers	Polypropylene	+0.24*	44	0.1-300	Schmerder et al., 2005

n.r.: Not reported, * Data graphically extrapolated

Fat polymorphism is affected by pressure as well, which favors more compact crystalline forms (Oh & Swanson, 2006). In biological structures, pressure-induced lipids crystallization was observed in phospholipids-based liposomes due to a tight packing of the system, which favored interchain Van der Waals interactions (Ichimori et al., 1998). Crystallization is favored by pressure even in semicrystalline polymeric materials typically used for food packaging (Hoque et al., 2022; Juliano et al., 2010). Pressure-induced crystallization of these matrices is attributable to both volume reduction and re-orientation of polymers chains in a more ordered configuration (Fleckenstein et al., 2014). The volume reduction induced by pressure also causes the permeability of packaging materials to decrease. In fact, the intermolecular spaces between polymer chains become smaller under hyperbaric conditions, hampering the diffusion of small molecules (*e.g.*, ketones) through the material (Schmerder et al., 2005).

Pressure-induced ion solvation is of particular interest in biological systems. Weak acids and bases dissociation have largely negative $\Delta V^{\neq}$ values, being thus strongly promoted in aqueous solutions even at pressure as low as 100 MPa (Neuman et al., 1973; Read, 1982).

Although pressure effects on the aforementioned chemical interactions are at the basis of pressure-induced changes in food, the overall outcome of the latter is not easily predictable. For instance, gelation of polysaccharides might be favored or hampered based on the nature of intra- and inter-molecular interactions that stabilize their structure (Gekko & Fukamizu, 1991; Gekko & Kasuya, 1985). By contrast, protein denaturation is always favored by pressure since occurring through a multi-step process involving not only solvation of polar groups, but also an overall decrease in protein molecular volume (Roche & Royer, 2018). The latter results in unfolding for globular proteins (Mazri et al., 2012) but in disruption for micellar and fibrillar structures (Bravo et al., 2015; Chapleau et al., 2004; MacFarlane & McKenzie, 1976).

Enzymatic proteins are known to be inactivated by high pressure, due to the loss of their quaternary and tertiary structures, but this generally requires pressure levels much higher ($P > 400$ - 600 MPa) than those typically applied in HS (Serment-Moreno et al., 2014). Under moderate pressure, structure changes might even potentiate enzymatic activity by (i) favoring the efficacious interaction between enzyme and substrate, (ii) modifying substrate structure and (iii) altering the organization of the environment (Eisenmenger & Reyes-De-Corcuera, 2009). Things are made even more complicated by the temperature dependence of the effect of pressure on enzymatic activity. Being the enzyme state diagram (pressure-temperature) elliptically shaped, an increase in pressure can result either in boosted or reduced enzymatic activity, depending on the temperature level (Serment-Moreno et al., 2014).

Lipid oxidation is likely to represent one of the main downsides of HS. Circumstantial evidence is the largely negative $\Delta V^{\neq}$ value of the formation of both hydroperoxides and secondary oxidative products, due to O_2 consumption and molecular rearrangements, respectively (Medina-Meza et al., 2014) (Table 1). These negative $\Delta V^{\neq}$ values are only partly counterbalanced by the positive ones associated to the formation of volatile end-products. It is noteworthy that lipid oxidation can be also triggered by the release of powerful pro-oxidants (*e.g.*, Fe^{2+}) upon protein denaturation and thus modification of muscle fibers in contact with lipids (Medina-Meza et al., 2014). Similar to oxidation, the multiple steps of non-enzymatic browning are affected by moderate pressure at different extents. The early condensation steps should be slightly impacted by pressure, whereas an intense inhibition effect would be observed for the advanced stages (Isaacs & Coulson, 1996; Martinez-Monteagudo & Saldaña, 2014; Tamaoka et al., 1991).

Pressure also influences cells and tissues functionality. For instance, pressure higher than 100 MPa affects membrane fluidity and functionality of transmembrane proteins, probably due to the modification of phospholipid packing and shifts in acid/base equilibria (Kato et al., 2002; Macdonald, 1978). At pressure higher than 220 MPa, membrane protein would unfold and the bilayer interface would separate, leading to membrane fragmentation.

Pressure lower than 100 MPa was found to inhibit motility, amino acids uptake and microbial cell division/growth/replication (Table 1), but microorganisms would easily recover when pressure is removed (Abe, 2007). If pressure is increased over 100 MPa, ribosomes dissociation is induced, DNA transcription is blocked and protein synthesis stops, causing microbial death (Gross, Lehle, et al., 1993). Pressure-induced microbial inactivation is strongly dependent on microorganism type. Gram(+) bacteria are more resistant to HS pressure as compared to Gram(-) ones (Huang et al., 2014). In fact, *Listeria monocytogenes*, *Listeria innocua* and sporogenic bacteria like *Clostridium botulinum*, were fully resistant to pressurization below 200 MPa (Lakshmanan & Dalgaard, 2004; Margosch et al., 2006; Tomasula et al., 2014). It can be thus inferred that HS performed among 100 and 250 MPa could have a partial bactericidal effect, being able to only impair the activity of the most pressure-sensitive microorganisms. The bactericidal effect would be synergistically enhanced by acidic conditions, which would further stress cell functionality (Paredes-Sabja et al., 2007).

Interestingly, bacterial toxins are commonly more resistant to pressure as compared to the bacteria they are generated by. The study published by Margosch et al. (2005) proved that pressure up to 800 MPa has no effect on the reactivity of toxins produced by *Vibrio cholerae* and *Staphylococcus aureus* and leads to an increase in reactivity of *Bacillus cereus* and *Escherichia coli* toxins. Whether

the production of these toxins would be enhanced or hampered under pressure has not been reported in the literature so far.

1.1.4 Effect of hyperbaric storage on food microbial counts

Based on evidence on the effect of pressure on cell functionality (Table 1), research performed prior to this Thesis has reported on the possibility of using HS to extend food microbial stability and shelf life in a more sustainable way than conventional refrigeration (4 °C). Studies have been performed by examining the effect of HS on the natural occurring spoilage microbes in solid (raw fish and meat, cooked ham and fresh cheese) and liquid foods (fruit juices), and in a model systems (McIlvaine buffer). Table 2 reviews the main literature relevant to the effect of HS on the evolution of microbial counts in these food categories.

Available literature suggests HS to be efficacious in reducing microbiological indicators of quality and hygiene. In particular, total bacteria count seems the most sensitive index, with inactivation levels ranging from 0.2 to 5 log units. The highest number of log reductions was detected in the case of strawberry juice, which presented a pH of *circa* 3.3, confirming the critical role of acidic condition in promoting microbial inactivation. The inactivation capacity of HS was further confirmed by challenge tests performed with specific surrogated pathogenic microorganisms. To this regard, the application of 75 MPa at 25 °C promoted a 3 log unit-reduction in inoculated *Listeria innocua* ATCC 33090 and *Escherichia coli* ATCC 25922 in bovine meat after 14 days of storage (Santos, Castro, et al., 2020). A similar result was obtained in watermelon juice by Pinto et al. (2017), with complete inactivation of *Listeria innocua* after 10 days and *Escherichia coli* after only 3 days. Coherently with literature on HHP, these results confirm the higher pressure-tolerance of Gram(-) bacteria and the protective food matrix effect (Campus, 2010).

An interesting feature of HS was reported to be the capability of inactivating pressure-resistant microbial spores. In fact, HS performed at 100 MPa for 1 or 2 months at room temperature was successful at inactivating endospores (4.5 log reductions) of *Alicyclobacillus acidoterrestris* and *Bacillus subtilis* in carrots and apple juice, respectively (Pinto et al., 2018, 2019). Contrarily to HHP, HS would efficaciously inactivate spores when a moderate pressure is applied for a sufficient time. In particular, during prolonged storage at 25-100 MPa spores would germinate, becoming far more sensitive to pressure. This mechanism allows HS to achieve spore inactivation levels not attainable by HHP, even under extreme pressure conditions.

Table 2: Logarithmic reduction of counts of total bacteria (*TBC*), *Enterobacteriaceae* (*ENT*), yeasts and molds (*YM*) upon hyperbaric storage of foods at different processing conditions.

Matrix	Process parameters			Microbial reduction (logCFU g^{-1})			Reference
	T (°C)	*P* (MPa)	*Storage* (days)	*TBC*	*ENT*	*YM*	
Hake loins	5	50	7	0.2	1.9	n.d.	Otero et al., 2017
Mackerel	5	50	12	0.6	2.0	n.d.	Otero et al., 2019
Salmon	10	60	50	1.3	1.5	n.d.	Fidalgo et al., 2019
	25	75	10	1.7	4.0	n.d.	Fidalgo et al., 2018*
Pork meat	10	60	60	2.4	1.5	2.3	Fernandes et al., 2019*
	25	75	60	2.3	1.5	1.8	
Bovine meat	25	75	60	2.5	2.0	4.2	Santos, Castro, et al., 2020*
		100		2.0	2.0	3.4	
	10	60	60	n.d.	3.3	3.4	Santos, Delgadillo, et al., 2020*
	25	75	60	3.1	3.3	3.4	
Watermelon juice	21	100	7	1.8	n.d.	2.5	Pinto et al., 2016*
	23	75	10	2.1	2.4	1.6	Pinto et al., 2017*
		100		3.1	2.4	2.6	
Strawberry juice	20	25	10	2.0	n.d.	1.3	Bermejo-Prada & Otero, 2016
		50		3.3	n.d.	2.8	
	20	50	15	2.2	n.d.	2.5	Segovia-Bravo et al., 2012
		220		5.0	n.d.	3.8	
Apple juice	23	25	30	2.7	n.d.	n.d.	Pinto et al., 2019*
		50		4.3	n.d.	n.d.	
		100		4.3	n.d.	n.d.	
Carrot juice	23	50	60	5.0	n.d.	n.d.	Pinto et al., 2018*
		100		4.4	n.d.	n.d.	
McIlvaine buffer	23	50	60	1.8	n.d.	n.d.	Pinto et al., 2018*
		100		2.6	n.d.	n.d.	
Watermelon juice	25	75	365	3.0	2.8	2.6	Lemos et al., 2020*

T: temperature, *P*: pressure, n.d.: Not determined, *: Data graphically extrapolated

The antimicrobial efficacy of HS would represent an undoubted advantage when compared to refrigeration, which mainly delays microorganisms growth with limited effects on their viability.

1.1.5 Effects of hyperbaric storage on food chemical, physical and sensory properties

Fruit and vegetables derivatives

In fruit and vegetables derivatives, HS affects a number of chemical and physical properties such as color, viscosity and cloudiness. These changes can be attributed to pressure related effects on endogenous enzymes. In addition, direct effects on the substrates of these enzymes, such as

polysaccharides and polyphenols, may occur. Color is affected by HS with great variability depending on products nature and storage parameters. For instance, watermelon juice stored under different pressure (25-100 MPa) and temperature conditions (15-25 °C) showed an increase in luminosity and a decrease in redness, especially at pressures higher than 75 MPa (Lemos et al., 2017, 2020; Pinto et al., 2017). The mechanism proposed for color changes has not been fully clarified, but it might involve the formation of yellow and brown pigments as a result of enzymatic and non-enzymatic oxidation of red pigments and polyphenols (Lemos et al., 2017). The latter is supposed to be the main mechanism of this effect, since polyphenoloxidase and peroxidase activities tend to decrease upon pressurized storage (Pinto et al., 2017). In addition, lycopene oxidation (up to 25 %) was reported for watermelon juice stored at 75 and 100 MPa at 25 °C for 10 days (Pinto et al., 2017). This result can be due to carotenoid ability to reduce polyphenols previously oxidized by polyphenoloxidase and peroxidase. Oppositely, in the case of strawberry juice, HS had some ability to prevent color fading, but refrigeration was better performing (Bermejo-Prada & Otero, 2016; Segovia-Bravo et al., 2012). Nevertheless, the volatile components were better preserved by HS (50 and 200 MPa for 15 days) as compared to refrigeration (Bermejo-Prada et al., 2017; Bermejo-Prada, Vega, et al., 2015). HS was also reported to affect juice cloud stability and viscosity by altering the activity of pectolytic enzymes (Bermejo-Prada, Segovia-Bravo, et al., 2015; Lemos et al., 2020; Pinto et al., 2016, 2017). Although the mechanism driving the increase in cloudiness has not been elucidated yet (Pinto et al., 2017), the role of these enzymes in the viscosity decay of strawberry juice was studied by Bermejo-Prada, Segovia-Bravo et al. (2015). In particular, HS up to 200 MPa at room temperature for 15 days resulted in an *in-situ* increase of pectinmethylesterase activity, which made more de-methylated pectin available for hydrolysis by polygalacturonase. However, the Authors suggested that other mechanisms, including the increase in the availability of the substrate, might be involved.

Fish, meat and dairy products

Beyond microbial inactivation (Table 1), a number of HS-induced changes have been observed in physical properties of fish and meat products. Such effects are mainly attributed to modifications in the structure of myofibrillar and sarcoplasmic proteins, as well as in myoglobin, which are actually characterized by a negative $\Delta V^{\neq}$ (Cheftel & Culioli, 1997).

Although denaturation of myofibrillar proteins and oxidation of myoglobin make meat appear whiter and less red (Cheftel & Culioli, 1997), these effects are rarely observed to remarkable extents under HS conditions, which do not promote severe protein changes. For instance, HS-RT for up

to 60 days at 100 MPa had minor effects on beef and pork meat color (Fernandes et al., 2019; Santos, Castro, et al., 2020; Santos, Delgadillo, et al., 2020). Nevertheless, a significant decrease in tissue water holding capacity (WHC) was noticed even at 50 MPa and no significant advantage was provided by performing HS-LT (10 °C) (Santos, Castro, et al., 2020; Santos, Delgadillo, et al., 2020). According to the Authors, this effect was correlated to the development of protein oxidation, which probably promoted a decrease in their solubility, leading to enhanced myofibrils disruption and sarcoplasmic proteins aggregation during HS (Santos, Delgadillo, et al., 2020; Van Laack, 1999). The observed changes in color and WHC were not detected when pressure was applied to meat tissue previously submitted to a thermal treatment, such as cooked ham. Once proteins have been thermally denatured, the application of pressure would be unable to further modify their structure (Fernandes et al., 2019; Rivalain et al., 2010). However, the absence of protein changes in ham was only assessed after 8 hours HS treatment, making necessary data validation at longer storage time. HS was also found to promote primary and secondary lipid oxidation in minced bovine and pork meat (Fernandes et al., 2019; Santos, Castro, et al., 2020), in agreement with the negative $\Delta V^{\neq}$ value of these reactions (Table 1).

Compared to meat, fish proteins are more susceptible to HS, with important differences depending on fish species. Whitening was observed in salmon after HS-RT at pressures as low as 50 MPa (Fidalgo et al., 2018), but it became negligible when HS was performed at 10 °C (HS-LT) (Fidalgo et al., 2018; Fidalgo, Simões, et al., 2020; Roche & Royer, 2018). The positive effect of low temperature on the preservation of myofibrillar structure of salmon was confirmed by Fidalgo, Delgadillo et al. (2020) and Fidalgo, Simões et al. (2020). These Authors reported HS-LT (60 MPa and 10 °C) not to cause any damage to tissue myofibrils, while extensive myofibrillar fragmentation was reported upon HS-RT at 75 MPa for 18 days. The preservation of myofibril structure under HS-LT agrees with the well-known antagonistic effects of low temperature and hydrostatic pressure on protein stability (Roche and Royer 2018). Pressure stability of fish muscle greatly depends on species. To this regard, whitening was observed even at HS-LT conditions in hake and mackerel due to the intense pressure-susceptibility of their proteins (Otero et al., 2017, 2019). However, the changes induced by pressure were completely nullified upon cooking. In fact, Otero et al. (2017, 2019) reported that, in hake loins and mackerel subjected to cooking, no significant difference was perceivable between samples stored under refrigeration and HS-LT (50 MPa at 10 °C for 12 days). Upon HS, oxidation might proceed much faster in fish than in meat, depending on the unsaturated fat content of the fish tissue. For instance, HS-RT in the pressure range 50 - 75 MPa strongly enhanced the rate of oxidation in salmon (Fidalgo et al., 2018).

Interestingly, application of HS-LT at 10 °C limited this phenomenon in both salmon and mackerel (Fidalgo et al., 2019; Otero et al., 2019).

1.1.6 Effects of pressure on food packaging properties

The plastic materials commonly employed for flexible food packaging (*e.g.*, pouches) are semicrystalline polymeric films, comprised by an amorphous matrix in which nanoscopic (50 nm) crystalline domains are finely dispersed (Lin et al., 2020). Studies relevant to HHP report that even moderate pressure (50-200 MPa) applied for brief times (5-30 min) can induce changes in the structural and functional (*i.e.*, barrier) properties of many of these materials (*e.g.*, polyethylene, polyamide, polypropylene, polyethylene-terephthalate) (Juliano et al., 2010). The most immediate effect of pressure is the reduction of the free volume of the polymers in the amorphous state, which makes the materials more compact and less permeable (Richter et al., 2010). These effects are usually reversible upon depressurization. However, if polymers develop exceptionally stable interactions under pressure, their compacted structure can be partially retained, with benefit of the barrier properties of the material (Caner et al., 2000, 2004). Under pressure, irreversible growth of the crystalline domains is also favored, leading to films becoming opaquer and potentially stained with white spots (Fleckenstein et al., 2014; Mensitieri et al., 2013). Since a higher crystallinity refers to more ordered polymeric chains, with lesser void spaces within the material matrix, an enhancement in barrier capacity and tensile strength is also achieved (Götz & Weisser, 2002). These effects of pressurization are usually not critical for packaging materials, and can even allow to improve their barrier and mechanical properties (Juliano et al., 2010). However, pressurized packaging materials, with particular reference to the multilayer ones, are also subjected to much more severe effects, such as delamination, embrittlement, wrinkling or puncturing (Galotto et al., 2008, 2010; Marangoni Júnior et al., 2020; Richter et al., 2010). In the literature, different elastic responses of adjacent layers to mechanical stress applied during pressurization was identified as the main cause of integrity loss of packaging (Fraldi et al., 2014). As a result, significant loss of mechanical and barrier properties was frequently observed (Fleckenstein et al., 2014). Besides the direct effects of pressurization, many literature studies have also shown that the presence of air or modified atmosphere gases inside the packaging frequently leads to critical damages (Al-Ghamdi et al., 2019; Dewimille et al., 1993). This is because under pressure higher than 8 MPa at room temperature (~ 20 °C), carbon dioxide is liquid, and oxygen and nitrogen are in the supercritical state (Knez et al., 2014). In these conditions, headspace gases easily dissolve into semicrystalline polymers (Bull et al., 2010; Götz & Weisser, 2002). Then, when pressure is suddenly removed

upon decompression, these solubilized gases rapidly expand in the films structure, causing pinholes and extensive delamination (Fleckenstein et al., 2014). In this intricate set of direct and indirect effects, further variability is provided by the nature of the packaged matrix subjected to pressurization. In particular, it was reported that contact with fatty simulants (*e.g.*, ethanolic solutions, olive oil, isooctane) during pressurization could yield to an exacerbation of physical defects (delamination) (Galotto et al., 2009). Despite the potentially critical relevance of the changes induced by pressure in food packaging, it is surprising that this aspect has been so far overlooked in HS studies. In fact, to our knowledge, there is no indication in the literature about the effects of HS on food packaging materials.

1.2 Challenges of hyperbaric storage and outline of the Thesis

1.2.1 Challenges and perspectives of hyperbaric storage

Based on the analysis of the literature regarding HS (Paragraph 1.1) the purpose of this Paragraph is to pinpoint potential challenges of the technology, which are summarized in Table 3.

Table 3: Pressure-sensitive phenomena and potential challenges of HS, with reference to food packaging, stabilization and functionalization.

	Pressure-sensitive phenomena	Challenges
Food packaging for HS	Plastic polymers compression and crystallization	Packaging material feasibility
Food stabilization by HS	Microbial inactivation	Non-thermal pasteurization
	Enzymatic inactivation	Non-thermal enzymatic stabilization
	Non-enzymatic browning	Control of color changes
Food functionalization by HS	Protein structure modification	Protein functionalization

Identification of feasible packaging solutions for HS of food is a mandatory requirement. The main *caveat* is here related to the fact that polymer compression and crystallization could induce visual defects of the packaging, such as white stains. Besides, more severe defects, like wrinkling or puncturing may occur even at moderate pressures if pressurization is prolonged. However, no evidence at all is available about the effects of prolonged pressurizations on the properties of food packaging materials.

Based on the evidence reporting the remarkable antimicrobial potential of HS, it is reasonable to hypothesize that HS could be used not only as a mere replacement of cold storage, but also as a novel, non-thermal approach to food pasteurization (Table 3). This application of HS would be particularly interesting in the case of perishable matrices conventionally requiring thermal treatment, and whose storage must be carried out under refrigerated conditions (*e.g.*, milk, fruit juices, egg derivatives). In fact, in these cases, non-thermal pasteurization and storage would be simultaneously performed by HS at room temperature, allowing to avoid both the nutritional loss

induced by heat treatment and the substantial energy expenditure associated with refrigeration. However, although the proof of concept for this application was demonstrated (Table 2), the proof of efficacy has never been provided. In fact, there is no evidence showing that microbial inactivation levels sufficient for food pasteurization (*i.e.*, at least 5 log reductions of relevant pathogenic species) are attainable by HS.

The technology could be used for scopes other than food safety. For instance, it has been circumstantially observed that HS might decrease the activity of some food-spoiling enzymes (*e.g.*, polyphenoloxidase, pectinmethylesterase) in selected food matrices (Bermejo-Prada, Segovia-Bravo, et al., 2015; Bermejo-Prada & Otero, 2016; Pinto et al., 2017), but, to our knowledge, no study has been specifically focused on the possibility to achieve enzymatic inactivation by pressurized storage so far.

Based on the hampering effect of pressure on phenomena characterized by a positive $\Delta V^{\neq}$, HS could be used to inhibit alterative chemical events which are typically associated with a volume expansion (Table 1), such as Maillard browning (Hill et al., 1996; Martinez-Monteagudo & Saldaña, 2014). The kinetics and mechanism of the Maillard reaction are extremely complex, and affected by a plethora of compositional and physical factors other than pressure, including pH and temperature. Such remarkable variability actually makes uncertain any prediction about the effect of HS on Maillard browning. To the best of our knowledge, this topic is a completely unexplored research gap.

Besides allowing to control undesired events such as microbial growth, enzymatic spoilage and chemical alteration, the available literature suggests that HS could be capable of delivering specific functionalities to foods. In particular, considering the unfolding of food proteins under moderate hydrostatic pressure (Table 1), this effect could be exploited to enhance the techno-functional properties (*e.g.*, gelling, foaming, emulsifying) of many protein-rich foods (*e.g.*, egg derivatives and milk). In these systems, HS could exert a functionalizing action during their storage under highly bacteriostatic conditions, with very low energetic cost. Although very promising, to our knowledge, this unconventional use of HS has never been tested.

Based on these considerations, the potential multi-role capability of the technology is clear (Table 3). If adequately demonstrated by sound experimental data, HS could become a multi-tasking technology, potentially capable of many different applications not only limited to food storage but also for food treatment, with potential extensive benefits for multiple stakeholders of the food chain.

1.2.2 Ph.D Thesis aim and outline

This Ph.D Thesis consisted of a set of investigations aimed at assessing the efficacy of hyperbaric storage in extending the stability and improving functionality of food.

The experimental work was organized as described in Table 4. Firstly, the effect of HS on plastic packaging materials was assessed with the objective of identifying the most appropriate solution for the subsequent experimental work. The effect of HS on the optical, structural, mechanical and barrier properties of four study-case plastic materials was tested. This activity was carried out in collaboration with the research group supervised by Prof. Fabio Licciardello, from the University of Modena and Reggio Emilia (Chapter 2).

The second Part of the Thesis had the objective to evaluate the capability of HS to stabilize food from a microbiological, enzymatic and chemical point of view (Chapter 3). Initially, the possibility to achieve food pasteurization by HS was evaluated. Durability and challenge tests were performed by applying HS to raw skim milk, which was considered as study-case based on its perishability and relevance in the industrial context. The investigation was then extended to the biological effects of HS on the activity of catalytic proteins occurring in food. To this aim, the capability of the technology to inactivate polyphenoloxidase, taken as a representative food-spoiling enzyme, was evaluated in model solutions and in apple juice. Then, the capability of HS to prevent chemical alterations in food was studied by assessing the effect of pressurized storage on the development of Maillard reaction in sugar-aminoacid model systems. This activity consisted of a kinetic study which was carried out in the laboratories of the Department of Chemistry of the University of Aveiro, under the supervision of Prof. Jorge Manuel Alexandre Saraiva.

In Chapter 4, the possibility to improve selected properties of food by HS was assessed. In particular, the attention was focused on the capability of HS to enhance the techno-functionality of proteins in raw skim milk, egg white, and egg yolk by inducing protein structural changes.

In the light of the results achieved with the experimental work of this Thesis, a critical perspective on the industrial readiness of HS was then reported in Chapter 5, highlighting the aspects still in need of assessment before the technology can be industrially scaled-up.

Finally, the outcomes of the work were critically discussed, suggesting possible future research needs (Chapters 6), and estimation of the scientific and personal impact of this Ph.D Thesis (Chapter 7).

Table 4: Challenges of HS and study-cases investigated within this Ph.D Thesis, applied HS conditions and methodologies for the evaluation of HS effects.

	Challenges	Study-case	Hyperbaric storage			Evaluation			
			T (°C)	*P (MPa)*	*Storage (days)*	*Microbiological Stability*	*Physical/chemical properties*	*Structural properties*	*Functional properties*
Chapter 2 Packaging for HS	Materials feasibility for HS	Industrially viable films	25	200	35		Luminosity (tristimulus colorimetry), Opacity (UV-Vis spectrophotometry)	UV-Vis spectrum, Thermal properties (DSC), Crystallinity (XRD)	Tensile strength, Elongation at break, WVTR
Chapter 3 Food stabilization by HS	Non-thermal pasteurization	Raw skim milk	25	150, 200	6	Native microflora count (TBC, LAB, TC, FC, C^+S), Inoculated pathogens count (*E. coli*, *S. aureus*)	Clotting (DLS), Color		
	Non-thermal enzymatic stabilization	PPO solutions	25	100, 200	2			PPO activity, Kinetic modelling	
		Apple juice	25	100, 200	6	Native microflora count (TBC, LAB, YM)	Color	PPO activity, Kinetic modelling	
	Control of color changes	Glucose-glycine model systems	20, 25, 43, 53, 63	15, 20, 30, 40, 50, 100, 200	88		Intermediates and melanoidins content, Kinetic modelling		
Chapter 4 Food functionalization by HS	Protein functionalization	Raw skim milk	25	150	6			Particle size (DLS), Whey protein profile (HPLC)	Foaming capacity, Foam stability
		Egg white	25	200	28	Inoculated pathogens count (*S. enterica*, *S. aureus*)	Color, Oxidative status (FT-IR), Peroxide value, Carotenoid content	Aromatic aminoacid exposure (Abs 280 nm), Turbidity (Abs 680 nm), Free SH groups, Thermal properties (DSC), Secondary structure (FT-IR), Particle size (DLS), Particle surface charge (DLS),	Viscosity, Solubility, Gelling capacity, Emulsifying activity, Foaming capacity, Foam stability
		Egg yolk	25	200	28				

Abbreviations in order of appearance: T: Temperature, P: Pressure, UV-Vis: ultraviolet-visible light, DSC: differential scanning calorimetry, XRD: X-ray diffraction, WVTR: water vapour transmission rate, TBC: total bacteria count, LAB: lactic acid bacteria, TC: total coliforms, FC: faecal coliforms, C^+S: coagulase-positive *Staphylococci*, DLS: dynamic light scattering, PPO: polyphenoloxidase, YM: yeasts and molds, FT-IR: Fourier transform infrared spectroscopy, HPLC: high-performance liquid chromatography.

Chapter 2: Packaging for hyperbaric storage

This Chapter of the Thesis reports a preliminary investigation carried out to explore the effects of hyperbaric storage on food packaging materials, with the objective of identifying plastic films adequate for packaging of food intended for HS.

2.1 Effect of hyperbaric storage on packaging materials

2.1.1 Introduction

The identification of appropriate packaging solutions for food subjected to hyperbaric storage is not a trivial issue, since any material proposed for HS applications should be: i) flexible, to guarantee that pressure is uniformly applied without breaking; ii) resistant, to avoid pressure-induced defects; iii) a good barrier, to prevent mass transfer from the pressurizing fluid to the food and *vice versa.* These requirements could be easily addressed by selecting materials with adequate mechanical and diffusional properties. Nevertheless, an extensive body of evidence (Chapter 1) suggests that even brief and moderate pressurizations (50 - 200 MPa for 30 min) can induce a complex set of undesired effects in plastic packaging materials, ranging from moderate crystallization to delamination and puncturing. In the HS context, even the less impactful defects occurring at a nanoscopic scale might build up to the point of becoming critical during long pressurizations, possibly resulting in dramatic visual defect and alteration of mechanical and barrier properties. By contrast, brief pressurization was also shown to enhance mechanical and barrier properties in many polymeric matrices by reducing free volume and increasing crystallinity (Chapter 1). Nevertheless, there is no evidence reporting the extent of the effect of pressure on packaging materials over time scales typical of HS.

This Chapter of the Thesis is dedicated to a preliminary investigation carried out to explore the effects of hyperbaric storage on food packaging materials with the objective of identifying plastic films adequate for packaging of food intended for HS. To this aim, four materials typically employed in the food industry were selected as study-cases: i) poly-amide/poly-ethylene (PA/PE) was chosen due to its widespread use in the literature studies about HS (Fidalgo et al., 2018; Lemos et al., 2017; Otero et al., 2017, 2019; Pinto et al., 2016, 2017, 2018, 2019; Santos, Fidalgo, et al., 2021); ii) poly-propylene/ethylene-vinyl-alcohol/poly-ethylene (PP/EVOH/PE) was chosen due to the known capability of EVOH-based multilayer materials to withstand even extreme pressurized conditions (up

to 800 MPa) without defects (Caner et al., 2004; Galotto et al., 2008; López-Rubio et al., 2005); iii) poly-ethylene-terephthalate (PET) was chosen based on its widespread use in the food industry (Ashby, 1988); iv) poly-lactic acid (PLA) was chosen as a biodegradable alternative to PET (Sousa et al., 2021). Pouches of each material were filled with D1 simulant. The latter was selected as a representative of foods with a dispersed fat matrix (*e.g.*, milk, egg derivatives), and based on the reported capability of fat-like simulants to promote pressure-induced damages in films (European Commission, 2011; Galotto et al., 2009). Samples were subjected to HS at 200 MPa at uncontrolled room temperature (20 ± 2 °C). At increasing time for up to 35 days, samples optical, mechanical, structural and diffusional properties were analyzed and compared to the ones of control samples stored at atmospheric pressure for the same timespan (0.1 MPa).

2.1.2 Materials and Methods

Samples preparation

PP/EVOH/PE (80 μm thickness) were obtained from Niederwieser Group S.p.A., (Campogalliano, Italy). PA/PE (90 μm thickness) were obtained from a local retailer. PET was obtained from DuPont Teijin Films™ (Dumfries, United Kingdom). PLA was obtained from Taghleef Industries (Newark, DE, U.S.A.).

Square pouches with 2 dm^2 internal surface were cut from each material and heat-sealed with minimal headspace (Orved VM-16, Musile di Piave, Italy) containing 30 mL of D1 simulant (50 % v/v ethanol).

Hyperbaric storage

The hyperbaric storage working unit described in Figure 1 (Chapter 1) was used. Pouches were stored at 200 MPa at 20 ± 2 °C and reference samples were stored at room pressure and temperature conditions (0.1 MPa, 20 ± 2 °C). At increasing time for up to 35 days, samples were removed from storage conditions and analyzed.

Luminosity

Samples luminosity was measured with a tristimulus colorimeter (Chromameter-2 Reflectance, Minolta, Osaka, Japan) equipped with a CR-300 measuring head. The instrument was standardized against a white tile before analysis. Samples were positioned on the standardization tile avoiding the

formation of wrinkles and air pockets, and analyzed. The L* parameter of the CIELab scale was considered as samples luminosity.

Ultraviolet and visible light barrier and opacity

Samples were obtained by manually cutting films into 2 x 2 cm squares. UV-Vis light transmission was measured with a spectrophotometer (VWR® Double Beam UV × VIS 6300 PC spectrophotometer, China) in the wavelength range 200-800 nm. The opacity value of the films was calculated with Eq. 3.

Eq. 3 $$Opacity = \frac{-\log T_{600}}{d}$$

Where T_{600} is the transmittance at 600 nm and d is the film thickness (nm).

Differential scanning calorimetry

Samples were manually cut into approximately 3 x 30 mm stripes, convoluted without wrinkling to fit a 100 µL aluminum crucible (Mettler-Toledo, Greifensee, Switzerland) and weighed to ± 0.0001 g precision. Differential scanning calorimetry (DSC) was performed with a DSC 3 Stare System differential scanning calorimeter (Mettler-Toledo). Samples were heated from 0 °C to 100 °C at 10 °C min^{-1} under continuous nitrogen flow (20 L min^{-1}). Glass transition temperature (T_g, °C) and peak enthalpies (ΔH, J g^{-1}) were computed from the thermograms using the program STARe ver. 16.10 (Mettler-Toledo).

X-ray diffraction

Films samples (2 x 2 cm) were subjected to X-ray diffraction (XRD) using an X'Pert PRO diffractometer (Marvel Panalytical, United Kingdom). XRD patterns were recorded using CuKα radiation (λ = 1.54 Å), at a voltage of 40 kV and a filament emission of 40 mA. Samples were scanned with ramping at 0.5° min^{-1} in an angle (2θ) range of 3°- 60°. A zero-background holder was used to avoid the detection of any peak not related to the sample. Background noise was quantified by running the diffractometer with empty sample holder and was subtracted to the spectra. Peak elaboration and integration were performed using Origin Pro 2021 (OriginLab, Northampton, MA, USA). Crystallinity index (CI) was calculated using Eq. 4.

Eq. 4 $CI\ (\%) = \frac{S_c}{S_t} * 100$

Where S_c is the sum of crystalline peaks area and S_t is the sum of total area under the spectra (Hato et al., 2017).

Mechanical properties

Samples were obtained by cutting films into rectangular strips (10 x 1.5 cm). Thickness of each sample was estimated by averaging three measurements performed in three random positions with a digital micrometer (IP65, SAMA Tools, Viareggio, Lucca, Italy). Mechanical properties (Tensile strength TS, elongation at break E%) were evaluated using a dynamometer (Z1.0, ZwickRoell, Ulm, Germany) equipped with a 1 kN load cell according to the standard method ASTM D882-12 (ASTM, 2001a). The TestXpert® II 161 software (v 3.31) (ZwickRoell, Ulm, Germany) was used to elaborate data.

Water vapour transmission rate

Water vapour transmission rate (WVTR) was determined according to the standard method ASTM E96 (ASTM, 2001b) with some modifications. Films were sealed on top of glass test cups (vials) with an internal diameter of 10 mm and a depth of 55 mm, filled with 2 g of anhydrous $CaCl_2$ (0% RH). The cups were placed in desiccator containing $BaCl_2$ (90% RH), which were maintained in incubators at 40 °C. The WVTR was calculated by plotting the weight gain of the vials as a function of time according to Eq. 5.

Eq. 5 $WVTR = \frac{\Delta W}{\Delta t} \cdot \frac{1}{A}$

Where $\frac{\Delta W}{\Delta t}$ is the slope of the line describing the weight increase of the bottles as a function of time (g day^{-1}), and A is the surface area of the exposed film (m^2).

Data analysis

Luminosity and DSC analyses were performed at least in triplicate. UV-Vis light barrier, opacity, mechanical properties and WVTR were measured at least in quintuple. XRD analysis was measured in duplicate. Analyses have been performed on three independent samples. Results are reported as mean ± standard deviation and were subjected to one-way analysis of variance (ANOVA) and Tukey's

Honest Significant Differences test ($p < 0.05$) using R v. 4.2.2 for Windows (The R foundation for statistical computing).

2.1.3 Results and Discussion

Films integrity and optical properties

The effect of hyperbaric storage on the packaging materials was firstly assessed visually, noting that PA/PE, PP/EVOH/PE and PET retained their integrity without macroscopic defects even after 35 days at 200 MPa. By contrast, the seals of PLA films were made significantly weaker by HS, as they immediately opened upon withdrawal from the hyperbaric chamber, spilling the food simulant. To this regard, few Authors have actually reported pressurization (up to 600 MPa for 20-60 min) to impair packaging seal strength (Dobiáš et al., 2004; Lambert et al., 2000b, 2000a; Masuda et al., 1992). As Fraldi et al., (2014) have demonstrated, pressure-induced stress would concentrate in the welded sides of packaging pouches, where they can even cause macroscopic damages (*e.g.*, delamination, wrinkling). Therefore, PLA seals could have progressively weakened over prolonged pressurization due to mechanical strain, ultimately failing when mild shear forces were applied upon manual removal of the pouches from the hyperbaric vessel. Based on these results, the optical properties of the tested materials were instrumentally assessed to detect possible changes related to structural modifications occurring during storage (Table 5).

Table 5: Luminosity (L*) and opacity of packaging films stored at 0.1 and 200 MPa for up to 35 days at room temperature (20 ± 2 °C). Standard deviations in brackets.

Pressure	Time	PA/PE		PP/EVOH/PE		PET		PLA	
(MPa)	(d)	L*	Opacity	L*	Opacity	L*	Opacity	L*	Opacity
0.1	0	95.25[a] (0.18)	5.78[a] (0.47)	96.13[a] (0.05)	7.06[a] (0.17)	95.91[a] (0.14)	17.44[a] (0.89)	96.57[a] (0.01)	15.47[a] (0.47)
	7	94.94[a] (0.03)	N.D.	95.52[b] (0.04)	N.D.	94.87[cd] (0.10)	N.D.	95.86[c] (0.13)	N.D.
	35	94.30[b] (0.25)	N.D.	95.54[b] (0.18)	N.D.	94.99[c] (0.04)	N.D.	96.10[b] (0.04)	N.D.
200	7	93.64[c] (0.09)	5.50[ab] (0.50)	94.70[c] (0.15)	6.87[a] (0.42)	94.63[d] (0.07)	16.31[b] (0.94)	95.34[e] (0.04)	14.48[b] (0.62)
	35	94.49[b] (0.10)	5.29[b] (0.67)	93.73[d] (0.35)	6.54[b] (0.41)	95.38[b] (0.13)	15.00[c] (0.97)	95.45[d] (0.02)	15.06[a] (0.73)

[a] Different letters in the same column indicate statistically different means (ANOVA; $p < 0.05$).

As expected, luminosity and opacity of films did not show dramatic changes during storage at 0.1 and 200 MPa for up to 35 days. Nevertheless, a small but statistically significant decrease ($p < 0.05$, ANOVA) of both indexes indicated a slight increase in the transparency of all materials (Table 5). In agreement with the literature, these effects are usually associated to a decrease in the crystallinity of polymeric matrices. In fact, a lower concentration of crystalline domains in the latter typically allows more light to be transmitted (Yoo et al., 2009). Pressurized storage seemed to slightly increase this effect, possibly indicating that HS favored crystallinity loss (Juliano et al., 2010). Regardless of the slight transparency increase, the UV-C light (≤ 200 nm) transmittance of all materials did not change during HS, remaining very low (< 0.5%) for up to 35 days. This indicates that HS did not affect the capability of the materials to screen foods against high-energy photons capable to beget a wide spectrum of alterations triggered by photo-oxidation (Haghighi et al., 2021).

Structural properties

The effect of hyperbaric storage (HS) on the crystalline fractions of packaging materials was assessed by X-ray diffraction (XRD). Analyses revealed that storage for up to 35 days did not cause significant change in the XRD spectra of PA/PE and PP/EVOH/PE samples (data not shown). On the other hand, the crystalline fractions of PET and PLA were significantly affected by storage both at atmospheric and hyperbaric conditions (Figure 3).

A single large peak was observed in X-ray diffractograms of control PET and PLA, at around 26.02 and 16.58°, respectively (Figure 3). In agreement with the literature, these angles corresponded to an interplanar distance (d) of 6.84 ± 0.00 and 5.36 ± 0.03 Å in the crystallites of PET and PLA, respectively (Greco & Ferrari, 2021; Stetsiv et al., 2021). Upon storage at 0.1 MPa for up to 35 days, no significant peak shift was observed, indicating the absence of changes in the interplanar distance of both PET and PLA crystalline fractions (data not shown). Conversely, a slight shift of the peak to higher angle was observed for both materials during HS, indicating that HS caused PET and PLA crystallites to become slightly more compact (6.72 ± 0.07 and 5.18 ± 0.03 Å, respectively). This is in agreement with the literature reporting compression of packaging materials even by brief (25 min) hydrostatic pressure processing at 200 MPa (Grassia et al., 2011). To understand the remarkable changes in peak intensity and area, the crystallinity index (CI, %) of the samples was calculated based on Eq. 4. In agreement with the largely crystalline character of the films (Figure 3), the CI of control PET and PLA was 77.68 ± 0.25 and 67.30 ± 4.38 %, respectively.

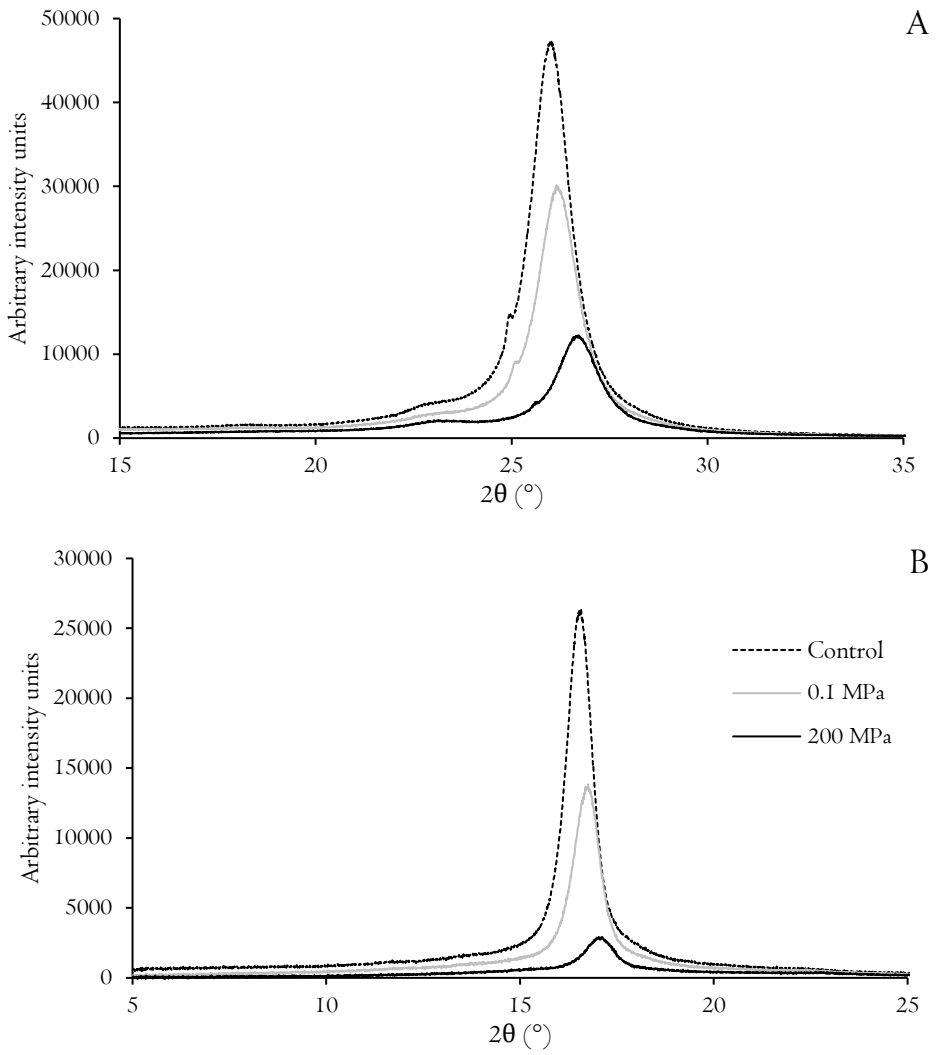

Figure 3: X-ray diffractograms of PET (A) and PLA (B) films before (control) and after storage at 0.1 and 200 MPa for 35 days at room temperature (20 ± 2 °C).

Interestingly, no significant changes in CI were observed in the case of PET stored for up to 35 days at 0.1 or 200 MPa. In particular, although the intensity of the XRD peak remarkably decreased after HS (Figure 3 A), the CI of the sample was still high and comparable with the one of the control film (75.85 ± 1.95 %). A very similar effect was observed in the case of PLA, in which only a slight reduction of CI was detected after 35 days under 200 MPa (52.65 ± 1.54 %). In agreement with the literature, these results indicate that, although HS slightly compressed PET and PLA crystallites, the applied pressure was not capable to significantly affect their relative abundance in the materials (Galotto et al., 2008, 2009).

Based on these results, the decrease in peaks area and intensity could be explained considering that the hydroalcoholic simulant might have swelled and diluted the materials during storage (Tang et al., 2020). In particular, since both PLA and PET are primarily hydrophobic, this effect was likely caused by the ethanolic component of the simulant rather than by water (Feigenbaum et al., 2000; Kirchkeszner et al., 2022; Mochizuki, 2009; Nasiri et al., 2016). As shown in Figure 3, such phenomenon would have been strongly favored under HS conditions. These results appear to contradict the literature reporting limited diffusion in pressurized polymeric matrices (Götz & Weisser, 2002; Schmerder et al., 2005). Nevertheless, even moderate pressurizations (200-300 MPa) were shown to cause microscopic irregularities (*e.g.*, valleys, depressions) when PET- and PLA-based materials were exposed to the simulant (Caner et al., 2003; Hoque et al., 2022; Tang et al., 2020).

In the light of these results, DSC was performed to study the effect of HS on the structure of the amorphous fraction of the films. Regardless of the applied pressure, storage for up to 35 days did not cause remarkable changes in the thermal behavior (T_g) of the amorphous regions of PA/PE, PP/EVOH/PE and PLA films (data not shown). However, interesting changes were observed in the case of PET (Figure 4).

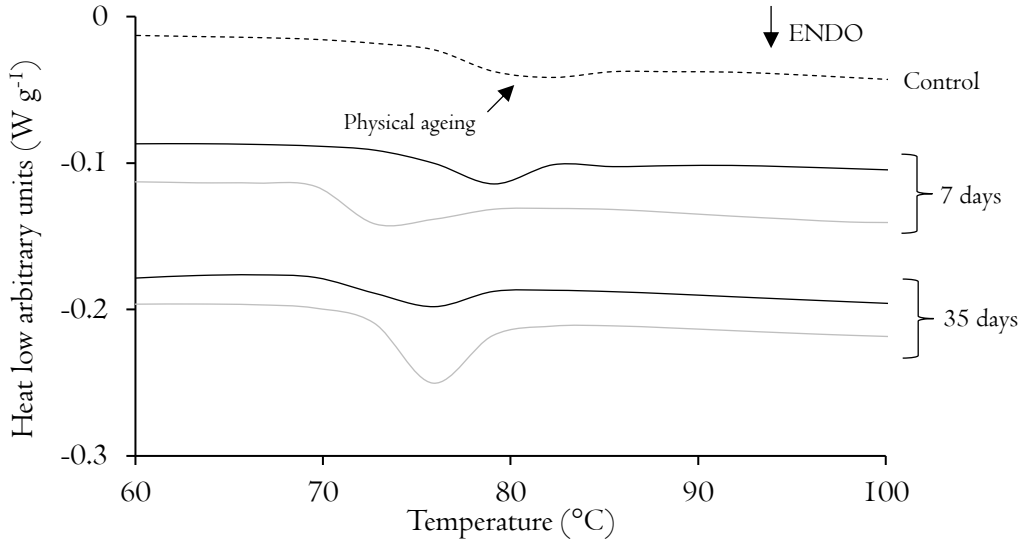

Figure 4: DSC thermograms of PET stored at 0.1 and 200 MPa for up to 35 days at room temperature (20 ± 2 °C).

As visible from Figure 4 and in agreement with the literature, the glass transition temperature (T_g) of the control PET film was around 80 °C (Jog, 1995). In this sample, DSC analysis revealed the presence

of a small endothermic peak in correspondence of the T_g, indicating that PET films were slightly physically aged before storage trials were performed. Physical ageing is a temperature-dependent phenomenon, affecting polymeric matrices stored for extended time (*i.e.*, days/weeks/months) below their T_g. It consists in the slow, progressive rearrangement of glassy polymer chains into non-crystalline ordered structures, which require more energy for rubbery transition when heated (Montserrat & Cortés, 1995; Rabinovitch & Summers, 1992). Due to physical ageing, polymeric materials usually become denser, with higher tensile strength and young modulus, but also embrittled (Lacatus & Rogers, 1986; Kong, 1986; Mininni et al., 1973; Munier et al., 2002; Tant & Wilkes, 1981).

Data reported in Figure 4 clearly indicate that storage conditions significantly affected the development of PET physical ageing. To better understand these changes, thermograms were elaborated, focusing the attention on the samples T_g and physical ageing peak enthalpy (ΔH) (Table 6). The T_g of PET significantly decreased after 7 days of storage at atmospheric pressure (0.1 MPa), without further significant changes for up to 35 days (Table 6). In accordance with previous discussion regarding data reported in Figure 3, plasticization was likely caused by the swelling of PET with simulant during storage (Feigenbaum et al., 2000; Kirchkeszner et al., 2022; Nasiri et al., 2016). When HS was applied, the decrease in T_g was slightly more pronounced (Table 6), likely due to the enhancement of the film swelling under pressure (Feigenbaum et al., 2000). In agreement with Figure 4, peak enthalpy (ΔH) progressively increased during storage at atmospheric pressure for up to 35 days (Table 6), indicating a remarkable development of physical ageing in these conditions (Montserrat & Cortés, 1995).

Table 6: T_g and physical ageing peak enthalpy (ΔH) of PET stored at 0.1 and 200 MPa for up to 35 days at room temperature (20 ± 2 °C).

Pressure (MPa)	Time (d)	T_g (°C)	ΔH (J g^{-1})
0.1	0	78.42 ± 0.40^{a}	0.45 ± 0.02^{c}
	7	71.16 ± 0.52^{cd}	0.81 ± 0.11^{b}
	35	71.91 ± 0.06^{c}	1.04 ± 0.03^{a}
200	7	74.30 ± 2.21^{b}	0.31 ± 0.06^{c}
	35	70.38 ± 0.47^{d}	0.38 ± 0.05^{c}

[a] Different letters in the same column indicate statistically different means (ANOVA; $p < 0.05$).

On the other hand, application of HS completely hampered the phenomenon, even showing a slight decreasing trend in ΔH under pressure (Table 6). These results not only demonstrate HS to be capable

of preventing physical ageing in PET, but provide evidence of the capability of the technology to reverse the phenomenon. To our knowledge, there is no information regarding the effect of hydrostatic pressure on polymers physical ageing. However, a reasonable explanation of this effect could be the enhancement of simulant swelling during HS, which could have mobilized amorphous PET molecules preventing their reorganization in stable structures. To this regard, it is interesting to note that physical ageing is always associated with a decrease in specific volume (Mininni et al., 1973; Struik, 1981). Therefore, based on the Le Chatelier principle and Transition State theory, this phenomenon should have been favored by pressure (Evans & Polanyi, 1935; Le Chatelier, 1891). Coherently with the literature (Fleckenstein et al., 2014), these results indicate that the outcome of packaging materials pressurization cannot be predicted based on theoretical kinetic principles solely. In particular, the interaction of the polymeric materials with the packaged foods or simulants (Figure 3, Table 6) appears to be a major source of deviation from ideality, and should thus be carefully considered.

Mechanical properties

In agreement with the absence of significant structural modification, PA/PE and PP/EVOH/PE films did not show any change in their mechanical properties (*i.e.*, tensile strength, elongation at break) during storage for up to 35 days, regardless of the applied pressure (Dobiáš et al., 2004; Galotto et al., 2008). Contrarily, the structural changes observed in PLA and PET affected the tensile strength and elongation at break of these materials (Figure 5).

PET and PLA samples initially showed values of tensile strength and elongation at break in line with those reported in the literature by several Authors (Jamshidian et al., 2012; Martino et al., 2009; Muller et al., 2017; Panowicz et al., 2021). During storage at atmospheric pressure, PET mechanical properties showed a fluctuating behavior, probably due to the complex set of changes in crystalline and amorphous domains previously observed (Figure 3, Table 6). It is worth noting that, after 35 days of storage at 0.1 and 200 MPa, both tensile strength and elongation at break of PET were statistically indistinguishable ($p > 0.05$, ANOVA) and showed very similar values compared to the ones of the control sample (Figure 5). Concerning PLA, storage at atmospheric pressure and under HS for up to 35 days caused a slight increase in tensile strength and elongation at break (Figure 5). In the pressurized films, the variation of mechanical properties during storage was quite irregular, resembling the trend showed by PET. As for the latter, these changes were probably caused by a series of interdependent effects of pressure and the prolonged contact with the ethanolic simulant (Fleckenstein et al., 2014).

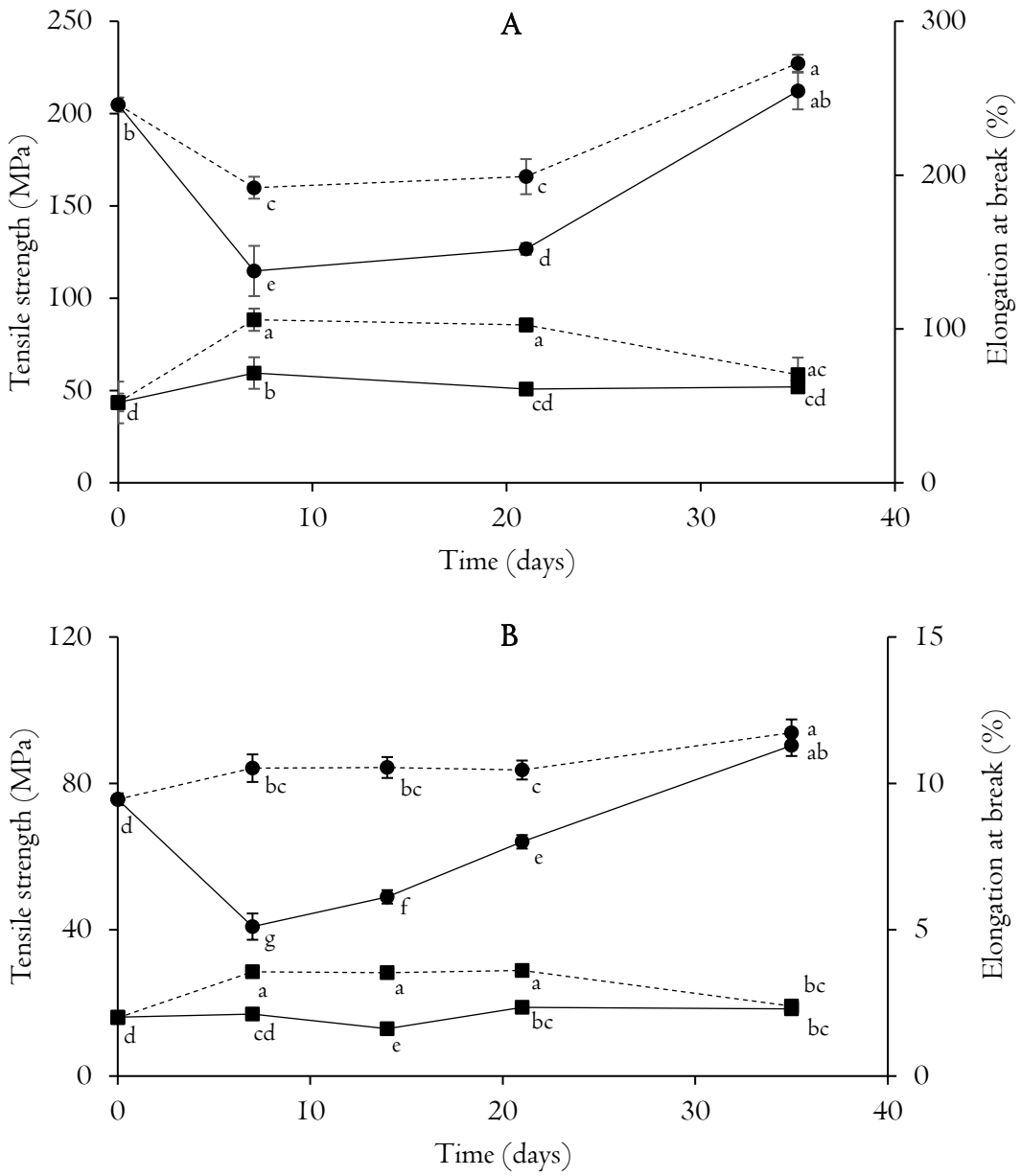

Figure 5: Tensile strength (●) and elongation at break (■) of PET (A) and PLA (B) films stored at 0.1 (...) and 200 (__) MPa for up to 35 days at room temperature (20 ± 2 °C); [a] Different letters for the same mechanical property for each film indicate statistically different means (ANOVA; $p < 0.05$).

Based on the critical role of this factor in shaping the structure and properties of PET and PLA, in the last part of this study the attention was focused on the evolution of the materials water vapour transmission rate (WVTR) under HS.

Diffusional properties

Given the commercial importance of WVTR (Jarvis et al., 2017), analyses were performed regardless of the presence or absence of HS-induced changes of films optical, structural or mechanical properties (Table 7).

Table 7: Water vapour transmission rate (WVTR; g day^{-1} m^{-2}) of packaging films stored at 0.1 and 200 MPa for up to 35 days at room temperature (20 ± 2 °C).

Pressure (MPa)	Time (d)	PA/PE	PP/EVOH/PE	PET	PLA
0.1	0	11.21 ± 1.06^{a}	7.13 ± 0.70^{a}	31.21 ± 3.68^{b}	300.00 ± 16.30^{c}
	7	12.10 ± 0.74^{a}	8.41 ± 1.14^{a}	41.40 ± 2.65^{a}	339.81 ± 7.60^{ab}
	21	12.31 ± 0.74^{a}	8.41 ± 1.14^{a}	N.D.	346.82 ± 9.44^{ab}
	35	12.74 ± 2.38^{a}	9.17 ± 0.57^{a}	40.45 ± 1.60^{a}	350.64 ± 8.41^{a}
200	14	10.70 ± 1.71^{a}	8.66 ± 1.07^{a}	42.29 ± 3.97^{a}	321.87 ± 6.41^{bc}
	35	10.45 ± 1.40^{a}	7.64 ± 1.56^{a}	36.18 ± 3.32^{ab}	320.59 ±17.39^{bc}

N.D. Not determined; [a] Different letters in the same column indicate statistically different means (ANOVA; $p < 0.05$).

In accordance with the lack of modification of PA/PE and PP/EVOH/PE structural and mechanical properties, the WVTR of these films did not significantly change ($p > 0.05$, ANOVA) during storage at 0.1 and 200 MPa (Table 7). In PET and PLA, storage for up to 35 days at 0.1 MPa resulted in a significant ($p < 0.05$, ANOVA) increase in WVTR (Table 7). This was probably due to films swelling with simulant, which would promote exposure of hydrophilic groups, enhancing their capability to interact with water (Ganesan et al., 2019). By increasing storage pressure up to 200 MPa, the increase in PET and PLA WVTR was slightly impaired (Table 7). These results are in apparent contradiction with the previously discussed enhancement of films swelling under pressure (Figure 3, Table 6). However, according to the reduction in interplanar distance observed in these materials after 35 days at 200 MPa (Figure 3), HS likely caused a slight irreversible compression of the films structure, which became less permeable to gases after storage (Götz & Weisser, 2002). Similar results have actually been obtained in some studies regarding the application of HHP (up to 800 MPa for 5-60 min) to different packaging materials (Juliano et al., 2010).

2.1.4 Conclusions

The results reported in this Chapter demonstrate that the effect of hyperbaric storage on food packaging films is highly material-dependent. Multilayer packaging seems to offer good resistance to pressurized storage, with no changes in structural, mechanical and diffusional properties. On the other hand, single-layer PET and PLA showed intense structural modifications upon simulant absorption even during storage at 0.1 MPa. These effects resulted in irregular changes in mechanical properties and in barrier capacity loss. Structural modifications of single-layer films were exacerbated by 200 MPa-HS, which caused PLA seals to fail. In addition, polymers compression slightly limited barrier decay.

These results clearly indicate that, among the tested materials, the two multi-layer solutions (PA/PE, PP/EVOH/PE) could represent appropriate choices for HS purposes. Based on these considerations, the experiments performed throughout the Thesis were performed using samples packed in PA/PE or PP/EVOH/PE pouches.

It would be interesting to study if polymer compression during HS could be exploited to enhance packaging barrier properties. This option would be particularly interesting for biodegradable or compostable materials other than PLA (*e.g.*, cellulose acetate), which would allow to further reduce the already low environmental impact of this innovative food storage approach.

Chapter 3: Food stabilization by hyperbaric storage

This Chapter of the Thesis aims at assessing the capability of hyperbaric storage to guarantee microbiological, enzymatic and chemical stability of food. The attention was focused on the possibility to: (i) obtain pasteurization of raw skim milk; (ii) inactivate polyphenoloxidase in model enzyme solutions and apple juice; and (iii) limit the development of non-enzymatic browning in model sugar-aminoacid systems. Since these topics are inherently different, they are addressed in three separate Paragraphs, each with its own "Introduction", "Material and Methods", "Results and Discussion" and "Conclusions" sections.

3.1 Non-thermal pasteurization by hyperbaric storage

3.1.1 Introduction

The remarkable antimicrobial capability of HS has been repeatedly demonstrated in the literature (Chapter 1). Among this body of evidence, the achievement of about 4.5-5.0 log reductions of endospores in perishable matrices like apple and carrot juice subjected to HS (25-100 MPa, up to 60 days) particularly stands out (Pinto et al., 2018, 2019) (Table 2). In fact, the well-known pressure resistance of *Alicyclobacillus acidoterrestris* and *Bacillus subtilis* endospores (Gänzle et al., 2007) could provide a strong proof of concept for the achievement of pasteurization via HS. This possibility could be of upmost value in the case of fresh milk, which is an industrially relevant food, conventionally obtained by thermal pasteurization of raw milk, and subsequent storage under refrigerated conditions (4 °C) (Lucey et al., 2017; Vasavada, 1988). As well known, despite guaranteeing microbiological safety, this approach is associated not only to milk thermal damage upon pasteurization (Syed et al., 2021), but also to the high environmental impacts of heat treatment and cold storage (James & James, 2010; Swain et al., 2005; Syed et al., 2021).

Despite HS-based milk pasteurization represents a potentially efficacious and sustainable alternative to milk preservation and refrigerated storage, milk pressurization is inherently challenging due to the high pressure-sensitivity of its proteins (Huppertz, Fox, et al., 2006). In particular, casein micelles disintegration has been often observed at pressure higher than ~ 250-300 MPa, due to solubilization of colloidal calcium phosphate, ultimately resulting in milk clotting (Anema, Lowe, et al., 2005;

Huppertz et al., 2002, 2004; Huppertz, Fox, et al., 2006; Kiełczewska et al., 2020; Needs, Capellas, et al., 2000). Nevertheless, this effect was not detected when pressure was applied in the HS range (Huppertz et al., 2004). Although circumstantial, this evidence suggests that HS might be applied to milk without inducing clotting phenomena. Nevertheless, the effects of prolonged pressurizations (*e.g.*, days/weeks) on raw milk and, in particular, on casein micelle structure, are unknown.

The objective of this Paragraph was to investigate the potentiality of HS as a non-thermal pasteurization approach for raw skim milk. Preliminary trials were performed to identify the optimal HS pressure for the treatment of raw skim milk. Optimal pressure was defined as the maximum pressure level applicable to raw skim milk without compromising its physical stability for up to 6 days, which is the typical shelf life of refrigerated pasteurized milk (Palmeri et al., 2019). The identified pressure level was then applied to evaluate the capability of HS to allow milk pasteurization. The latter was tested based on the achievement of two specific microbiological criteria within 6 days under pressure: (i) control of the naturally occurring milk microflora, assessed with a durability test, and (ii) achievement of at least 5 log reductions of inoculated *Escherichia coli* and *Staphylococcus aureus*, assessed with a challenge test. These pathogenic bacteria were selected as representative Gram(-) and Gram(+) strains, commonly found in raw milk due to contamination during harvesting and processing (Bartolomeoli et al., 2009; EFSA, 2015). Challenge tests were performed in both raw skim milk and ultra-high-temperature sterilized skim milk, in order to assess the efficacy of HS on pathogens with and without the interference of milk native microflora. Results were compared with the ones obtained in raw skim milk stored under conventional refrigeration (0.1 MPa, 4 °C).

3.1.2 Materials and methods

Samples preparation

Ultra-high-temperature sterilized (UHT), and raw skim milk were obtained at a local food retailer and a local milk processing plant, respectively. For the inoculum, bacteria suspensions containing *Escherichia coli* 8048 and *Staphylococcus aureus* 226 were prepared. Strains were maintained at -80 °C in Brain Heart Infusion broth (BHI, Oxoid, Milan, Italy) with 30% sterile glycerol as cryoprotectant until use. From stock cultures, the strains were plated on BHI culture media, and incubated at 37 °C for 24 h. The inoculations were carried out by suspending plated pure cultures of each microorganism in 5 mL of BHI at 37 °C for 24 h. Subsequently, the cells were collected by centrifugation at 14,170 × *g* for 10 min at 4 °C (Beckman, Avanti TM J-25, Palo Alto, CA, USA)

and washed three times with Maximum Recovery Diluent (MRD, Oxoid, Milan, Italy). The final pellet was suspended in MRD. An aliquot of the bacteria suspension was added to approximately 50 mL UHT milk or raw milk to obtain a final concentration of 10^5 - 10^6 CFU mL^{-1}. Milk samples were then poured in poly-propylene/ethylene-vinyl-alcohol/poly-ethylene pouches (Niederwieser Group S.p.A., Campogalliano, Italy), and heat-sealed with headspace not exceeding 5% of samples volume (Orved, VM-16, Musile di Piave, Italy).

Hyperbaric storage

The hyperbaric storage working unit described in Figure 1 (Chapter 1) was used. Packaged samples were introduced in the vessel and pressurized at 150 and 200 MPa at room temperature (20 ± 2 °C). Control samples for microbiological trials were stored under refrigerated conditions (0.1 MPa, 4.0 ± 0.5 °C). At increasing time during storage for up to 6 days, samples were removed from the HS vessel or the refrigerator, and analyzed.

Color

A tristimulus colorimeter (Chromameter-2 Reflectance, Minolta, Osaka, Japan) equipped with a CR-300 measuring head was used to determine milk color. The instrument was standardized against a white tile before analysis. Samples were poured into Petri dishes, positioned on top of the standardization tile and analyzed. Color was expressed in L*, a* and b* scale parameters.

Casein micelles size

Casein micelles size was determined by DLS analysis adapting the method from Segat et al. (2015). Milk samples were diluted 1:100 (v/v) with MilliQ water and inserted into 1 cm optical pathway cuvettes. Particle size was determined at 20 °C by using a dynamic light scattering system (NanoSizer 3000, Malvern Instruments, Malvern, UK) equipped with a Peltier temperature control system. The refractive index was set at 1.333 and the viscosity was approximated to that of pure water at 20 °C. The occurrence of milk clotting was identified by formation of aggregates with size higher than 5 μm.

Microbiological analyses

Decimal dilutions of milk samples were prepared in MRD (Oxoid, Milan, Italy) and plated in specific culture media according to the microorganisms analyzed. TBC was enumerated on Plate Count Agar

(PCA, Oxoid, Milan, Italy) and the plates were incubated at 30 ± 1 °C for 48–72 h; *S. aureus* and C^+S were plated and counted on Baird Parker agar (BP, Oxoid, Milan, Italy) after incubation at 37 ± 1 °C for 24–36 h; *E. coli*, FC and TC were determined on ColiID (bio-Merieux, Grassina, Italia) and the plates were incubated at 37 ± 1 °C for 24 h; LAB were enumerated on Man Rogosa Sharp agar (MRS, Oxoid, Milan, Italy) after incubation at 30 ± 1 °C for 48 h. The results were expressed as logCFU mL^{-1}; the detection of limit (L.o.D.) was 0 logCFU mL^{-1} for *E. coli*, FC and TC, and 1 logCFU mL^{-1} for *S. aureus*, C^+S, TBC, and LAB.

Data analysis

Data of particle size and color were obtained by at least triplicate measurements. These data are reported as mean ± standard deviation and were subjected to one-way analysis of variance (ANOVA) and Tukey's Honest Significant Differences test ($p < 0.05$) using R v. 3.6.1 for Windows (The R foundation for statistical computing). Microbiological analyses were performed in single on samples from two independent experiments and are reported as mean ± standard deviation.

3.1.3 Results and Discussion

Identification of pressure conditions for hyperbaric storage of milk

Preliminary trials were performed to identify the maximum pressure level that could be applied to milk without leading to significant changes in its physical stability within the typical shelf life of refrigerated pasteurized milk (*i.e.*, 6 days) (Palmeri et al., 2019). To this aim, samples were stored at 200 and 150 MPa until milk clotting was detected by DLS as large aggregates (Table 8). Milk showed the presence of a monodispersed (polydispersity index = 0.09 ± 0.04) particle family with 169 nm size, representing casein micelles (de Kruif, 1999). Under HS at 200 MPa, two distinct phenomena were observed (Table 8): a progressive increase in casein micelles size and the appearance of a novel family of smaller particles (about 50 nm). The latter became evident after 30 min-HS and was associated to sub-micellar particles, which occurred as a consequence of pressure-induced micelle fragmentation and reassociation (Gebhardt et al., 2006). After 1.5 h of HS, casein micelles aggregated to form large particles exceeding 5 μm in size, indicating the onset of clotting. When HS was performed at 150 MPa, the increase in casein micelle size and their fragmentation occurred at a much slower rate. In particular, sub-micellar particles became detectable only after 2 days (Table 8).

Table 8: Size and content of casein micelles and sub-micellar particles in raw skim milk during storage for increasing time under hyperbaric conditions (150 and 200 MPa, 20 ± 2 °C).

Pressure	Time	Micelles		Sub-micellar particles		Aggregates	
		size	Intensity	size	Intensity	size	Intensity
(MPa)	(h)	(nm)	(%)	(nm)	(%)	(nm)	(%)
0	0	169.1 ± 2.6[g]	100.0 ± 0.0[a]	-	-	-	-
150	0.5	173.2 ± 2.3[g]	100.0 ± 0.0[a]	-	-	-	-
	1	170.9 ± 2.8[g]	100.0 ± 0.0[a]	-	-	-	-
	2	167.1 ± 4.6[g]	100.0 ± 0.0[a]	-	-	-	-
	3	172.5 ± 5.0[g]	100.0 ± 0.0[a]	-	-	-	-
	15	217.1 ± 5.2[e]	100.0 ± 0.0[a]	-	-	-	-
	18	223.1 ± 4.1[e]	100.0 ± 0.0[a]	-	-	-	-
	24	237.0 ± 4.0[d]	100.0 ± 0.0[a]	-	-	-	-
	48	275.8 ± 7.9[b]	96.7 ± 3.1[a]	52.1 ± 8.0[a]	6.5 ± 1.4[ab]	-	-
	120	377.9 ± 11.0[a]	96.5 ± 3.3[a]	51.1 ± 2.8[a]	5.9 ± 0.9[ab]	-	-
	144	371.1 ± 8.1[a]	99.8 ± 0.5[a]	-	-	5280.0 ± 396.0[a]	2.0 ± 0.8[a]
200	0.17	175.4 ± 3.1[fg]	100.0 ± 0.0[a]	-	-	-	-
	0.33	186.8 ± 3.2[f]	100.0 ± 0.0[a]	-	-	-	-
	0.5	212.6 ± 4.9[c]	97.2 ± 0.2[a]	46.0 ± 2.2[a]	2.8 ± 0.2[b]	-	-
	1	248.5 ± 6.2[cd]	92.7 ± 0.5[ab]	58.4 ± 2.8[a]	7.3 ± 0.5[ab]	-	-
	1.5	256.3 ± 11.8[c]	90.9 ± 2.5[b]	52.6 ± 4.7[a]	9.1 ± 2.6[a]	5344.5 ± 304.8[a]	1.7 ± 0.8[a]

- : not detectable; [a] Different letters indicate significantly different means (ANOVA; $p < 0.05$) in the same column.

As casein better tolerated less intensive HS, milk clotting was detected only after 6 days. It is worth noting that, when milk clotted, casein micelles were significantly larger (370 nm) if milk was stored at 150 MPa rather than at 200 MPa (250 nm). This indicates that milk clotting was not the result of micelle enlargement solely. In fact, many Authors reported that pressure-induced clotting primarily occurs due to aggregation of sub-micellar particles, whereas an increased micelle size is mainly attributable to interactions between micelles and pressure-unfolded whey proteins (Anema, Lowe, et al., 2005; Huppertz et al., 2004; Huppertz & de Kruif, 2007; Needs, Capellas, et al., 2000; Needs, Stenning, et al., 2000).

Independently on storage conditions, no changes in luminosity were observed in all samples (data not shown), indicating that casein micelle modifications (Table 8) did not affect the optical properties of milk colloidal system. The effects of 150 MPa-HS on milk appearance were also evaluated by assessing color parameters a* (redness) and b* (yellowness) (Figure 6). A very slight but statistically significant ($p < 0.05$) increase in milk redness and yellowness was progressively detected during HS (Figure 6). Although not visually perceivable to the naked eye, this minor color change could be attributed to pressure-triggered non-enzymatic browning. Reportedly, the early condensation steps of the Maillard reaction can be favored by pressure since, in some cases, they can be characterized by a negative activation volume (Hill et al., 1996; Isaacs & Coulson, 1996).

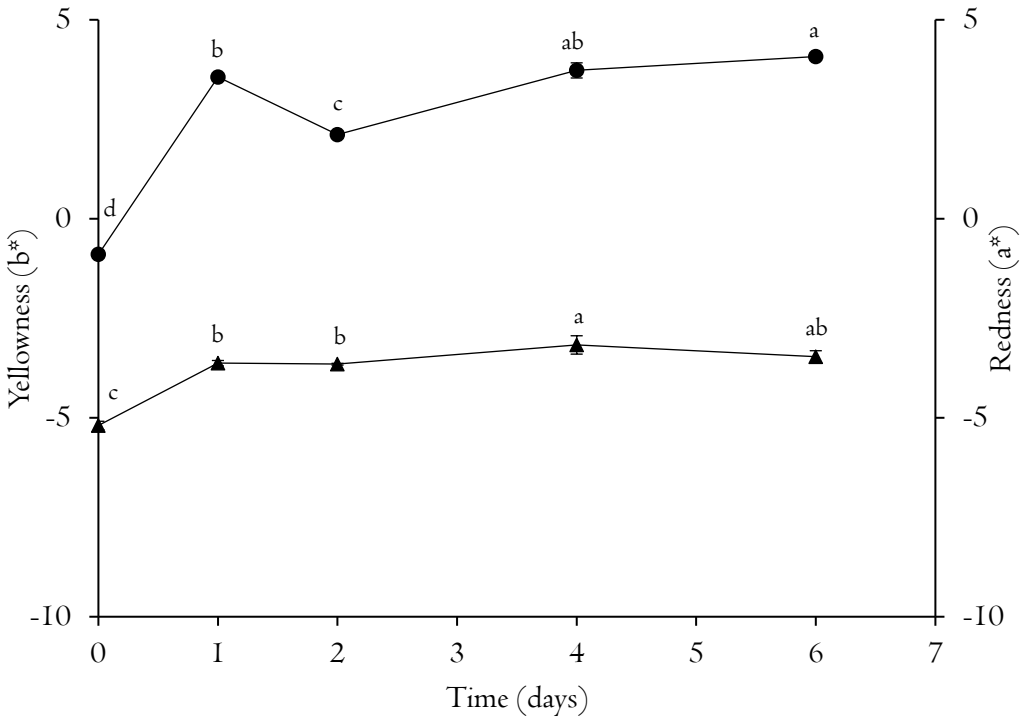

Figure 6: Redness (a*, ●) and yellowness (b*, ▲) of raw skim milk stored for up to 6 days under hyperbaric conditions (150 MPa, 20 ± 2 °C); [a] Different letters for the same color parameter indicate significantly different means (ANOVA; $p < 0.05$).

Based on these results, milk physical stability could be guaranteed for up to 6 days by storing it at pressure as high as 150 MPa. The latter was thus deemed as the optimal pressure level for milk HS, and further experiments were conducted by applying these conditions.

Milk pasteurization by hyperbaric storage

Since milk is not an inherently sterile matrix, a durability test was firstly performed to assess the effect of HS on the naturally occurring microflora. To this aim, total bacteria count (TBC), lactic acid bacteria (LAB), coagulase-positive *Staphylococci* (C^+S), fecal coliforms (FC) and total coliforms (TC) microbiological quality indexes were considered. The latter were followed during pressurized storage for up to 6 days, using refrigerated milk as reference (Table 9).

In fresh raw milk, the value of all the considered indexes was relatively high, ranging from about 2 to circa 4 logCFU mL^{-1} (Table 9). The detection of FC and C^+S indicated the potential occurrence of dangerous microorganisms, such as *E. coli* and *S. aureus*. During refrigerated storage for up to 6 days, all the microbial indexes progressively increased with the only exception of C^+S, which remained relatively stable (Table 9). In particular, TBC and FC grew by more than 2 logCFU mL^{-1} after 6 days, whereas LAB and TC increased by less than 1 log unit.

Table 9: Total bacteria (TBC), lactic acid bacteria (LAB), coagulase-positive *Staphylococci* (C^+S), fecal coliforms (FC) and total coliforms (TC) counts in raw skim milk stored for up to 6 days under refrigerated (0.1 MPa, 4.0 ± 0.5 °C) and hyperbaric conditions (150 MPa, 20 ± 2 °C). Results are expressed as logCFU mL^{-1}.

Storage	Time (days)	TBC	LAB	C^+S	FC	TC
Fresh	0	3.89 ± 0.16	3.44 ± 0.42	2.91 ± 0.28	2.38 ± 0.03	2.70 ± 0.22
Refrigerated	1	3.85 ± 0.15	3.82 ± 0.03	2.95 ± 0.12	2.13 ± 0.29	2.66 ± 0.17
	2	3.88 ± 0.07	3.43 ± 0.28	2.57 ± 0.03	2.22 ± 0.01	2.50 ± 0.11
	4	3.80 ± 0.03	3.41 ± 0.52	3.11 ± 0.05	2.72 ± 0.17	2.88 ± 0.08
	6	5.98 ± 0.09	4.12 ± 1.08	2.51 ± 0.22	4.69 ± 0.44	3.56 ± 0.16
Hyperbaric	1	3.41 ± 0.38	3.59 ± 0.05	2.41 ± 0.57	< L.o.D.**	1.70 ± 0.29
	2	3.41 ± 0.30	2.99 ± 0.50	2.10 ± 0.45	< L.o.D.**	< L.o.D.**
	4	2.95 ± 0.31	2.29 ± 0.25	1.95 ± 0.24	< L.o.D.**	< L.o.D.**
	6	< L.o.D.*	< L.o.D.*	< L.o.D.*	< L.o.D.**	< L.o.D.**

*L.o.D.: 1 logCFU mL^{-1}

** L.o.D.: 0 logCFU mL^{-1}

These results are in agreement with the well-known weak bacteriostatic capacity of refrigeration in raw milk (Griffiths et al., 1987), potentially allowing the development of pathogens. On the contrary, HS

at 150 MPa caused the reduction of all microorganisms below the detection limit (Table 9). In particular, FC and TC were inactivated within 1 and 2 days, respectively. Differently, the Gram(+) species comprising C^+S and LAB better withstood pressurized conditions and, similarly to TBC, were reduced below the detection limit only after 6 days-HS. Based on these results, the efficacy of HS in inactivating pathogens was assessed with a challenge test. To this aim, counts of milk spiked with *E. coli* and *S. aureus* (5-6 logCFU mL^{-1}) pressurized at 150 MPa for up to 6 days were compared to those of analogous samples submitted to refrigeration. Possible interferences provided by the presence of native milk bacteria (Table 9) were made negligible by firstly performing the challenge test using UHT-sterilized skim milk. Results are shown in Table 10.

Table 10: Counts of inoculated *E. coli* and *S. aureus* in UHT skim milk stored for up to 6 days under refrigerated (0.1 MPa, 4.0 ± 0.5 °C) and hyperbaric conditions (150 MPa, 20 ± 2 °C). Results are expressed as logCFU mL^{-1}.

Storage	Time (days)	*E. coli*	*S. aureus*
Fresh	0	5.49 ± 0.13	5.33 ± 0.08
Refrigerated	1	5.49 ± 0.16	5.32 ± 0.09
	2	5.56 ± 0.11	5.38 ± 0.00
	4	5.55 ± 0.24	5.29 ± 0.05
	6	5.25 ± 0.09	5.19 ± 0.02
Hyperbaric	1	1.47 ± 0.18	4.94 ± 0.08
	2	< L.o.D.*	4.13 ± 0.18
	4	< L.o.D.*	2.43 ± 0.19
	6	< L.o.D.*	< L.o.D.**

*L.o.D.: 0 logCFU mL^{-1}

** L.o.D.: 1 logCFU mL^{-1}

The application of refrigerated conditions did not affect the load of the inoculated microorganisms, which remained unchanged during the 6 days-storage (Table 10). Oppositely, HS progressively reduced both *E. coli* and *S. aureus* loads below the detection limit. The complete inactivation of *S. aureus* required the application of 150 MPa for 6 days, whereas *E. coli* was undetectable in milk samples after just 2 days (Table 10). It is likely that the remarkably higher resistance of Gram(+) bacteria to pressure, which is due to their thick peptidoglycan cell wall layer, allowed *S. aureus* to better withstand HS

conditions as compared to *E. coli* (Wuytack et al., 2002). Similar results were previously observed during HS of watermelon juice spiked with *E. coli* and *L. innocua* (Pinto et al., 2017).

With the aim of validating the encouraging results obtained with UHT-sterilized milk, the challenge test was repeated on raw skim milk. In this case, the presence of native milk microorganisms was evaluated by performing TBC counts concomitantly to *E. coli* and *S. aureus* ones. The results are reported in Table 11.

Similar to what observed for UHT-sterilized skim milk, the application of refrigeration did not induce any variation in the counts of inoculated *E. coli* and *S. aureus* while increased TBC by roughly 1 log unit (Table 11). On the other hand, milk TBC counts decreased during HS, showing a reduction that ranged from about 3 to 5 logCFU mL^{-1}. Moreover, pressurized storage promoted 5 log units-inactivation of both *E. coli* and *S. aureus*, with high similarity with the inactivation efficacy observed in UHT milk (Table 10). It is noteworthy that a 5-log reduction has been suggested as a reasonable criterion by different Authors to assess the potential of non-thermal technologies for milk pasteurization (Alberini et al., 2015; Matak et al., 2005; Mussa & Ramaswamy, 1997; Ruiz-Espinosa et al., 2013; Stratakos et al., 2019).

Table 11: Counts of inoculated *E. coli* and *S. aureus*, and relevant TBC (in brackets) in raw skim milk stored for up to 6 days under refrigerated (0.1 MPa, 4.0 ± 0.5 °C) and hyperbaric conditions (150 MPa, 20 ± 2 °C). Results are expressed as logCFU mL^{-1}.

Storage	Time (days)	*E. coli* (TBC)		*S. aureus* (TBC)	
Fresh	0	5.13 ± 0.33	(5.16 ± 0.02)	5.66 ± 0.93	(5.56 ± 0.83)
Refrigerated	1	5.00 ± 0.17	(5.15 ± 0.15)	5.67 ± 1.04	(5.51 ± 0.67)
	2	5.12 ± 0.28	(5.30 ± 0.08)	5.50 ± 0.71	(6.07 ± 1.52)
	4	4.97 ± 0.21	(5.13 ± 0.07)	5.47 ± 0.81	(5.52 ± 0.93)
	6	4.99 ± 0.30	(6.07 ± 0.11)	5.59 ± 0.94	(6.05 ± 0.26)
Hyperbaric	1	2.25 ± 0.25	(3.69 ± 0.04)	5.20 ± 0.92	(5.20 ± 0.85)
	2	< L.o.D.*	(3.02 ± 0.17)	3.83 ± 1.86	(4.28 ± 1.27)
	4	< L.o.D.*	(2.43 ± 0.19)	2.67 ± 1.02	(2.94 ± 0.08)
	6	< L.o.D.*	(<L.o.D.**)	< L.o.D.**	(2.10 ± 0.02)

*L.o.D.: 0 logCFU mL^{-1}

** L.o.D.: 1 logCFU mL^{-1}

Data shown in Tables 10 and 11 clearly evidence that such a criterion can be reached by storing milk at 150 MPa for 6 days. This result demonstrates the potentiality of HS for non-thermal pasteurization of milk.

To evaluate the capability of HS to extend the shelf life of milk after depressurization, inoculated and pressurized raw skim milk samples were further stored under refrigerated conditions for 12 days. During this period, *E. coli* and *S. aureus* remained undetectable, and TBC values did not change (data not shown). This result demonstrates the irreversibility of HS-induced microbial inactivation and highlights the capability of the technology of extending milk microbiological stability for several days after decompression.

3.1.4 Conclusions

The results reported in this Paragraph demonstrate the potentiality of hyperbaric storage (150 MPa for 6 days) as a novel, non-thermal approach for milk pasteurization. HS irreversibly inactivated 5 log units of *E. coli* and *S. aureus* in raw skim milk, allowing to achieve at least two weeks of microbiological safety. Milk HS at 150 MPa for 6 days caused casein enlargement while 1.5 h at 200 MPa was sufficient to induce clotting. These effects clearly indicate that HS might induce remarkable modification in food protein structure. This supports the hypothesis that HS could be used for both the inactivation of enzymes responsible for food spoilage and the improvement of the technological functionality of protein-rich foods (*e.g.*, milk, egg derivatives). These topics are addressed in Paragraph 3.2 and in Chapter 4 of the Thesis, respectively.

In addition, HS induced slight milk browning, which was tentatively attributed to the onset of Maillard reaction. The effect of hyperbaric storage on the kinetics of the Maillard reactions are further investigated in Paragraph 3.3.

3.2 Non-thermal enzymatic stabilization by hyperbaric storage

3.2.1 Introduction

As clear from the substantial body of evidence on the application of HS (Chapter 1), fruit juices are particularly feasible for pressurized storage (Otero, 2019). Due to their very high water activity, fruit juices alteration during storage is mainly due to microbial growth and enzymatic activity (Erkmen & Bozoglu, 2016). In these foods, the activity of catalytic proteins can lead primarily to color changes and loss of cloud stability, due to the development of enzymatic browning and pectin hydrolysis, respectively (Ribeiro et al., 2010) Sporadic and contradictory evidence of enzymatic inactivation under HS conditions (50-200 MPa, 4-15 days) is only available with reference to watermelon and strawberry juice (*e.g.*, polyphenoloxidase, pectinmethylesterase, peroxidase) (Bermejo-Prada, Segovia-Bravo, et al., 2015; Bermejo-Prada & Otero, 2016; Pinto et al., 2017). The irregular or non-linear dependence of enzymatic activity on pressurization intensity and time agrees with abundant literature reporting the highly variable effects of HHP (250-1200 MPa, 5-30 min) on catalytic proteins, primarily due to the structural complexity of the enzymes (Eisenmenger & Reyes-De-Corcuera, 2009; Mozhaev et al., 1996). Such variability could be a serious issue in the HS context, since it would not only impair the inactivation efficacy of the technology but also promote undesired catalytic activity.

The goal of the present work was to study the possibility to use hyperbaric storage to obtain food enzymatic inactivation. The attention was focused on the case of polyphenoloxidase, selected as a study-case enzyme due to its critical role for the quality of plant derivatives like fruit juices (Yoruk & Marshall, 2003). The work was divided in two parts. Initially, a kinetic study of mushroom polyphenoloxidase inactivation by HS at pressure up to 200 MPa was performed in model solutions with different initial enzyme concentration (2-26 U). Following, the results obtained in model systems were validated in apple juice stored at 100 and 200 MPa. During storage for up to 6 days, the juice was analyzed not only for polyphenoloxidase activity but also for color and quality-related microbial indexes (*i.e.*, total bacterial count, lactic acid bacteria and yeasts and molds) to show the industrial relevance of HS in the stabilization of fruit derivatives.

3.2.2 Materials and Methods

Materials

Golden delicious apples were obtained at a local retailer and kept at 4 °C until analysis. 3,4-dihydroxy-

-L-phenylalanine (L-DOPA), dihydrogen- and monohydrogen-potassium phosphate were obtained by J. T. Baker (Teugseweg, Deventer, Netherlands). Mushroom tyrosinase (5771 U mg^{-1}) was obtained by Sigma-Aldrich (Milano, Italy). Plate count agar (PCA), Oxytetracycline Glucose Yeast Extract Agar (OGY), and De Man, Rogosa and Sharpe Agar (MRS) were obtained from Oxoid (Milan, Italy).

Samples preparation

Mushroom (*Agaricus bisporus*) tyrosinase (*i.e.*, polyphenoloxidase) model solutions were prepared by solubilizing increasing amounts of enzyme in pH 7 potassium phosphate buffer with 0.1 M ionic strength. Solutions were frozen and maintained at -30 °C until use to prevent loss of activity (Anese et al., 1994).

Apple juice (dry matter (d.m.) = 11.89 ± 0.05 % (w/w), pH 3.7) was obtained from *Golden delicious* apples as previously described by Manzocco et al., (2009). Briefly, apples were cored and cut into approximately 3 x 3 x 3 cm cubes. Apple cubes were pressed using a domestic juicer (FP800 Kenwood electronic, Havanthants, UK), collecting the juice in a beaker kept in a water ice bath. The obtained juice was clarified by centrifugation at 3,700 × g at 4 °C for 5 min (Avanti J-25, Beckman Inc., Palo Alto, CA, USA).

Appropriate aliquots of PPO solutions (1 mL) or apple juice (10 mL) were packaged inside poly-propylene/ethylene-vinyl-alcohol/poly-ethylene pouches (Niederwieser Group S.p.A., Campogalliano, Italy) and heat-sealed (Orved VM-16, Musile di Piave, Italy) with minimal headspace.

Hyperbaric storage

The hyperbaric storage working unit described in Figure 1 was used. Samples were stored for up to 10 days at 100 and 200 MPa at room temperature (20 ± 2 °C). Control samples were stored at room pressure and temperature conditions (0.1 MPa, 20 ± 2 °C).

Polyphenoloxidase activity

Polyphenoloxidase activity of mushroom PPO solutions and apple juice samples was determined during storage according to Manzocco et al. (2009, 2013b). Briefly, 20 μL of PPO solutions or apple juice were added to 1980 μL of 1.5 mM L-DOPA in 0.10 M potassium phosphate buffer pH 7. Following the addition of the enzyme to L-DOPA, absorbance at 420 nm was determined at increasing time for up to 10 min using a UV-2501 PC spectrophotometer (Shimadzu Kyoto, Japan). Absorbance increase rate (Abs min^{-1}) was calculated by applying a zero-order kinetic model to the absorbance curves within

the first 3 min of assay. Fitting of the kinetic model was deemed acceptable with values of the adjusted determination coefficient (R^2_{adj}) > 0.9. The enzymatic unit (U) was defined as the amount of enzyme capable to induce a 0.001 Abs min^{-1} increase in absorbance at 420 nm in the described testing conditions. Samples residual activity was calculated during storage using Eq. 6.

Eq. 6 $$RA\ (\%) = \frac{A_t}{A_0} * 100$$

Where RA is the residual polyphenoloxidase activity, A_t (Abs min^{-1}) is the polyphenoloxidase activity of the samples stored for a time t (h) and A_0 (Abs min^{-1}) is the activity of the samples before storage.

Kinetic modelling

Zero-, first-, second- and n^{th}-order models were used to fit data. The two-fraction model (Weemaes et al., 1998) was used to fit PPO inactivation curves showing a biphasic behavior during storage (Eq. 7).

Eq. 7 $$RA_t = RA_0^f \cdot exp(-k^f t) + RA_0^s \cdot exp(-k^s t)$$

Where RA_t (%) is the estimated residual polyphenoloxidase activity at storage time t (h), RA_0^f and RA_0^s (%) are the estimated initial polyphenoloxidase activity of the two isozymes, and k^f and k^s (h^{-1}) are the inactivation kinetic rate of the two enzymatic fractions.

First-order kinetic rates (k, h^{-1}) were used to estimate the decimal reduction time under pressure (D_p, h) and pressure sensitivity (z_p, MPa) of PPO according to Manzocco et al. (2016). In particular, D_p was computed using Eq. 8.

Eq. 8 $$D_p = \frac{2.303}{|k|}$$

The decimal logarithm of D_p was then linearly regressed versus storage pressure (*P*), according to the Bigelow model (Eq. 9).

Eq. 9 $$log_{10}(D_p) = \frac{-P}{z_p}$$

Where P is the storage pressure (MPa). z_p was derived as the regression line slope negative reciprocal.

Microbiological analyses

Apple juice samples were appropriately diluted and plated on PCA for total bacteria count (TBC), OGY for yeasts and molds (YM), and MRS agar for lactic acid bacteria (LAB). Plated samples were

incubated at 30 °C, for 24-48 h for TBC and LAB, and for 48-72 h for YM. Analyses were carried out in sterile conditions and microbial counts were expressed as logCFU mL^{-1}.

Color

Apple juice color was determined using a tristimulus colorimeter (Chromameter-2 Reflectance, Minolta, Osaka, Japan) equipped with a CR-300 measuring head and calibrated against a standard tile before use. 4 mL aliquots of apple juice samples were poured into a Petri dish (5 cm diameter, 1 cm height) positioned over the instrument calibration tile. Color measurements were taken onto the juice surface.

Image acquisition

Images (300 dpi vertical and horizontal resolution) were acquired using an image acquisition cabinet (Immagini & Computer, Bareggio, Italy) equipped with a digital camera (EOS 550D, Canon, Milano, Italy) placed on an adjustable stand positioned 45 cm above a black cardboard base. Uniform lighting was guaranteed by 4100 W frosted photographic floodlights.

Statistical analysis

Microbial counts were performed in single on a single experiment. Polyphenoloxidase activity and color measurements were performed at least in duplicate on at least two experiments. Kinetic modelling of PPO residual activity during storage was performed using the Nonlinear Fit function of Origin Pro 2021 (OriginLab, Northampton, MA, USA). Goodness of fit was evaluated based on R^2_{adj} and normalized root-mean-squared error (NRMSE). The latter was calculated by dividing the root-mean-squared error by the highest value on the residual activity curves scale. Data from color measurements were expressed as mean ± standard deviation and were subjected to one-way analysis of variance (ANOVA) and Tukey's Honest Significant Differences test ($p < 0.05$) using R v. 4.2.2 for Windows (The R foundation for statistical computing).

3.2.3 Results and Discussion

Effect of HS on PPO in model systems

buffer was analyzed for enzymatic activity during hyperbaric storage at 100 and 200 MPa at room temperature (Figure 7). An analogous control solution was stored at ambient pressure (0.1 MPa). Independently on pressure, PPO activity progressively decreased during storage in all samples. Many enzymes, including polyphenoloxidase, are known to lose activity when solubilized in aqueous media (Anese et al., 1994; Liu & Cheng, 2000; Rosenthal et al., 2002; Sadana, 1988).

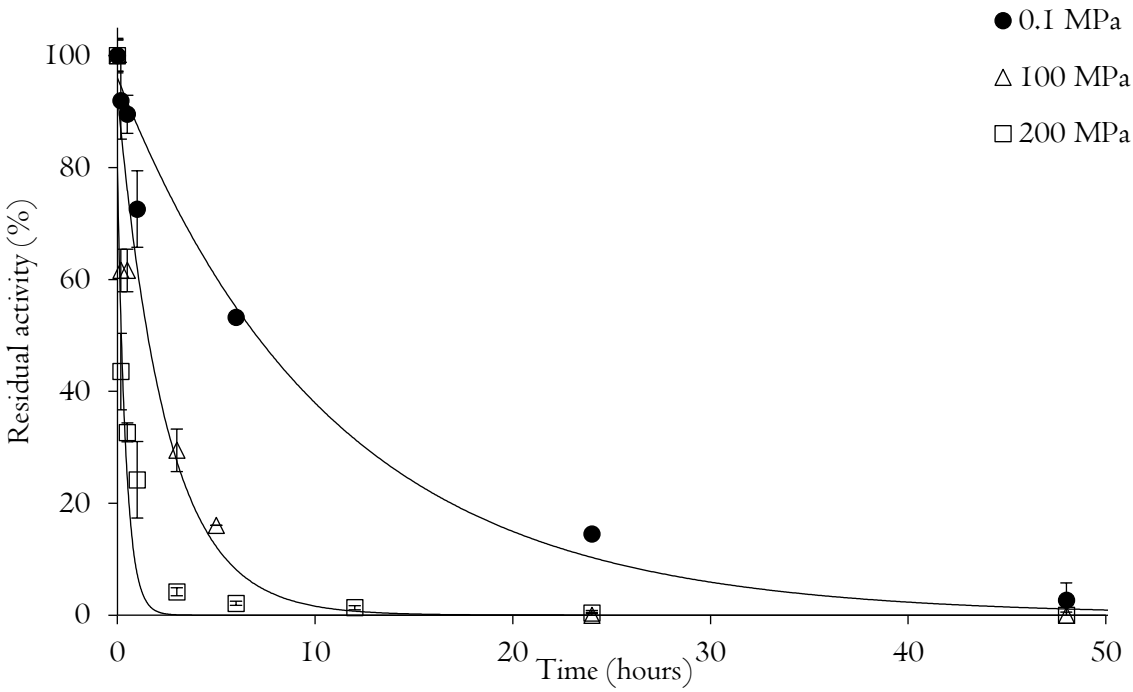

Figure 7: Residual polyphenoloxidase activity of mushroom PPO solution (0.1 M phosphate buffer pH 7) containing 2 U of enzyme during storage at 0.1, 100 and 200 MPa at room temperature (20 ± 2 °C). First-order (__) models fitting activity data are also shown.

In fact, enzyme molecules in diluted aqueous environments are highly mobile and easily undergo structural modifications that hamper their catalytic activity (Zaks & Russell, 1988). In the case of PPO, this decay was made significantly faster by the application of HS. In fact, PPO complete inactivation occurred in 48 h at environmental pressure (control), while only 24 and 12 h were needed when samples were stored at 100 and 200 MPa, respectively. This indicates that the application of pressure during storage promoted PPO inactivation, which spontaneously occurs in diluted solution at environmental

pressure. Samples showing complete loss of polyphenoloxidase activity were further checked for possible reactivation upon refrigeration (4 °C, 0.1 MPa) for up to 4 days. However, no enzyme activity recovery was detected, indicating that PPO inactivation was not only complete but also irreversible.

PPO activity data (Figure 7) were subjected to kinetic elaboration according to zero-, first-, second- and n^{th}-order kinetic equations. The first-order kinetic model well fitted the experimental data and showed the lowest NRSME and the highest R^2_{adj} (data not shown). Based on this result and in agreement with the literature (Henley & Sadana, 1985; Illera et al., 2019; Sadana, 1988), the first order kinetic model was used to estimate PPO inactivation rate during storage (Table 12).

Table 12: First-order inactivation rate ($k \pm$ standard error) and model fitting parameters (NRMSE; R^2_{adj}) of increasing units of polyphenoloxidase in 0.1 M, pH 7 phosphate buffer solution during storage at 0.1, 100 and 200 MPa at room temperature (20 ± 2 °C).

Enzymatic units (U)	Pressure (MPa)	Inactivation rate, k (h^{-1})	NRMSE	R^2_{adj}
2	0.1	0.093 ± 0.007	0.039	0.9920
	100	0.405 ± 0.058	0.078	0.9620
	200	2.395 ± 0.453	0.113	0.9068
6	0.1	0.031 ± 0.002	0.041	0.9875
	200	0.031 ± 0.001	0.024	0.9961
14	0.1	0.019 ± 0.001	0.047	0.9763
	200	0.019 ± 0.001	0.028	0.9936
26	0.1	0.021 ± 0.003	0.109	0.8906
	200	0.013 ± 0.001	0.072	0.9508

Kinetic elaboration confirmed that PPO inactivation rate increased with storage pressure (Table 12). Inactivation rate data were then used to estimate PPO decimal reduction time under pressure (D_p), which was defined as the time (h) required to achieve a 90 % decrease in the enzyme activity. D_p values resulted 23.5, 5.6 and 0.2 h at 0.1, 100 and 200 MPa, respectively. Based on these results, the pressure sensitivity (z_p) of PPO, defined as the pressure increase needed to cause a 90% reduction of D_p, was computed by linear regression of the $\log_{10}(D_p)$ versus pressure ($R^2_{adj} = 0.9088$, $p < 0.05$, NRMSE = 0.019). The obtained z_p was 140.8 MPa, which was comparable with the one reported in the literature

(156.3 MPa) for PPO solutions subjected to brief HHP treatments (750-900 MPa) (Guerrero-Beltrán et al., 2005).

Further tests were performed by hyperbaric storage of model solutions having higher initial polyphenoloxidase activity (Table 12). In particular, samples containing 6, 14 and 26 U polyphenoloxidase were considered. According to the kinetic rates calculated using the first-order model, the increase in initial PPO concentration up to 14 U decreased both inactivation rate and the effect of HS on inactivation itself. This result indicates that enzyme concentration in the solution not only inhibited PPO activity decay, but also made the enzyme pressure resistant (Table 12). This intense stability is likely due to enzyme self-crowding (Helm & Miiller, 1991; Liu & Cheng, 2000; Manzocco et al., 2013b), which limits conformational changes of protein molecules in close proximity with each other (Minton, 2005; Van den Berg et al., 1999). As a consequence, structure-dependent enzymatic inactivation may be significantly hampered (Manzocco et al., 2013b). By further increasing PPO initial concentration to 26 U, enzyme inactivation under hyperbaric conditions became even lower than that observed at environmental pressure (0.1 MPa) (Table 12). This unexpected result might be ascribed to the packing effect of hydrostatic pressure on crowded proteins, which would be forced to come closer to each other, further inhibiting structural changes and enzyme inactivation (Boonyaratanakornkit et al., 2002).

Based on these results, it is reasonable to infer that HS exerts two opposite effects on PPO, depending on the enzyme concentration: i) enzyme inactivation by modification of its structure in diluted environment; ii) enzyme stabilization by forced packing in crowded environment.

Effect of HS in apple juice

Based on the interesting results observed in model systems, the effect of HS on PPO was evaluated in apple juice, taken as an example of a real food matrix affected by the browning action of this enzyme. Microbiological analyses were preliminarily performed to validate the known efficacy of HS in guaranteeing apple juice hygiene (Pinto et al., 2019). In particular, TBC, LAB, and YM were counted in samples stored at 0.1 (control), 100 and 200 MPa.

Expectedly, during storage at room pressure, microbial counts increased from approximately 2 to more than 6 logCFU mL^{-1} within 4 days. At this point, the microbiological trials were interrupted, since samples were considered unacceptable for consumption. On the contrary, HS induced a substantial decrease of apple juice hygienic indicators. In particular, 200 MPa-HS led to the complete and

irreversible inactivation (data not shown) of all the considered microbial indexes within 24 h. These results agree with the bactericidal effect of HS reported in the literature for various foods, including apple, watermelon, and strawberry juices (Fidalgo et al., 2014, 2019; Lemos et al., 2017; Otero & Pérez-Mateos, 2021; Pinto et al., 2019; Segovia-Bravo et al., 2012). Given the antimicrobial efficacy of HS and in agreement with the aims of this work, the attention was focused on the effect of HS on apple juice PPO.

The initial PPO activity in apple juice was 1.76 ± 0.13 U in the tested conditions, equal to 0.76 ± 0.04 U $mg^{-1}_{(d.m.)}$. Figure 8 shows that apple juice PPO activity progressively decreased during storage, reaching the complete inactivation after 2 and 6 days at 100 and 200 MPa, respectively. By contrast, at room pressure, the complete inactivation of PPO was not observed since the experiment was interrupted due to sample microbial spoilage.

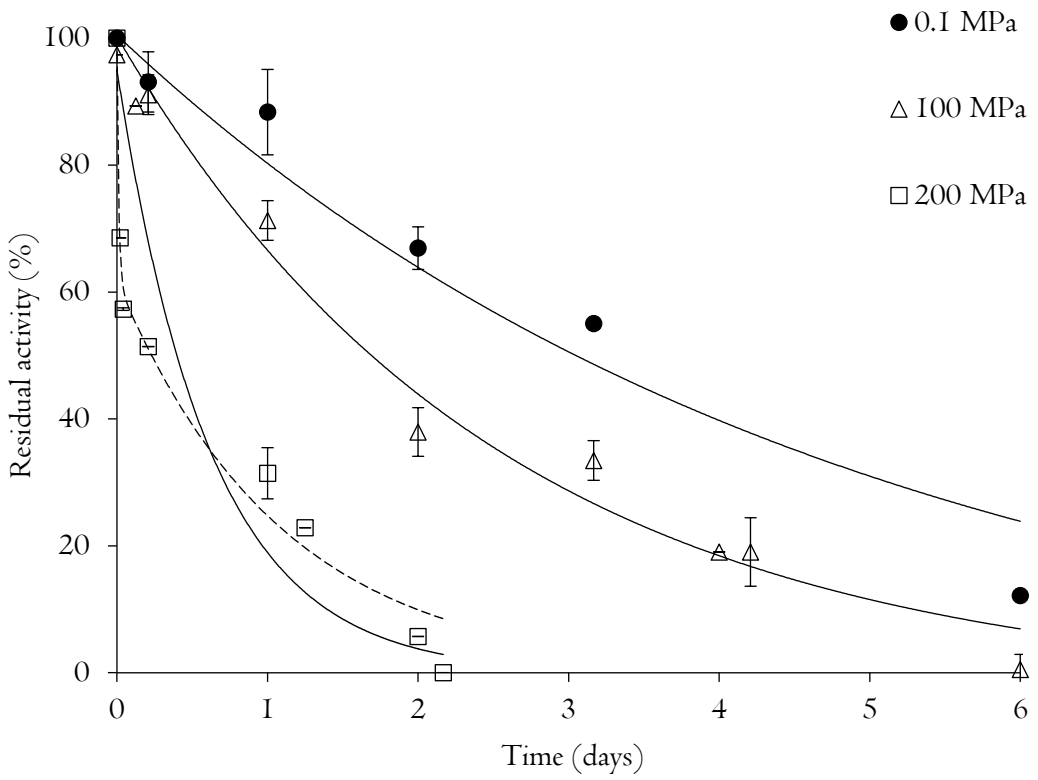

Figure 8: Residual polyphenoloxidase activity of apple juice during storage at 0.1, 100 and 200 MPa at room temperature (20 ± 2 °C). First-order (—) and biphasic first-order (----) models fitting activity data are also shown.

Data shown in Figure 8 were further elaborated according to a first-order kinetic model (Table 13). Kinetic elaboration confirmed the faster inactivation of PPO under 100 and 200 MPa-HS as compared to control conditions, and yielded a z_p value equal to 227.3 MPa ($R^2_{adj} = 0.9429$, $p < 0.05$), indicating apple PPO to be less pressure-sensitive than the mushroom one (140.8 MPa).

Table 13: First-order inactivation rate ($k \pm$ standard error) and model fitting parameters (NRMSE; R^2_{adj}) of polyphenoloxidase in apple juice during storage at 0.1, 100 and 200 MPa at room temperature (20 ± 2 °C).

Pressure (MPa)	Inactivation rate, k (h^{-1})	NRMSE	R^2_{adj}
0.1	0.009 ± 0.001	0.079	0.9313
100	0.016 ± 0.001	0.061	0.9725
200	0.067 ± 0.018	0.174	0.7147

This could be attributed to the different enzyme structures and to the presence in apple juice of sugars, salts, polysaccharides, and other proteins. Such components are likely to have stabilized the conformation of apple juice PPO by allowing a larger number of interactions with the close environment (Weemaes et al., 1998).

It must be highlighted that, as indicated by the fitting parameters ($R^2_{adj} = 0.7147$, Table 13), the first-order model was less efficacious in describing PPO inactivation data obtained at 200 MPa than those relevant to storage at 0.1 and 100 MPa ($R^2_{adj} > 0.93$). In fact, PPO decay at 200 MPa (Figure 8) clearly showed a discontinuity point at about 1 h storage, suggesting a biphasic inactivation trend at these pressure conditions. This might be attributed to the presence in apple juice of at least two fractions of PPO isozymes with different pressure sensitivity. Data fitting was thus performed using a biphasic first-order model ($R^2_{adj} = 0.9727$; NRMSE = 0.053). The latter is also known as the two-fraction model (Eq. 7) and is often applied to describe heat- or pressure-induced enzymatic inactivation (Illera et al., 2019; Weemaes et al., 1998). In particular, the model accounts for the coexistence of isozymes by grouping them into two fractions: a labile one, which was fast inactivated, and a stable one, whose activity was longer retained (Illera et al., 2019). k_f and k_s account for the inactivation rates of the two isozymes fractions, and resulted equal to 3.458 ± 1.623 and 0.038 ± 0.004 h^{-1}, respectively. This clearly indicated a difference in the pressure stability between apple PPO fractions. Based on the

value of RA_0^f, the relative abundance of the pressure sensitive PPO fraction was estimated to be about 40% of the overall apple PPO. In accordance with the inactivation effect of HS on apple PPO (Figure 8, Table 13), pressurized storage allowed to better maintain the visual appearance of the juice (Table 14).

Table 14: Visual appearance, luminosity (L*), redness (a*) and yellowness (b*) of apple juice during storage at 0.1 and 200 MPa at room temperature (20 ± 2 °C).

Pressure	Time (days)	Visual appearance	L*	a*	b*
0.1 MPa	0		67.12 ± 0.84[a]	1.13 ± 0.14[c]	22.61 ± 0.57[d]
	1		53.87 ± 1.86[c]	2.78 ± 0.53[b]	30.49 ± 0.58[ab]
	2		47.71 ± 1.63[d]	6.06 ± 0.88[a]	30.26 ± 2.23[ab]
	3		42.06 ± 0.88[de]	7.27 ± 0.23[a]	26.77 ± 0.81[c]
	6	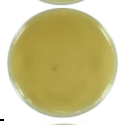	39.29 ± 1.12[e]	6.39 ± 0.06[a]	22.83 ± 1.19[d]
200 MPa	1		63.18 ± 2.59[b]	N.D.	N.D.
	2		53.76 ± 1.45[c]	2.49 ± 0.35[b]	30.89 ± 0.38[ab]
	3		53.57 ± 1.62[c]	2.95 ± 0.27[b]	32.26 ± 0.75[a]
	6		53.82 ± 0.61[c]	2.63 ± 0.08[b]	32.10 ± 0.16[a]

[a] Different letters for the same color parameter indicate significantly different means (ANOVA; $p < 0.05$).

N.D. Not determined

In particular, storage at 200 MPa significantly limited the decrease in luminosity and the increase in redness ($p < 0.05$), which are typically associated with the formation of brown polymers upon PPO-catalyzed oxidation of phenols (Bermejo-Prada & Otero, 2016). Differently, the application of pressurized storage caused apple juice yellowness to increase significantly more than under room pressure conditions. This result apparently contradicts the observed decrease in PPO activity during pressurized storage. Nevertheless, the increase in yellowness was likely due to disruption of apple cells organelles (*e.g.*, plastids, chromoplasts) upon pressurization with release of yellow pigments (*e.g.*, lutein, zeaxanthin) in the juice (Gonzalez & Barrett, 2010; Saini et al., 2015) and potential increase of its overall appeal to consumers.

3.2.4 Conclusions

Hyperbaric storage was shown to accelerate the spontaneous inactivation of polyphenoloxidase in aqueous model systems and apple juice. The inactivating effect of HS on PPO depends on enzyme nature and concentration, and primarily relies on protein conformational modifications favored by pressure. The results acquired by subjecting apple juice to HS clearly indicate that the technology can contemporarily guarantee food microbiological growth and prevent enzymatic browning, suggesting its potential use in the stabilization of many other fresh foods.

The observed effect of HS on enzymes confirms the capability of the technology to modify protein structure (Paragraph 3.1) and further supports the hypothesis that HS could be used to steer protein technological functionality (Chapter 4).

It is due noting that food color alteration during storage does not depend on the activity of catalytic proteins solely. The development of Maillard reaction is actually regarded as a major source of spoilage in many foods stored at room temperature, thus having remarkable relevance in the HS context. For this reason, the effect of HS on the kinetics of Maillard reaction is examined in the following Paragraph (3.3).

3.3 Effect of hyperbaric storage on Maillard reaction kinetics

3.3.1 Introduction

The knowledge about the effect of HS on the development of alterative chemical events is still limited. Information is only available regarding lipid peroxidation in raw meat and fish, oxidative color fading in fruit juices, and production of unpleasant volatiles in meat and strawberry juice (Bermejo-Prada, Vega, et al., 2015; Bermejo-Prada & Otero, 2016; Fidalgo et al., 2018; Pinto et al., 2017; Santos, Matos, et al., 2021). No literature evidence is however available regarding the effect of HS on the development of the Maillard reaction, despite this event might be a major source of alteration during food storage (Van Boekel, 2001, 2008). Since Maillard browning is characterized by positive $\Delta V^{\neq}$ (Chapter 1), the reaction should be always hampered by pressure, with kinetics described by the Eyring equation (Eq. 2).

The kinetics of Maillard reaction under pressure could be influenced by many factors, with temperature and pH playing a pivotal role (Lund & Ray, 2017). The effect of these parameters is only known at room pressure or upon brief HHP treatments (Martins & Van Boekel, 2005; Van Boekel, 2008). In particular, the reaction is well known to be boosted by alkaline pH. Similarly, the accelerating effect of temperature on the reaction rate is widely recognized and typically described by the Arrhenius equation (Arrhenius, 1901; Martins & Van Boekel, 2005; Van Boekel, 2001). The possibility to predict the combined effect of pressure and temperature on the development of Maillard reaction is still to be demonstrated. Some Authors have proposed a model based on the Arrhenius and Eyring equations to describe the development of phenomena other than non-enzymatic browning (e.g., starch swelling and oxidative reactions) during brief HHP treatments (up to 900 MPa, 20-130 °C) (Ahromrit et al., 2007; Huang et al., 2019; Verbeyst et al., 2010, 2011). This approach could be scientifically sound to study also the combined effects of pressure and temperature on Maillard browning kinetics during HS.

The aim of the work reported in this Paragraph was to study the effect of HS on the kinetics of Maillard reaction. In particular, glucose-glycine solutions, with pH adjusted to 6 and 8 to simulate perishable foods, were considered. Samples were subjected to 0.1, 15, 50 and 100 MPa for up to 96 h at 43, 53 and 63 °C. At increasing time during HS, Maillard intermediates and melanoidins (abs at 294 and 420 nm) were measured, and the reaction rates were estimated according to the first-order kinetic model. The dependence of reaction rates on temperature and pressure was described using a

combined model based on Arrhenius and Eyring equations. The reliability of the model was then validated by using external data.

3.3.2 Materials and Methods

Samples preparation

Glucose-glycine model solutions were obtained by dissolving 1.71 M D-glucose monohydrate (Labchem, Lisbon, Portugal) and 2.05 M glycine (Biochem Chemopharma, Cosne-Cours-sur-Loire, France) in double-distilled water. Complete solubilization was ensured by vigorous stirring at room temperature for up to 1 h. Solutions were divided into two aliquots whose pH was adjusted at 6 and 8 by addition of 1 M NaOH or HCl. Aliquots of 1 mL of each solution were then introduced in 5 x 3 cm poly-amide/poly-ethylene plastic pouches and heat-sealed with minimum headspace using a SK heat-sealing bar (Albipack, Águeda, Portugal).

Hyperbaric storage

Samples were subjected to pressurized storage (0.1 - 200 MPa) for up to 88 days at different temperatures (20 - 63 °C). Depending on the temperature applied during hyperbaric storage, different working units were used, as described below. In all cases, a 60:40 (v/v) mixture of propylene glycol (96% propylene glycol and 4% of inhibitors and water, Dowcal N fluid, Dow Chemical) and tap water was used as pressurizing fluid.

For storage at 20 °C, the hyperbaric storage working unit described in Figure 1 was used to store samples at 20 ± 2 °C at 200 MPa for up to 88 days.

Storage trials at 25 °C were performed using a SFP FPG13900 hyperbaric storage experimental equipment (Stansted Fluid Power, Stansted, UK) with three independent 0.4 L steel vessels. Samples were stored at 20, 30 and 40 MPa for up to 14 days at 25 ± 2 °C. Pressure was generated inside the vessels using the integrated pneumatic pressure multiplier of the equipment coupled with a DPC10QTC (capacity = 9.4 L, maximum pressure = 12 bar, engine power = 1.5 cv) air compressor (DeWalt, Baltimore (MD), U.S.A.).

Pressurized storage at 43, 53 and 63 °C was performed using an U33 high-pressure system (Unipress Equipment Division, Institute of High Pressure Physics, Warsaw, Poland) equipped with a 0.1 L jacket-thermostated pressure vessel. For each temperature tested, samples were maintained at 0.1, 15, 50 and 100 MPa for up to 96 h. In this case, the 60:40 (v/v) propylene glycol:water mixture employed

as pressurizing fluid was also used to control the temperature in the vessel thermostating jacket. The fluid was heated and circulated in the vessel jacket by a FA 90 thermostatic bath (FALC Instruments, Treviglio, Italy).

Absorbance readings

At increasing time during hyperbaric storage, the working units were depressurized and samples were collected from the pressure vessels. Samples stored at 43, 53 and 63 °C were cooled with fresh running tap water and conditioned for at least 30 min at 4 °C. Samples absorbance at 294 and 420 nm was read at 25 °C in UV-grade microplates using a Multiskan Go microplate spectrophotometer (Thermo Scientific, Waltham, EUA). Samples showing absorbance values higher than 0.7 were appropriately diluted in double-distilled water to reach absorbance values in scale.

Kinetic modelling

Kinetic modelling was performed adapting the procedure used by Huang et al. (2019). The increase in sample absorbance (A) at 294 and 420 nm as a function of storage time (t, h) at increasing pressure (0.1 - 200 MPa) and temperature (20 - 63 °C) was fitted with a first-order model (Eq. 10).

Eq. 10 $\ln A/A_0 = k * t$

Where A_0 is the sample absorbance at $t = 0$ h and k is the kinetic rate constant (h^{-1}). The dependence of k on storage temperature (T, K) was modelled in the 43 - 63 °C temperature range using the reparametrized Arrhenius equation (Eq. 11).

Eq. 11 $\ln(k) = -\frac{E_a}{R}\left(\frac{1}{T} - \frac{1}{T_{ref}}\right) + \ln k_{T_{ref}}$

Where E_a is the activation energy (kJ mol^{-1}), R is the universal gas constant ($8.314 \cdot 10^{-3}$ kJ K^{-1} mol^{-1}), T_{ref} is the reference temperature, which was selected as the midpoint of the temperature experimental range (53 °C, *i.e.* 326 K), and $k_{T_{ref}}$ is the frequency factor (*i.e.*, kinetic rate at the reference temperature). The average activation energy $\overline{E_a}$ was expressed as mean values ± standard deviation.

The dependence of $k_{T_{ref}}$ on storage pressure (P, MPa) was modeled in the 0.1-100 MPa pressure range using the reparametrized Eyring equation (Eq. 12).

Eq. 12 $\ln k_{T_{ref}} = -\frac{\Delta V^{\neq}_{T_{ref}}}{RT_{ref}}\left(P - P_{ref}\right) + \ln k_{T_{ref};P_{ref}}$

Where $\Delta V^{\neq}_{T_{ref}}$ is the activation volume (mL mol^{-1}) at T_{ref}, P_{ref} is the reference pressure, which was selected as the midpoint of the pressure experimental range (50 MPa), and $k_{T_{ref};P_{ref}}$ is the kinetic rate at T_{ref} and P_{ref}.

The equation predicting the rate of the increase in sample absorbance as a function of the combined changes of temperature and pressure was finally obtained by substituting the logarithm of the frequency factor, $\ln k_{T_{ref}}$ in Eq. 11, thus obtaining Eq. 13.

Eq. 13 $\ln k = -\frac{\overline{E_a}}{R}\left(\frac{1}{T} - \frac{1}{T_{ref}}\right) - \frac{\Delta V^{\neq}_{T_{ref}}}{RT_{ref}}\left(P - P_{ref}\right) + \ln k_{T_{ref};P_{ref}}$

Model validation

The capability of Eq. 13 to predict the kinetic rate (*k*) of the increase in absorbance at 294 and 420 nm of glucose-glycine solutions was validated on external data relevant to analogous samples submitted to hyperbaric storage at 20, 30 and 40 MPa at 25 ± 2 °C (samples with pH 6 and 8), and at 200 MPa at 20 ± 2 °C (only samples with pH 6). These conditions were selected among those typically applied during food hyperbaric storage, focusing on pressure values lower and higher than the ones employed to build the model. Model accuracy was evaluated by linear correlation between the predicted *k* values and the ones that were experimentally obtained in the storage conditions used for validation.

Statistical analysis

Absorbance data were obtained by at least three determinations per sample. Measurements accuracy was evaluated based on the variation coefficient (CV). Data with CV > 5 % were discarded from the dataset. Kinetic modelling based on first-order, Arrhenius and Eyring equations were performed using Origin Pro 2021 (OriginLab, Northampton, MA, USA). Calculated parameters were expressed as estimate ± standard error and goodness of fit was assessed based on the determination coefficient (R^2_{adj}) and root-mean square error (RMSE).

One-way analysis of variance (ANOVA), Tukey's Honest Significant Differences post-hoc test ($p<0.05$) and non-parametric Kendall rank-based correlation test for model validation were performed

using R (v. 4.2.2) for Windows (The R foundation for statistical computing). Goodness of correlation was evaluated based on the coefficient of correlation (r) and the p-value.

3.3.3 Results and Discussion

Maillard kinetics during hyperbaric storage at 43, 53 and 63 °C

Glucose-glycine model solutions with pH 6 and 8 were subjected to hyperbaric storage in a wide range of pressure (0.1, 15, 50 and 100 MPa) and temperature (43, 53 and 63 °C) conditions. At increasing time during storage, sample absorbance at 294 and 420 nm was read to monitor the development of Maillard α-dicarbonyl intermediates and melanoidins, respectively (Nicoli et al., 1991). In agreement with the high Maillard reactivity of glucose-glycine solutions, absorbance at both wavelengths progressively increased in all samples without occurrence of a lag phase (Van Boekel, 2001). As an example, Figure 9 shows the increase in absorbance at 294 (A) and 420 (B) nm during storage at 43 °C of glucose-glycine solution having pH 8. Absorbance data were expressed as logarithmic ratio between the absorbance at a given storage time t (A) and the initial absorbance of the samples (A_0), and fitted with the first-order kinetic model (Eq. 10) (Figure 9).

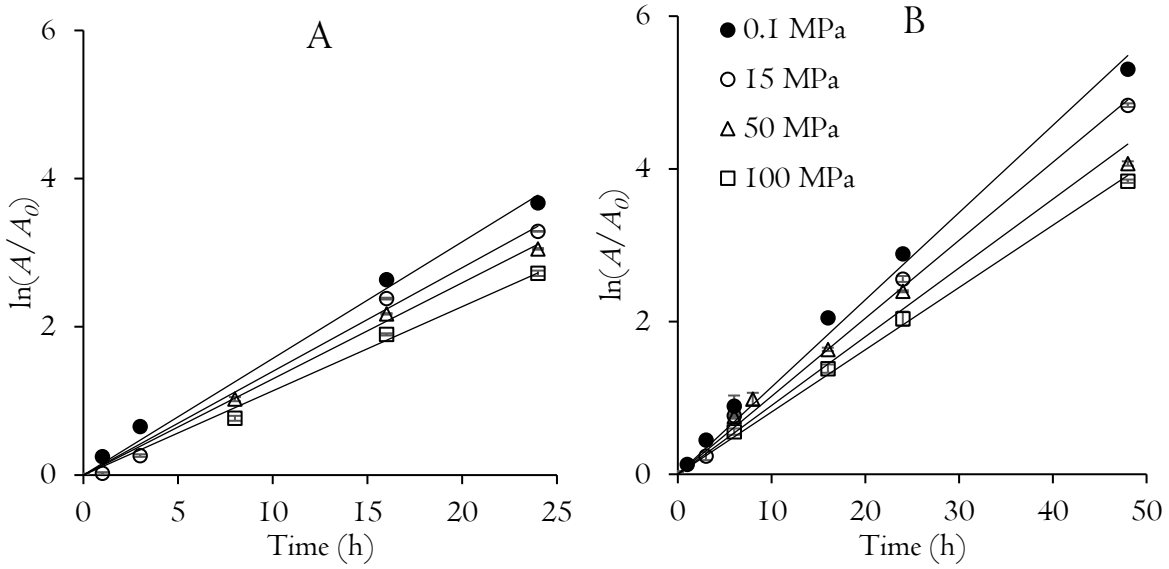

Figure 9: Absorbance at 294 (A) and 420 (B) nm of glucose-glycine solution at pH 8 stored at 43 °C at increasing pressure. Regression lines (__) obtained according to first-order kinetic model are also shown.

From Figure 9, it can be noted that, in agreement with the literature, the first-order model adequately fitted experimental data (Van Boekel, 2001). This equation was thus used to estimate the reaction rate (k, $R^2_{adj} > 0.96$; RMSE < 0.34) in samples having different pH and stored at increasing temperature (43-63 °C) and pressure (0.1-100 MPa) conditions (Table 15).

Table 15: First-order kinetic rates (k) of the increase in absorbance at 294 and 420 nm of glucose-glycine solutions with different pH stored at increasing temperature and pressure.

Wavelength (nm)	Temperature (°C)	Pressure (MPa)	k ± S.E. (h^{-1}) pH 6	pH 8
294	43	0.1	0.094 ± 0.002	0.157 ± 0.002
		15	0.081 ± 0.001	0.140 ± 0.002
		50	0.069 ± 0.004	0.130 ± 0.001
		100	0.056 ± 0.001	0.115 ± 0.002
	53	0.1	0.247 ± 0.002	0.379 ± 0.013
		15	0.214 ± 0.003	0.340 ± 0.009
		50	0.178 ± 0.002	0.317 ± 0.008
		100	0.152 ± 0.002	0.294 ± 0.004
	63	0.1	0.815 ± 0.008	1.255 ± 0.032
		15	0.705 ± 0.002	1.128 ± 0.015
		50	0.592 ± 0.006	1.069 ± 0.020
		100	0.539 ± 0.010	0.933 ± 0.011
420	43	0.1	0.076 ± 0.002	0.114 ± 0.001
		15	0.061 ± 0.001	0.102 ± 0.001
		50	0.053 ± 0.002	0.089 ± 0.002
		100	0.043 ± 0.003	0.082 ± 0.001
	53	0.1	0.179 ± 0.002	0.309 ± 0.010
		15	0.162 ± 0.003	0.260 ± 0.006
		50	0.140 ± 0.002	0.242 ± 0.004
		100	0.112 ± 0.002	0.221 ± 0.008
	63	0.1	0.536 ± 0.011	0.866 ± 0.030
		15	0.468 ± 0.009	0.826 ± 0.005
		50	0.380 ± 0.007	0.727 ± 0.021
		100	0.315 ± 0.002	0.612 ± 0.018

In accordance with the literature, reaction rates of the formation of Maillard intermediates and melanoidins were higher when the sample pH was 8 (Ajandouz & Puigserver, 1999; Ashoor & Zent, 1984; Reyes & Wrolstad, 1982; Van Boekel, 2001). To this regard, Martins & Van Boekel (2005) have demonstrated that the boosting effect of alkaline pH on the Maillard reaction is primarily exerted in the early sugar isomerization step, which is a base-catalyzed reaction. As expected, an increasing trend was observed in reaction rates with increasing storage temperature (Table 15) (Martins et al., 2000). By contrast, at each storage temperature, the increase in pressure caused a decrease in reaction rate (Table 15).

As reported in the literature (Hill et al., 1996, 1999; Isaacs & Coulson, 1996; Martinez-Monteagudo & Saldaña, 2014) hyperbaric conditions can hamper non-enzymatic browning phenomena based on two independent mechanisms. The first one is related to the compression of the reaction environment, which impairs any chemical event associated with a volumetric expansion (Bristow & Isaacs, 1999; Isaacs & Coulson, 1996; Tamaoka et al., 1991). At the present moment, very little is known about which, among the hundreds of events typically occurring during non-enzymatic browning, are the pressure-sensitive ones, able to exert a bottleneck effect on Maillard reaction products. Secondly, pressure-promoted dissociation of weak acid moieties (*e.g.*, aminoacids carboxylic group) has been suggested to cause a local pH decrease. As a consequence, early-stage sugar isomerization would become slower, affecting the rate of all the subsequent Maillard reaction steps (Hill et al., 1996).

Dependence of kinetic rates on temperature

The effect of temperature on the formation rate (k) of Maillard intermediates (294 nm) and melanoidins (420 nm) at different pressure was modelled according to the reparametrized Arrhenius equation (Eq. 11). Results of this elaboration are shown, with reference to pH 6 glucose-glycine systems, in Figure 10.

The reparametrized Arrhenius model well-fitted experimental data ($R^2_{adj} > 0.98$, RMSE < 0.13), allowing to estimate the activation energy (E_a) and the frequency factor $k_{T_{ref}}$ at each storage pressure. As known, E_a indicates the amount of energy required to activate the reaction, and is an indication of temperature dependence of the phenomenon, whereas $k_{T_{ref}}$ represents the frequency of collisions between reactant molecules at the reference temperature T_{ref} (326.15 K, *i.e.* 53 °C) (Piskulich et al., 2019).

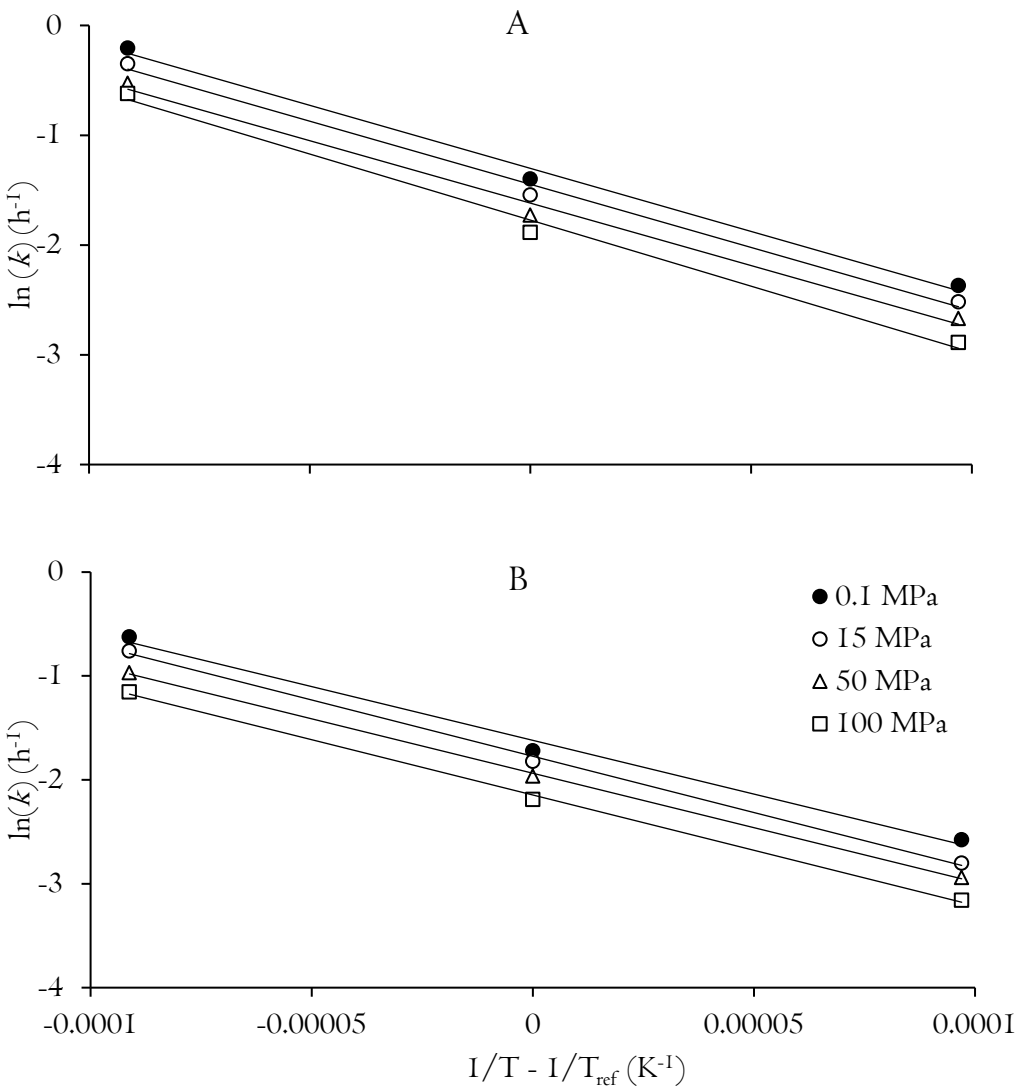

Figure 10: Arrhenius plots of the increase in absorbance at 294 (A) and 420 (B) nm in glucose-glycine solutions with pH 6 stored at increasing temperature (43-53 °C) and pressure (0.1-100 MPa). Regression lines (__) obtained according to reparametrized Arrhenius model are also shown.

The values of the Arrhenius parameters E_a and $k_{T_{ref}}$ were thus estimated for glucose-glycine solutions having pH 6 and 8 (Table 16).

Activation energy values were coherent with those reported by several Authors for the development of Maillard compounds in near-neutral, glucose-glycine model systems at 20-60 °C (*i.e.*, 88-96 kJ mol^{-1}) (Van Boekel, 2001). Almost no effect of pressure was observed on the temperature sensitivity of both

Maillard reaction indicators (absorbance at 294 and 420 nm) in all samples, as indicated by very similar E_a values in the 0.1-100 MPa pressure range (Table 16).

Table 16: Activation energy (E_a), average activation energy ($\overline{E_a}$) and $k_{T_{ref}}$ of the increase in absorbance at 294 and 420 nm in glucose-glycine solutions with pH 6 and 8, stored at increasing temperature (43 - 53 °C) and pressure (0.1 - 100 MPa).

pH	Wavelength (nm)	Pressure (MPa)	E_a ± S.E. (kJ mol^{-1})	$\overline{E_a}$ ± S.D. (kJ mol^{-1})	$k_{T_{ref}}$ ± S.E. (h^{-1})
6	294	0.1	95.53 ± 3.67	96.41 ± 2.40[a]	0.272 ± 0.014
		15	95.57 ± 3.29		0.235 ± 0.011
		50	94.58 ± 0.69		0.198 ± 0.009
		100	99.94 ± 2.28		0.170 ± 0.008
	420	0.1	86.44 ± 6.55	87.97 ± 1.54[c]	0.197 ± 0.008
		15	89.94 ± 4.44		0.170 ± 0.003
		50	87.13 ± 3.16		0.144 ± 0.001
		100	88.37 ± 5.18		0.117 ± 0.002
8	294	0.1	91.55 ± 2.14	92.27 ± 0.62[b]	0.430 ± 0.046
		15	92.01 ± 2.07		0.385 ± 0.036
		50	92.28 ± 2.10		0.361 ± 0.032
		100	92.52 ± 5.56		0.323 ± 0.018
	420	0.1	89.63 ± 0.24	90.89 ± 1.84[bc]	0.319 ± 0.006
		15	92.23 ± 0.72		0.286 ± 0.016
		50	92.69 ± 1.35		0.256 ± 0.007
		100	89.01 ± 3.65		0.227 ± 0.003

[a] Different letters indicate statistically different E_a ($p < 0.05$, ANOVA)

These results were in agreement with circumstantial evidence reporting high pressure (600 MPa) not to affect the activation energy of Maillard browning in glucose-lysine solutions with pH 10.4 maintained at 40 – 60 °C for up to 22 h (Hill et al., 1996). Therefore, it was assumed that, for each indicator and pH, a unique E_a value could be used to model the temperature dependence of the

Maillard reaction, independently on the pressure applied during storage. Average activation energy ($\overline{E_a}$) was thus calculated for the increase in absorbance at 294 or 420 nm of each model solution (Table 16). This allowed also to appreciate the effect of pH on E_a. In particular, by increasing the pH from 6 to 8, the $\overline{E_a}$ of the formation of α-dicarbonyls significantly decreased ($p < 0.05$, ANOVA), whereas no difference was observed in the $\overline{E_a}$ of browning development (Table 16). This was reasonably due to the remarkable pH-dependence of the initial and intermediate steps of the Maillard reaction, as compared to the very low sensitivity to the environmental proton concentration of the advanced stages (Martins & Van Boekel, 2005).

The Arrhenius frequency factor was affected not only by pH but also by the applied pressure, in agreement with the effect of both these variables on *k* values reported in Table 15. In particular, a clear decrease of $k_{T_{ref}}$ was observed by increasing storage pressure (Table 16). From a kinetic point of view, this result suggests that pressurized storage did not affect the temperature sensitivity of Maillard reaction events, but decreased the number of effective collisions among reactants. In agreement with the literature, this indicates that pressure decreased the overall amount of compounds formed during the development of the reaction, without substantially modifying its pathway (Hill et al., 1996; Piskulich et al., 2019).

Based on these results, the dependence of $k_{T_{ref}}$ on pressure was further studied, with the aim of building a modified Arrhenius model predicting the combined effect of changes in temperature and pressure on the rate of the Maillard reaction.

Dependence of pre-exponential factor on pressure

Given the pressure-dependence of the Arrhenius frequency factor, the attention was focused on modelling $k_{T_{ref}}$ values, shown in Table 16, as a function of the pressure applied during storage. In agreement with the literature, the reparametrized Eyring equation (Eq. 12) was used (Huang et al., 2019; Martinez-Monteagudo & Saldaña, 2014). It is interesting to note how a clear parallelism can be found in the physical meaning of Arrhenius and Eyring parameters. In particular, while the Arrhenius E_a quantifies the sensitivity of a phenomenon kinetics on temperature at a given pressure, the activation volume ($\Delta V^{\neq}$, mL mol^{-1}) of the Eyring equation defines the dependence of a phenomenon on pressure at a given temperature (Zamora et al., 2021). To this regard, $\Delta V^{\neq}$ can be also intended as a mathematical representation of the volume change associated with any given phenomenon (Evans &

Polanyi, 1935). In fact, it is well known that phenomena favored by pressure have a negative $\Delta V^{\neq}$ and *vice-versa* (Chapter 1). Also, the Arrhenius parameter $k_{T_{ref}}$ has a physical meaning analogous to the one of the Eyring parameter $k_{P_{ref}}$, which identifies the number of effective collisions among reactants at the selected reference pressure. In the present work, the Eyring frequency factor is referred to reference temperature and pressure conditions (53 °C, 50 MPa) and was thus identified as $k_{T_{ref};P_{ref}}$. By modelling $k_{T_{ref}}$ as a function of storage pressure using the Eyring equation, a very high fitting accuracy ($R^2_{adj} > 0.97$; RMSE < 0.09) was obtained, with $\Delta V^{\neq}_{T_{ref}}$ and $k_{T_{ref};P_{ref}}$ estimates reported in Table 17.

Table 17: Activation volume ($\Delta V^{\neq}_{T_{ref}}$) and $k_{T_{ref};P_{ref}}$ of the increase in absorbance at 294 and 420 nm in glucose-glycine solutions with pH 6 and 8, stored at 53 °C (T_{ref}) at increasing pressure (0.1 - 100 MPa).

pH	Wavelength (nm)	$\Delta V^{\neq}_{T_{ref}}$ ± S.E. (mL mol^{-1})	$k_{T_{ref};P_{ref}}$ ± S.E. (h^{-1})
6	294	12.18 ± 2.04	0.21 ± 0.01
	420	13.53 ± 1.27	0.15 ± 0.01
8	294	7.13 ± 1.12	0.36 ± 0.01
	420	8.70 ± 1.04	0.26 ± 0.01

In accordance with the literature about the Maillard reaction in sugar-aminoacid model systems under pressure, the activation volume of α-dicarbonyls and melanoidins formation was around 10 mL mol^{-1} in all samples with small differences (Hill et al., 1996, 1999; Isaacs & Coulson, 1996). Such order of magnitude is typical of chemical reactions that are moderately hampered by the application of pressure (Table 1) (Martinez-Monteagudo & Saldaña, 2014). At the same pH, formation of α-dicarbonyls and melanoidins had almost identical estimated activation volume (Table 17), indicating similar pressure sensitivity of the formation of intermediate- and late-stage Maillard compounds. Activation volume was mostly affected by solutions pH. In particular, in samples with initial pH 6, $\Delta V^{\neq}_{T_{ref}}$ was higher for the increase in absorbance at 294 and 420 nm (Table 17), indicating that the development of Maillard reaction was more pressure-sensitive in acidic environment. According to Hill et al. (1996), this would

be due to the higher pH drop resulting from pressure-induced dissociation of aminoacids carboxylic groups in acidic environments.

Model validation

The combined effect of storage temperature and pressure on the formation of Maillard intermediates and melanoidins in solutions with different pH was predicted by integrating the Arrhenius and Eyring equations (Eq. 13) with parameters reported in Table 16 ($\overline{E_a}$) and 3 ($\Delta V^{\neq}_{T_{ref}}$ and $k_{T_{ref};P_{ref}}$).The reliability of this equation was tested by external validation. To this aim, reaction rates (k) obtained from glucose-glycine solutions with pH 6 and 8, stored at temperature and pressure conditions typical of HS and different from those employed for model development, were used. In particular, samples were stored for up to 19 days at 25 °C, at 20, 30 and 40 MPa, and for up to 88 days at 20 °C, at 200 MPa. Reaction rates predicted by using Eq. 13 were thus compared to the experimental reaction rates by linear correlation (Figure 11).

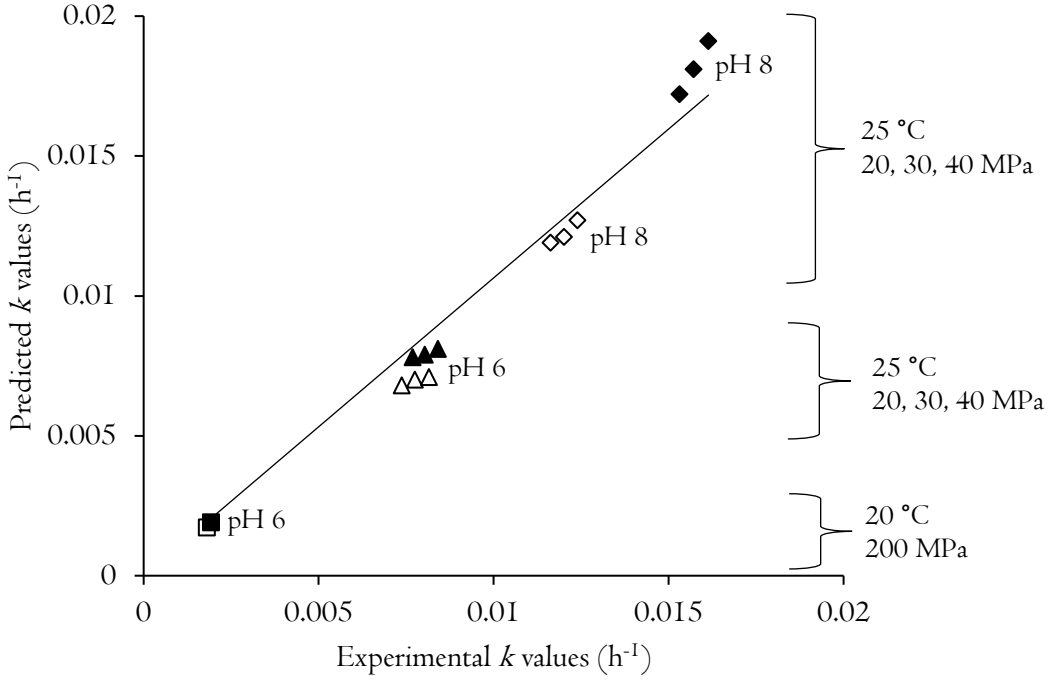

Figure 11: Linear correlation between experimental and predicted (Eq. 13) reaction rates (k) of the increase in absorbance at 294 (black symbols) and 420 (empty symbols) nm in glucose-glycine solutions with different pH and stored at different temperature and pressure.

As clearly visible from Figure 11, and as substantiated by a high correlation coefficient ($r = 0.9341$) and a very low p-value ($p < 0.0001$), the developed model could accurately predict the rate of formation of both intermediates and melanoidins in glucose-glycine systems in all the conditions considered for validation.

3.3.4 Conclusions

In this part of the work, the effect of HS on the development of Maillard intermediates and melanoidins in model systems is studied for the first time. The rate of the reaction depends both on compositional and environmental factors, increasing with solutions pH and storage temperature (43-63 °C), and decreasing with storage pressure (0.1-100 MPa). Kinetic analysis provided information about temperature sensitivity, pressure sensitivity, and frequency factor of the reaction under HS. A model based on the Arrhenius and Eyring equations was thus developed to accurately ($r = 0.9341$) predict the reaction rate at temperature and pressure conditions outside its building range (20-25 °C; 20-40 MPa, 200 MPa).

Based on these results, it is reasonable to infer that hyperbaric storage could be used to control the development of Maillard reaction in foods. In this context, the proposed modelling approach could represent a starting point to develop specific predictive tools. However, it must be highlighted that the structural and compositional complexity of real food could represent a remarkable source of variability, making even harder the prediction of reaction rate during HS. The role of these factors on the development of Maillard reaction during HS is definitely unknown and certainly worthy of future investigations.

Chapter 4: Food functionalization by hyperbaric storage

This fourth Chapter of the Thesis has the objective of studying the possibility of improving food technological functionality of protein-rich foods by hyperbaric storage. The effect of HS on food protein structure and techno-functionality was investigated in three study-cases, selected due to their different protein organization (*i.e.*, raw skim milk, egg white and egg yolk). Since the specific objective of this Part of the Thesis is tackled by the adoption of similar analytical techniques, common "Introduction" and "Materials and Methods" Paragraphs are firstly provided to avoid repetition. For the sake of clarity, the results relevant to each one of the three food matrices are discussed in three consecutive Paragraphs. Finally, differences among the effect of HS in the three matrices are critically discussed in an overall "Conclusions" Paragraph.

4.1 Introduction

The changes induced by pressure in protein structure and techno-functionality strictly depend on the native organization of proteins, which shapes their pressure sensitivity (Balny & Masson, 1993). As reported in Chapter 1, pressurization (200-800 MPa, 1-30 min) of globular proteins generally results in unfolding and networking, due to the promotion of intra- and inter-molecular non-covalent bonds. On the other hand, more complex structures, such as protein-lipid complexes and micelles, typically disintegrate or aggregate under pressure (Fertsch et al., 2003; Gebhardt et al., 2006; Huppertz, Kelly, et al., 2006; Speroni et al., 2005). When different types of protein structures are present in the pressurized matrix, peculiar interactions can also occur, such as the complexation of partially destabilized proteins (Patel & Huppertz, 2014).

In this very complicated framework, the influence of pressurization time has been studied only with reference to brief and intense HHP treatments. In particular, prolonging pressurization time, within HHP time scales, typically exacerbates structural modification and changes in techno-functionality of globular proteins and lipoproteins (Li, Mao, et al., 2018; Naderi et al., 2017; Singh & Ramaswamy, 2013; Van der Plancken et al., 2007). Conversely, pressurization time was reported not to affect the aggregation state of micellar casein (Anema, 2008, 2012; Anema, Stockmann, et al., 2005; Gaucheron et al., 1997; Huppertz et al., 2004). Based on data relevant to HHP treatments, it would be reasonable

to assume that, in the HS context, matrices more prone to techno-functionality changes could be the ones containing primarily globular proteins and protein-lipid complexes, such as egg white and egg yolk. On the other hand, matrices containing micellar proteins, such as milk, would only suffer minor changes. Nevertheless, this hypothesis apparently contradicts with the progressive clotting of milk during HS, as described in Paragraph 3.1. Based on these considerations, the role of HS on protein structure and functionality appears worthy of being studied in more detail.

The attention is here focused on the capability of HS to steer protein structural and techno-functional properties in food. To this aim, the work was organized by focusing on three highly perishable food matrices, namely milk, egg white and egg yolk, which are particularly relevant for their techno-functionality, and characterized by the presence of proteins with considerably different native structure. Paragraph 4.3 is thus dedicated to the study of the effect of HS on raw skim milk proteins. Milk was subjected to the same storage conditions applied in Paragraph 3.1 for HS pasteurization (*i.e.*, 150 MPa), since they were observed to beget protein modification without leading to physical alteration (*i.e.*, clotting). At increasing time for up to 6 days, milk was analysed for whey protein profile and foaming properties, using refrigerated (0.1 MPa, 4.0 ± 0.5 °C) milk as a reference.

The focus of Paragraph 4.4 is on the effect of HS on protein structure and techno-functionality of egg white. Samples were stored at 200 MPa for up to 28 days. The use of HS on egg white was validated from a microbiological standpoint, based on the possibility to achieve inactivation of inoculated *Staphylococcus aureus* and *Salmonella enterica* within 28 days. These bacteria were specifically selected based on their frequent occurrence in egg produce (EFSA, 2014; Le Loir et al., 2003). Following, the effect of HS on the structural (color, particle size and Z-potential, sulfhydryl groups, absorbance at 280, 380 and 680 nm, denaturation temperature, secondary structure) and techno-functional (viscosity, solubility, gelling capacity, and foaming properties) properties of egg white was evaluated. The effects of HS on egg white were compared to those of conventional refrigeration (0.1 MPa, 4.0 ± 0.5 °C).

Analogously to the previous one, Paragraph 4.5 describes the effect of HS on egg yolk. After the antimicrobial efficacy of HS was confirmed, the capability of the technology to preserve egg yolk chemical stability (oxidative status, peroxide value, carotenoid content) was assessed. Similar to the approach adopted in the case of egg white, egg yolk samples were analyzed for protein structure and functionality. Given the specific emulsifying activity of egg yolk, this property was also addressed.

4.2 Materials and Methods

4.2.1 Samples preparation

Raw skim milk was obtained as reported in Paragraph 3.1. Aliquots of 100 mL of milk were poured in poly-ethylene/ethylene-vinyl-alcohol/poly-propylene pouches (Niederwieser Group S.p.A., Campogalliano, Italy), which were heat-sealed with minimal headspace (Orved, VM-16, Musile di Piave, Italy).

Fresh hen (*Gallus gallus domesticus*) eggs were purchased from a local retailer. Egg white and egg yolk were obtained by manual separation. The chalazae were carefully removed and discarded. Egg whites and yolks were gently, manually stirred for 2 min at room temperature to mix the naturally occurring fractions of each matrix (*i.e.*, thick and thin egg white, light-colored and dark-colored egg yolk). Aliquots of 100 mL of milk and 200 mL of egg white or egg yolk were poured inside poly-ethylene/ethylene-vinyl-alcohol/poly-propylene pouches (Niederwieser Group S.p.A., Campogalliano, Italy), which were heat-sealed with headspace not exceeding 5 % of samples volume (Orved, VM-16, Musile di Piave, Italy).

Egg white and egg yolk samples for microbiological analyses were prepared separately. Egg shells were cleaned with hydroalcoholic solution (ethanol 70%) and allowed to air dry for a few minutes before aseptic breaking. The egg white was manually separated from the yolk and chalazae under sterile conditions. The chalazae were discarded. Each egg fraction was collected in sterilized beakers. For the inoculum, bacteria suspensions were prepared using strains of *Salmonella enterica* subsp. *Enterica* 9898 DSMZ and *Staphylococcus aureus* 226. Strains were maintained at -80 °C in Brain Heart Infusion broth (BHI, Oxoid, Milan, Italy) with 30% sterile glycerol as cryoprotectant until use. Strains were incubated in BHI at 37 °C for 24 h, subsequently cultured in 5 mL of BHI at 37 °C for 24 h, and finally collected by centrifugation at 14,170 × g for 10 min at 4 °C (Beckman, Avanti TM J-25, Palo Alto, CA, USA) and washed three times with Maximum Recovery Diluent (MRD, Oxoid, Milan, Italy). The final pellets were suspended in MRD. An adequate aliquot of the bacteria suspension was added to egg white and egg yolk samples to obtain a final concentration of 10^{3-4} CFU g^{-1}. The latter was specifically selected to allow the detection of either an increase or a decrease of microorganisms population using the viable count method (Choi et al., 2019; Pinto et al., 2017). Inoculated egg white and yolk were distributed in 50 g aliquots and packaged as for the other samples.

4.2.2 Hyperbaric storage

The hyperbaric storage working unit described in Figure 1 was used. Raw skim milk was stored at 150 MPa for up to 6 days at 20 ± 2 °C. Egg white and egg yolk samples were stored at 200 MPa for up to 28 days at 20 ± 2 °C. Control samples for all matrices were stored under refrigerated conditions (0.1 MPa, 4.0 ± 0.5 °C). Additional control samples for egg white consisted of in-shell eggs stored at room temperature conditions (20 ± 2 °C, 0.1 MPa). At increasing time during storage for up to 28 days, samples for microbial analyses were removed from the HS vessel or from the refrigerator and analyzed. Other samples were divided in two aliquots. The first one was submitted to analysis within 24 h from depressurization. The second aliquot was removed from the pouches, frozen in thin layer at -30 °C in a shock freezer ("air-o-chill", Electrolux Professional S.p.A., Pordenone, Italy) and freeze-dried (Mini-Fast Edwards, mod. 1700, Edwards Alto Vuoto, Milan, Italy). Freeze dried samples were stored until further analyses in desiccators placed in the dark, at room temperature and at -18 °C for egg white and egg yolk, respectively.

4.2.3 Microbiological analyses

From each pouch, 20 g of egg white or egg yolk sample inoculated with *S. enterica* or *S. aureus*, was diluted (1:5 v/v) in MRD (Oxoid, Milan, Italy). 0.1 mL aliquots of appropriate dilutions were plated onto Plate Count Agar (Oxoid, Milan, Italy) and incubated (37 °C) for 24 h and 36-48 h for *S. enterica* and *S. aureus* counts, respectively. Preliminary trials were carried out on non-inoculated samples to check the *S. enterica* or *S. aureus* presence. For *S. aureus*, 20 g of sample was diluted 1:5 v/v in MRD and 0.1 mL aliquots of appropriate dilutions were plated onto Baird Parker agar (BP, Oxoid, Milan, Italy), incubated (37 °C, 24 h). For *S. enterica*, 25 g of non-inoculated sample were diluted with 225 mL of Buffered Peptone Water (BPW, Oxoid, Milan, Italy), homogenized in a Stomacher for 2 min and incubated at 37 °C for 24 h. A volume of 0.1 mL of sample diluted in BPW was added with 9.9 mL Rappaport Vassiliadis (RV, Oxoid, Milan, Italy) and incubated at (42–43 °C; 18-24 h). Presence/absence of *S. enterica* was checked by spreading onto Xylose-Lysine-Desoxycholate agar (Oxoid, Milan, Italy) and incubated (37 °C, 24 h).

4.2.4 Color

A tristimulus colorimeter (Chromameter-2 Reflectance, Minolta, Osaka, Japan) was used. The instrument was equipped with a CR-300 measuring head, was calibrated against a standardized white

tile and used to determine samples color in the L*a*b* (CIELAB) color space. Approximately 10 mL aliquots of egg white and egg yolk sample were poured into Petri dishes and positioned over the calibration tile for analysis.

4.2.5 Particle size and Z-potential

Freeze dried egg white and egg yolk samples were diluted to a concentration of 0.01 and 0.015 g mL^{-1}, respectively, in 0.05 M Tris-HCl buffer pH 9.0 containing 0.04 M NaCl. Samples were very gently stirred at 4 °C overnight to ensure solubilization. This buffer was specifically selected to optimize protein stability during analyses (Ohba et al., 1993). Egg white samples were filtered through Whatman n °1 paper and, subsequently, through 25 mm PVDF syringe filters (cutoff 0.45 μm; Lab Logistics Group GmbH, Meckenheim, Germany). Filtered samples were further diluted 1:100 (v/v) with Tris-HCl buffer at 4 °C. Egg yolk samples were further diluted 1:1000 (v/v) with 0.1 % (v/v) SDS in Tris-HCl buffer at 4 °C, and filtered through Whatman n °1 paper. Particle size and Z-potential were determined at 4 °C to minimize protein aggregation during analyses, which were carried out using a dynamic light scattering system (NanoSizer 3000, Malvern Instruments, Malvern, UK) equipped with a Peltier temperature control system. The refractive index was set at 1.333 and the viscosity was approximated to that of pure water at 4 °C.

4.2.6 Protein denaturation temperature

Egg white and egg yolk thermograms were obtained by differential scanning calorimetry (DSC). Samples (15 and 20 mg of egg yolk and egg white, respectively, sealed into 40 μL aluminum pans) were heated from 45 to 95 °C at a 5 °C min^{-1} rate using a DSC 3 Stare System differential scanning calorimeter (Mettler-Toledo, Greifensee, Switzerland). An empty sealed pan was used as reference. Peak temperature and enthalpy were calculated using the program STARe ver. 16.10 (Mettler-Toledo, Greifensee, Switzerland). The transition peak associated to egg white ovalbumin unfolding was deconvoluted using Origin Pro 9 (OriginLab, Northampton, MA, USA). Multiple peak fitting was applied adopting $R^2_{adj} > 0.997$ as goodness of fit threshold.

4.2.7 Oxidative status by FTIR

The oxidation state of egg yolk was evaluated by Fourier transform infrared spectroscopy (FT-IR). The analysis was performed at 25 ± 1 °C on freeze-dried samples finely ground with a domestic

blender. An Alpha-P (Bruker Optics, Milan, Italy) infrared spectrometer, equipped with a Zn–Se crystal accessory, was used to record samples attenuated total IR reflection. Spectra from 4000 to 400 cm^{-1} were acquired in absorbance mode by performing 32 scans per measurement with a resolution of 4 cm^{-1}. After baselining and smoothing the recorded spectra, peak height of the bands associated to lipid oxidation was determined (Origin Pro 9, OriginLab, Northampton, MA, USA).

4.2.8 Peroxide value

Peroxide value analysis was carried out according to the method described by the International Olive Council (2017). Briefly, approximately 2 g of freeze-dried egg yolk was dissolved in 25 mL of chloroform (Sigma Aldrich, Milan, Italy) in acetic acid (VWR, Leuven, Belgium) (2:3 v/v) solution. A 1 mL aliquot of supersaturated KI (Sigma Aldrich, Milan, Italy) solution in MilliQ water was added and the mix was vigorously stirred with a magnetic stirrer. After 5 min incubation at room temperature in the dark to develop color, 75 mL of MilliQ water was added to stop the reaction and the free iodine was titrated with 0.01 N $Na_2S_2O_3$ (Sigma Aldrich, Milan, Italy) aqueous solution, using potato starch as indicator. The peroxide value was determined according to Eq. 14.

Eq. 14 $$PV = \frac{V \times T \times 1{,}000}{m}$$

where V (mL) is the volume of 0.01 N $Na_2S_2O_3$ added to induce color change of the mix, T (mol/L) is the exact molarity of the $Na_2S_2O_3$ solution, and m is the mass (g) of the tested egg yolk sample.

4.2.9 Carotenoid content

Total carotenoids content was evaluated on freeze-dried samples according to the AOAC method (AOAC, 1973). Briefly, 0.5 g of freeze-dried egg yolk powder was dissolved into 50 mL acetone (Merck, Darmstadt, Germany) and stirred for 10 min. The egg yolk suspension was filtered through Whatman n° 4 paper. The retentate was washed with fresh acetone and filtered again. The filtrates were pooled and the volume was made up to 100 mL with fresh acetone. Absorbance at 450 nm was read in 1 cm path-length cuvettes using a UV-Vis spectrophotometer (UV-2501 PC, Shimadzu Kyoto, Japan). Results were expressed as optical density values at 450 nm (OD_{450}).

4.2.10 Whey protein profile

Whey was obtained from milk samples by isoelectric precipitation (pH 4.6) of casein by addition of HCl 1 M. Whey samples were frozen and kept at – 18 °C until analysis. Thawed samples were diluted 1:5 (v/v) with MilliQ water and subjected to reverse-phase high performance liquid chromatography (RP-HPLC) as previously described by De Noni et al. (2007). The RP-HPLC apparatus was a 230 Pro Star (Varian Inc, Palo Alto (CA), USA), equipped with a 7725i injector (Rheodyne, Cotati (CA), USA) and a PLRP-S column (4.6 mm i.d. × 150 mm, 5 mm, 300 Å from Polymer Laboratories, Shropshire, UK) kept at 40 °C. The detector was a Varian 330 Pro Star UV-Vis spectrophotometer set at 205 nm. Samples were eluted by applying a gradient of solvents: A (0.1% (v/v) trifluoroacetic acid in MilliQ water); B (0.1% (v/v) trifluoroacetic acid in acetonitrile; Sigma Aldrich, Milan, Italy). Eluting solvents were filtered through 0.45 μm cutoff HV DURAPORE® membrane filters (Merck Millipore Ltd., Tullagreen, Carrigtwohill, Cork, Ireland). The elution gradient, as solvent B proportion (v/v), was as follows: 0-8 min, 25-35%; 8-10 min, 35-36%; 10-17 min, 36-38%; 17-23 min, 38-45%; 23-23.5 min, 45-100%; 23.5-25 min, 100-25%. The flow rate was 1.0 mL min^{-1}. Peak assignment was performed according to Innocente et al. (2011). β-Lactoglobulin (β-Lg) was quantified by using a calibration curve obtained from standard solutions (Sigma Aldrich. Milan, Italy) in the 0-2 g L^{-1} concentration range (R^2_{adj} = 0.9843).

4.2.11 Free SH groups

Free sulfhydryl groups content was determined using Ellman's reagent (5′,5-dithiobis (2-nitrobenzoic acid), DTNB) (Sigma Aldrich. Milan, Italy), adapting the method of Manzocco, Panozzo, & Nicoli (2013a). Briefly, freeze dried egg white and egg yolk samples were diluted 1:1000 and 1:150 (w/v), respectively, in Tris–glycine buffer (10.4 g Tris, 6.9 g glycine, 1.2 g EDTA per liter, pH 8.0) containing 1% (w/v) NaCl (Sigma Aldrich, Milan, Italy) by very gentle stirring overnight. For egg white, 1.93 mL of 0.5% SDS in Tris–glycine buffer was added to 0.067 mL of diluted sample and 0.013 mL of Ellman's reagent (4 mg mL^{-1} DTNB in Tris–glycine buffer). For egg yolk, an aliquot of 1.67 mL 0.5 % (w/v) sodium-dodecyl sulfate (SDS) in TGE was added to 0.116 mL of diluted sample and 0.018 mL of Ellman's reagent. The SDS-TGE solution was previously sonicated for 30 min (Ultrasonic Cleaner, VWR, Leuven, Belgium) and bubbled with pure nitrogen for 15 min under gentle stirring to purge solubilized oxygen. Egg yolk samples were then centrifuged at 12,700 × g at 4 °C for

15 min (Mikro 120, Hettich Zentrifugen, Tuttlingen, Germany). All samples were incubated for 15 min at 20 °C in the dark to develop color and absorbance was measured at 412 nm by a UV–VIS spectrophotometer (UV-2501 PC, Shimadzu Kyoto, Japan). Concentration of free sulfhydryl groups ($\mu M\ g^{-1}$) was calculated using Eq. 15.

Eq. 15 $SH = \frac{73.53 \cdot A \cdot D}{C}$

where A is the absorbance; C is egg white or egg yolk concentration ($mg\ mL^{-1}$); D is the dilution factor; and 73.53 is derived from $\frac{10^6}{1.36 \cdot 10^4}$; $1.36 \cdot 10^4$ is the molar absorptivity (Ellman, 1959).

4.2.12 UV-Vis absorbance

Freeze dried egg white and egg yolk samples were prepared as previously described for particle size and Z-potential analyses. Egg white was further diluted 1:10 (v/v) with Tris-HCl buffer pH 9 at 4 °C before readings. Egg yolk was diluted 1:200, 1:150 and 1:60 (v/v) with the same buffer at 4 °C before readings at 280, 380 and 680 nm, respectively. Absorbance of egg white and egg yolk at 280, 380 and 680 nm was read at 4 °C to minimize protein aggregation with a UV-VIS spectrophotometer (UV-2501 PC, Shimadzu Kyoto, Japan) in 1 cm path-length quartz cuvettes.

4.2.13 Protein secondary structure

Fourier transform infrared spectroscopy (FT-IR) analysis was performed at 25 ± 1 °C on freeze-dried egg white samples using an Alpha-P (Bruker Optics, Milan, Italy) instrument equipped with an attenuated total reflection accessory and a Zn-Se crystal, as previously described by Melchior et al. (2020). Spectra were acquired by performing 32 scans per measurement in the 4000 - 400 cm^{-1} wavelength range, with a resolution of 4 cm^{-1}. Amide I band of every spectra (1700 - 1600 cm^{-1}) was extrapolated, smoothed, baselined and normalized using the OPUS software (version 7.0 for Microsoft Windows, Bruker Optics, Milan, Italy). Amide I band Fourier self-deconvolution and Gaussian multiple peak fitting were performed using Origin Pro 9 (OriginLab, Northampton, MA, USA). $R^2_{adj} > 0.997$ was adopted as goodness of fit threshold.

4.2.14 Solubility

Egg white and egg yolk solubility was evaluated adapting the method from Melchior et al., (2020).

Freeze dried samples were solubilized (10 g L^{-1}) in 0.05 M Tris-HCl buffer pH 9.0 containing 0.04 M NaCl. Complete solubilization was achieved by very gentle stirring at 4 °C overnight. Samples were centrifuged (Mirko 120, Hettich Italia S.r.l., Milan, Italy) at 13,500 × g for 5 min. The residual pellet (insoluble fraction) was dried in a vacuum oven (Vuotomatic 50, Bicasa, Milan, Italy) overnight and weighed to ± 0.00001 g precision. Sample solubility was calculated by Eq. 16.

Eq. 16 $Solubility\ (\%\ w/w) = \frac{S-I}{S} \cdot 100$

Where S (mg) is the initial sample weight and I (mg) is the weight of the dried insoluble fraction.

4.2.15 Viscosity

A RS6000 Rheometer (ThermoScientific Rheo Stress, Haake, Germany) equipped with a Peltier temperature control system, was used to determine egg white and egg yolk apparent viscosity at 20 °C. Flow curves were obtained in the 0.1 - 200 s^{-1} shear rate range by using a bob-cup geometry with a gap of 27.2 mm (bob: CC25 DIN Ti; cup: CCB25 DIN/SS; ThermoScientific, Haake, Germany). Samples apparent viscosity was compared at 4.472 and 21.79 s^{-1} shear rate, for egg yolk and egg white, respectively, to better highlight occurring differences between samples.

4.2.16 Gelling capacity

Aliquots of 50 mL of egg white and egg yolk samples were heated at 90 °C for 15 min in 50 mL-capacity sealed plastic Falcon tubes. Samples were then rapidly cooled in ice and stored at 4 °C for 12 h. The gelled samples were extracted from the Falcon tubes and manually cut with a sharp knife to obtain 1.5 ± 0.1 mm thick slices. Mechanical spectra of the heat-set gels were obtained using a RS6000 Rheometer equipped with a parallel plates geometry having 40 mm diameter and 1 mm gap. To determine samples linear visco-elastic stress domain, stress sweep analysis was performed by increasing the applied stress from 1 to 200 Pa at 1 Hz frequency. Frequency sweep analysis was performed by increasing oscillatory frequency from 0.1 to 16 Hz, applying a stress within the linear visco-elastic domain. Gelling capacity was expressed as the elastic modulus of gelled samples at a frequency of 1 Hz.

4.2.17 Foaming properties

For milk, two different foaming methods, based on mechanical agitation or on steam injection, were used. For the mechanical-based method, the procedures applied by Ho et al. (2019) and Kamath et al.

(2008) were adapted. In particular, 25 mL milk aliquots were poured into 100 mL beaker, equilibrated at 20 °C for 1 h, heated to 50 ± 3 °C in a microwave oven (Panasonic Ne-1643, 1600 W, applied for 8 s) and foamed using a commercially available mechanical milk frother for 15 s. For the steam-based method, 90 mL of milk was poured into 250 mL beakers and the foam was generated using a steam injection system purposedly built to simulate catering steam frothers. Steam was injected in the samples for 5 s, so that milk reached a temperature of 70 ± 5 °C. For both methods, the height of the milk surface (h_i) from the bottom of the beaker was measured with a Metrica monobloc precision venier caliper (Metrica S.p.A., San Donato M.se, MI, Italy). Foam height was measured after (h_0 and 15 min (h_{15}) and the foaming capacity and foam stability were calculated using Eq. 17 and 18, respectively.

Eq. 17 $Foaming\ capacity\ (\%) = h_0/h_i \cdot 100$

Eq. 18 $Foam\ stability\ (\%) = h_{15}/h_0 \cdot 100$

In the case of egg white and egg yolk, foaming properties were determined by adapting the method from Melchior et al. (2020). Briefly, 10 mL of sample was diluted 1:10 (w/w) with MilliQ water and homogenized (Polytron DI 25 basic, IKA Werke GmbH & Co., Staufen im Breisgau, Germany) for 3 min at 9,500 rpm in a graduated cylinder. The total volume of the foamed samples was measured after 0 and 15 min. Foaming capacity and foam stability were calculated using Eq. 19 and 20, respectively.

Eq. 19 $Foaming\ capacity\ (\%) = \frac{V_0 - V_i}{V_i} \cdot 100$

Eq. 20 $Foam\ stability\ (\%) = 100 - \left(\frac{V_0 - V_{15}}{V_0} \cdot 100\right)$

Where V_0 (mL) is the sample volume after homogenization, V_i (mL) is the initial sample volume (10 mL) and V_{15} (mL) is the sample volume after 15 min from homogenization.

4.2.18 Emulsifying activity

Emulsifying properties were evaluated by determining the emulsifying activity index (EAI) of freeze-dried samples adapting the methods of Anton & Gandemer (1997) and Yan et al. (2010). Briefly, 60 mL egg yolk solutions (3 %, w/v) were prepared in 0.05 M Tris-HCl buffer (pH 9) containing 0.04 M NaCl. Sunflower oil (17 mL) was subsequently added and pre-emulsified by applying a high-speed blender (Polytron DI 25 basic, IKA Werke GmbH & Co., Germany) at 8,000 rpm for 1 min. Stable

emulsions were obtained by passing the pre-emulsion through a lab-scale two-stage (first stage valve: 50 MPa; second stage valve: 5 MPa) high pressure homogenizer (Panda Plus 2000, GEA Niro Soavi, Parma, Italy). Exactly 7 mL of the obtained emulsion were transferred into 10 mL glass vials. 10 μL aliquots were then quickly withdrawn from the center of the vials, 10 mm above the bottom, using an automatic pipette, and diluted 1:6000 (v/v) in MilliQ water. Absorbance at 500 nm of diluted emulsions was measured with a UV-Vis spectrophotometer (UV-2501 PC, Shimadzu Kyoto, Japan) and EAI was calculated using Eq. 21.

Eq. 21 $EAI = \frac{2 \times 2.303 \times A_0 \times DF}{C \times \phi \times (1-\theta) \times 1{,}000}$

Where 2×2.303 is the conversion factor of samples light absorption value to turbidity, A_0 is the absorbance of the diluted samples, DF is the dilution factor, C is the initial concentration of the sample, ϕ is the cuvette optical path, θ is the oil fraction in the emulsion (0.283).

4.2.19 Statistical analysis

Microbiological analyses were performed in single on samples from two independent experiments. These data are reported as mean ± standard deviation. Data of oxidative status, peroxide value, carotenoid content, color, absorbance spectroscopy, free sulfhydryl groups content, secondary structure, particle size, Z-potential, solubility, emulsifying activity, foaming properties were obtained by triplicate measurements. These data are reported as mean ± standard deviation and were subjected to one-way analysis of variance (ANOVA) and Tukey's Honest Significant Differences test ($p < 0.05$) using R v. 3.6.1 for Windows (The R foundation for statistical computing). Data of whey protein profile, denaturation temperature, apparent viscosity and gelling properties were obtained in duplicate and reported as mean ± standard deviation.

4.3 Milk functionalization by hyperbaric storage

4.3.1 Effect of hyperbaric storage on milk protein structure

To understand the effect of hyperbaric storage on milk proteins, the attention was focused on the role of whey proteins in the micelle enlargement induced by HS, to provide an explanation to the phenomenon (Paragraph 3.1, Table 8). Whey was thus recovered from differently stored milk and subjected to RP-HPLC. In accordance with De Noni et al. (2007), chromatograms indicated the presence of the full whey protein spectrum in fresh milk (Figure 12).

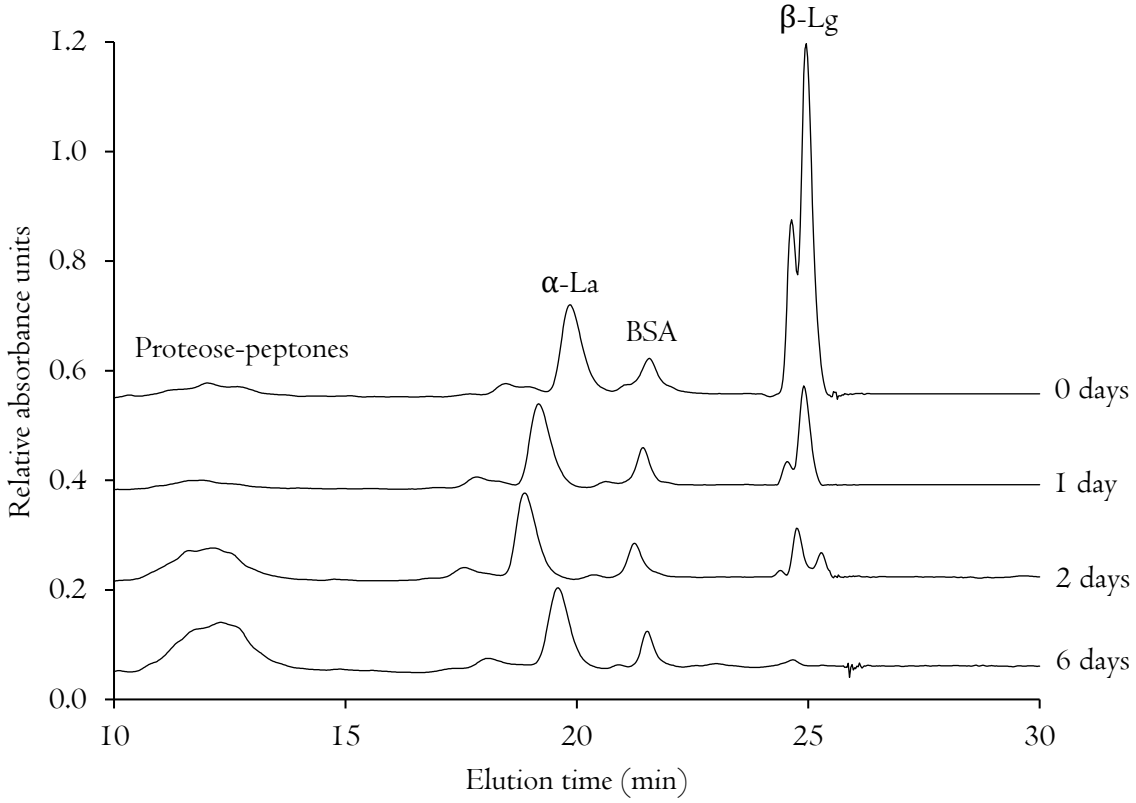

Figure 12: RP-HPLC chromatogram of raw skim milk samples during HS at 150 MPa (20 ± 2 °C) for up to 6 days. Peak assignment of proteose-peptones, α-La, BSA and β-Lg is also displayed.

In particular, α-lactalbumin (α-La), bovine serum albumin (BSA) and β-lactoglobulin (β-Lg) were eluted at about 20, 22 and 25 min, respectively. Moreover, the presence of proteose-peptones was clearly indicated by the occurrence of a broad, irregular peak at 13 min (Innocente et al., 2011). During refrigerated storage, milk whey proteins content did not change (chromatograms not shown), indicating

optimal maintenance of their structure. Contrarily, a significant loss of β-Lg was observed in the samples stored at 150 MPa (Figure 12). Quantitative analysis showed that β-Lg concentration decreased from 2.38 ± 0.28 (fresh sample) to 0.44 ± 0.10 and 0.11 ± 0.08 g L^{-1} after 1 and 6 days of hyperbaric storage, respectively. These results are probably due to extensive pressure-induced unfolding of β-Lg, which is highly pressure-sensitive (Huppertz et al., 2004; Huppertz, Fox, et al., 2006) and prone to interact with κ-casein molecules in relatively stable complexes (Cho et al., 2003). It can be thus inferred that milk whey was deprived of β-Lg since it separated along with casein. Based on the literature and on the results observed regarding the enlargement of casein micelles during 150 MPa-HS (Paragraph 3.1, Table 8), it can be inferred that casein micelles would locally support aggregation of pressure-unfolded β-Lg molecules, which would have accumulated onto their surfaces (Patel & Huppertz, 2014). This hypothesis was further corroborated by statistical analysis, which revealed strong negative correlation (r = -0.838) between β-Lg concentration and casein micelles size. HS also induced a progressive increase in proteose-peptones content (Figure 12), suggesting that casein hydrolysis by native milk proteases (*e.g.*, plasmin) was favored by HS (Garcia et al., 2017). According to García-Risco et al. (2000), this phenomenon resulted from pressure-induced modification of micelles structure, which made them prone to proteolytic enzymes.

4.3.2 Effect of hyperbaric storage on milk techno-functionality

The observed effects of HS on milk proteins indicate the possibility to employ pressurized storage to improve the technological performance of milk. For instance, due to their exceptional surface activity, unfolded β-Lg and proteose-peptones formed by HS could be of peculiar interest for milk foaming.

To assess whether protein structural changes induced by hyperbaric storage could steer the attitude of milk to be further processed into foams, differently stored milk samples were analyzed for foaming properties by using two alternative methods (Table 18). The first one was based on mechanical agitation and moderate heating. According to the literature, besides being representative of milk foaming processes carried out at domestic level (Silva et al., 2008), this procedure allows to accurately evaluate foaming performances. Subsequently, a steam injection-based method was also applied, which can be considered the gold standard for foamed milk preparations (*i.e.*, *cappuccino*, *macchiato*, and *latte*) in the catering sector (Silva et al., 2008).

Table 18: Foaming capacity and foam stability determined by mechanical agitation or steam injection in raw skim milk stored for up to 6 days under refrigerated (0.1 MPa, 4.0 ± 0.5 °C) or hyperbaric conditions (150 MPa, 20 ± 2 °C).

Storage	Time	Mechanical agitation		Steam injection	
		Foaming capacity	Foam stability	Foaming capacity	Foam stability
	(days)	(%)	(%)	(%)	(%)
Fresh	0	72.5 ± 4.4[d]	72.6 ± 4.1[a]	112.7 ± 6.0[b]	50.2 ± 6.6[ab]
Refrigeration	4	83.4 ± 9.5[d]	62.3 ± 15.5[a]	N.D.	N.D.
	6	92.8 ± 5.1[d]	71.4 ± 6.8[a]	106.6 ± 6.9[b]	60.2 ± 0.8[a]
Hyperbaric	1	119.5 ± 7.9[c]	75.0 ± 5.6[a]	N.D.	N.D.
	2	123.4 ± 8.5[c]	79.6 ± 6.6[a]	122.4 ± 0.7[ab]	51.6 ± 0.7[ab]
	4	197.2 ± 6.5[b]	71.2 ± 0.8[a]	127.4 ± 2.9[ab]	54.9 ± 3.5[ab]
	6	267.3 ± 15.7[a]	71.7 ± 1.5[a]	147.5 ± 15.3[a]	49.3 ± 2.2[b]

[a] Different letters indicate significantly different means (ANOVA; $p < 0.05$) in the same column.

In agreement with the literature, refrigeration had no significant effect on milk foaming properties (Ho et al., 2019). Differently, HS caused a remarkable progressive increase (~ 4-fold after 6 days) in mechanically-induced foaming capacity, without detriment to the foam stability (Table 18).

Similar to the mechanical procedure, the steam injection foaming method highlighted a progressive increase in the foaming capacity (about 35% after 6 days) and no changes in the foam stability of pressurized milk (Table 18). Data confirm the hypothesis that unfolding of β-Lg and formation of proteose-peptones during HS improved milk foaming capacity (Figure 2) (Buccioni et al., 2013; Innocente et al., 2011). However, based on their excellent foaming activity, proteose-peptones were reasonably the major driver of these phenomena, as also supported by the strong positive correlation ($r = 0.9085$) between foaming capacity and proteose-peptones RP-HPLC peak area (data not shown). These results indicate that the enhancement of milk foaming induced by HS would be relevant for both domestic and catering-related uses, suggesting that preparations based on foamed milk might be attained using lower amounts of milk if the latter was previously subjected to pressurized storage.

4.4 Egg white functionalization by hyperbaric storage

4.4.1 Validation of the antimicrobial efficacy of hyperbaric storage in egg white

Preliminary microbial analyses were carried out on non-inoculated egg white and to ensure the absence of *Salmonella* and *S. aureus*, which resulted always below the detection limit (1.7 logCFU g^{-1}). Egg white was then inoculated with *S. enterica* (4.05 ± 0.35 logCFU g^{-1}) and *S. aureus* (3.96 ± 0.20 logCFU g^{-1}) and the evolution of the counts of these bacteria were followed throughout storage under hyperbaric and refrigerated conditions over 28 days (Table 19).

Table 19: *Salmonella enterica* and *Staphylococcus aureus* counts (logCFU g^{-1}) in egg white stored for up to 28 days under refrigerated (0.1 MPa, 4.0 ± 0.5 °C) or hyperbaric conditions (200 MPa, 20 ± 2 °C).

Time (days)	*S. enterica*		*S. aureus*	
	Refrigerated	Hyperbaric	Refrigerated	Hyperbaric
0	4.05 ± 0.35	4.05 ± 0.35	3.96 ± 0.20	3.96 ± 0.20
1	3.85 ± 0.35	< L.o.D.	3.95 ± 0.21	< L.o.D.
3	3.50 ± 0.07	< L.o.D.	3.75 ± 0.22	< L.o.D.
7	3.40 ± 0.57	< L.o.D.	3.70 ± 0.25	< L.o.D.
14	3.08 ± 0.11	< L.o.D.	3.38 ± 0.11	< L.o.D.
21	3.05 ± 0.07	< L.o.D.	2.62 ± 0.17	< L.o.D.
28	2.37 ± 0.05	< L.o.D.	2.43 ± 0.02	< L.o.D.

L.o.D. 1.7 logCFU g^{-1}

After just 3 hours under hyperbaric conditions, values below the detection limit were reached for *S. enterica*. Interestingly, these values were maintained throughout the 28 days storage, suggesting the capability of hyperbaric storage to maintain egg white microbiological stability as long as pressure is applied. Such findings are coherent with the literature on HS applied to fresh meat, fresh fish and fruit juices (Fidalgo et al., 2018; Pinto et al., 2017; Santos, Delgadillo, et al., 2020; Segovia-Bravo et al., 2012). Conversely, in the refrigerated samples, values of *S. aureus* remained almost the same as the initial concentrations, and these values remained similar until the 14th day of storage. Prolonging the

storage period up to 28 days, the *S. aureus* concentration decreased to reach a concentration of about 2.43 logCFU g^{-1}. Regarding *S. enterica* under refrigerated condition, a behavior similar to *S. aureus* was observed, even though significant count reduction occurred only after 14 days. By comparing the results observed under hyperbaric and refrigerated conditions, it appears that pressure actively induces microbial inactivation, while, on the other hand, low temperature only prevents microbial growth. Such behavior has been repeatedly observed in other food matrices subjected to hyperbaric storage (Segovia-Bravo et al., 2012). Based on these interesting results, the effects of hyperbaric storage on *S. enterica* and *S. aureus* counts were investigated within 24 hours under hyperbaric conditions to evaluate the differences in their inactivation under hyperbaric conditions (Table 20).

Table 20: *Salmonella enterica* and *Staphylococcus aureus* counts (logCFU g^{-1}) in egg white stored for up to 3 hours under hyperbaric conditions (200 MPa, 20 ± 2 °C).

Time (hours)	*S. enterica*	*S. aureus*
0	3.50 ± 0.07	3.96 ± 0.20
0.5	2.30 ± 0.36	3.52 ± 0.35
3	< L.o.D.	3.19 ± 0.06

L.o.D. 1.7 logCFU g^{-1}

As a result, a reduction of *Salmonella* of about 1.3 log was observed after just 30 min of storage (Table 20). Subsequently, the count value reached the detection limit after only 3 hours. On the other hand, *S. aureus* was more resistant to pressure. In fact, after 3 hours, only a slightly decrease of the microorganism was observed (Table 20). This behavior might be explained by the higher pressure resistance of Gram(+) bacteria (*e.g.*, *Staphylococcus* spp.) as compared to Gram(-) ones (*e.g.*, *Salmonella* spp.). This is known to be due to the presence of a thick peptidoglycan layer in the cell wall of Gram(+) bacteria (Wuytack et al., 2002). These results indicate that hyperbaric storage at 200 MPa allows an efficient performance on microbial growth inhibition and inactivation for both *S. enterica* and *S. aureus* in egg white. In particular, 1 day of storage seems sufficient to achieve a satisfactory level of inactivation of these microorganisms.

4.4.2 Effect of hyperbaric storage on egg white protein structure and techno-functionality

In the light of the encouraging results relevant to the effect of hyperbaric storage on the hygienic properties of egg white, further analyses were performed, focusing on the physical properties of egg white. Egg white samples were initially analyzed for color changes. Figure 13 compares the evolution of luminosity and yellowness of egg white during storage under hyperbaric and refrigerated conditions.

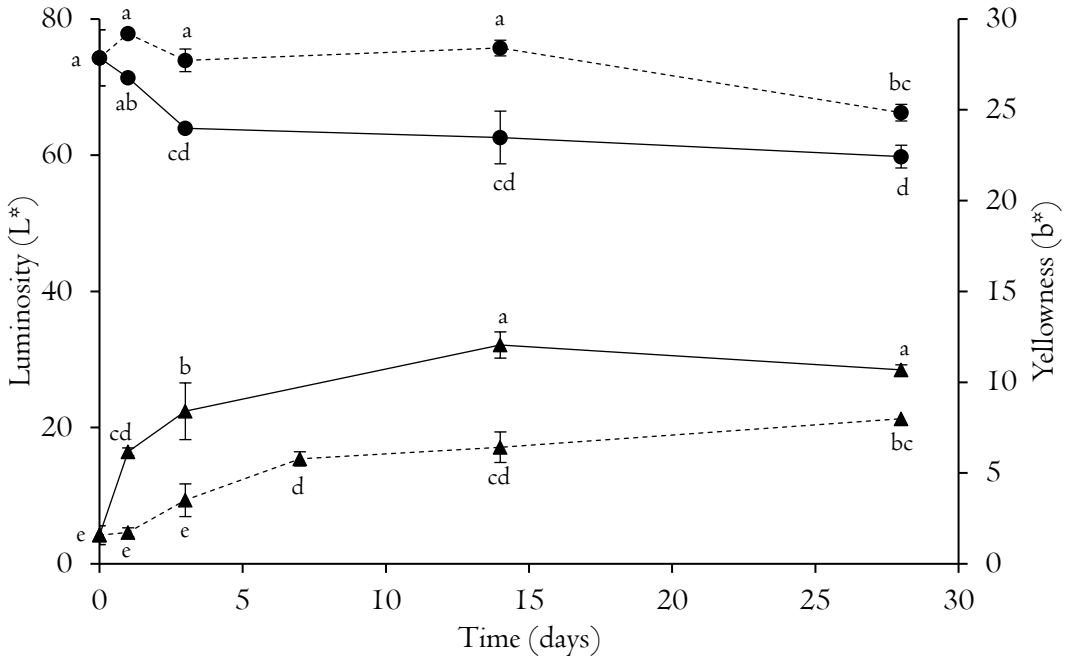

Figure 13: Luminosity (●) and yellowness (▲) of egg white stored for increasing time under refrigerated (----, 0.1 MPa, 4.0 ± 0.5 °C) or hyperbaric (—, 200 MPa, 20 ± 2 °C) conditions. [a] Different letters for the same color parameter indicate significantly different means (ANOVA; $p < 0.05$).

A progressive decrease in egg white luminosity and a significant increase in yellowness were detected during hyperbaric storage, whereas much less pronounced color changes were observed under refrigeration. These changes were also confirmed by measurements of absorbance at 380 nm. The latter remained almost constant (0.057 ± 0.004) during refrigeration for 28 days, while almost triplicated (0.150 ± 0.007) during pressurized storage at room temperature. Although being mainly constituted by proteins, egg white also contains small amounts of reducing sugars, which could make the matrix particularly prone to non-enzymatic browning (Isaacs & Coulson, 1996; Sisak et al., 2006). In fact, as

reported in Paragraph 3.3 with reference to glucose-glycine model systems, Maillard reaction easily occurs even during HS. In addition, a further yellowing mechanism could involve egg white riboflavin. Literature actually reports that this pigment occurs in egg white as complexed with a riboflavin-binding protein. Pressure-induced dissociation of this complex would thus increase the amount of free riboflavin, which has a higher absorption capacity at 380 nm (Li et al., 1976; Shiga et al., 1979).

Protein structural changes were investigated by FT-IR analysis of freeze-dried samples. Spectra (not shown) exhibited the typical peaks of amide I and amide II within the range 1500 - 1700 cm^{-1}, associated to C=O and N–H stretching, and bending of the peptide bonds, respectively (Ami et al., 2013). Deconvolution of Amide I peak (1600 – 1700 cm^{-1}) clearly showed the presence of three protein components. Peaks identified at 1630, 1654 and 1684 cm^{-1} were associated to low-frequency β-sheet, α-helix highly overlapped to random coil and high-frequency β-sheet structures, respectively (Uygun-Sarıbay et al., 2017). Data relevant to refrigerated egg white showed the occurrence of minor fluctuations in the α-helix/random coil domain (Table 21).

Table 21: Percentage of secondary structures of egg white stored for up to 28 days under refrigerated (0.1 MPa, 4.0 ± 0.5 °C) or hyperbaric conditions (200 MPa, 20 ± 2 °C).

Storage	Time (days)	α-helix and random coil (%)	Low frequency β-sheet (%)	High frequency β-sheet (%)
Fresh	0	33.50 ± 5.82[bc]	49.83 ± 3.59[a]	16.67 ± 2.97[a]
Refrigerated	14	28.86 ± 2.88[c]	50.26 ± 3.23[a]	17.62 ± 3.84[a]
	28	34.30 ± 3.48[ab]	49.95 ± 3.41[a]	15.30 ± 2.35[a]
Hyperbaric	5	37.17 ± 2.44[ab]	47.11 ± 1.63[ab]	15.72 ± 1.66[a]
	7	38.45 ± 3.72[ab]	46.42 ± 1.63[ab]	15.92 ± 2.28[a]
	14	37.82 ± 2.01[ab]	46.54 ± 2.44[ab]	15.64 ± 0.59[a]
	28	39.88 ± 3.62[a]	45.01 ± 3.22[b]	15.69 ± 2.48[a]

[a] Different letters in the same column indicate significantly different means (ANOVA; $p < 0.05$).

In the pressurized samples, only a slight increase in the average value of the percentage of α-helix/random coil was noticed (Ngarize et al., 2004), suggesting that the secondary structure of egg white proteins was largely retained during hyperbaric storage. Nevertheless, pressurized egg white appeared significantly more turbid then the refrigerated one, as indicated by the increase in absorbance

at 680 nm (Table 22). This effect typically indicates the occurrence of protein denaturation phenomena (Manzocco et al., 2013a; Smith et al., 1996). To better study structural changes leading to protein denaturation, egg white samples were also analyzed for absorbance at 280 nm, particle size and Z-potential (Table 22).

Table 22: Absorbance at 680 and 280 nm, particle size and Z-potential of egg white stored for up to 28 days under refrigerated (0.1 MPa, 4.0 ± 0.5 °C) or hyperbaric conditions (200 MPa, 20 ± 2 °C).

Storage	Time (days)	Absorbance 680 nm	Absorbance 280 nm	Particle size (nm)	Z-potential (mV)
Fresh	0	0.020 ± 0.001[b]	0.376 ± 0.005[b]	224.65 ± 4.97[a]	-12.25 ± 0.78[a]
Refrigerated	14	0.018 ± 0.003[bc]	0.391 ± 0.009[b]	226.63 ± 11.71[a]	-12.48 ± 1.02[a]
	28	0.016 ± 0.001[c]	0.410 ± 0.009[a]	225.50 ± 11.47[a]	-12.14 ± 0.24[a]
Hyperbaric	14	0.050 ± 0.005[a]	0.382 ± 0.010[b]	198.29 ± 4.20[b]	-15.95 ± 0.53[b]
	28	0.046 ± 0.005[a]	0.377 ± 0.006[b]	192.78 ± 5.26[b]	-15.15 ± 0.91[b]

[a] Different letters in the same column indicate significantly different means (ANOVA; $p < 0.05$).

Under refrigerated conditions, a minor increase in absorbance at 280 nm was observed, suggesting a marginally higher exposure of tyrosine, tryptophan and cysteine residues. Under hyperbaric conditions, no significant changes in absorbance at 280 nm were observed. The lack of changes in cysteine groups exposure was also confirmed by data relevant to sulfhydryl group, which remained almost constant (about 51 μM g^{-1}), independently on storage condition and time. This confirms that S-S/SH exchange plays a negligible role during egg white storage under both refrigerated and hyperbaric conditions. By contrast, dynamic light scattering analysis indicated that the size of pressurized egg white proteins was significantly lower than that of proteins in fresh and refrigerated-stored samples (Table 22). A concomitant increase in the absolute value of the Z-potential also indicated a slightly higher stability of hyperbarically stored proteins towards inter-particle interactions. Similar Z-potential changes were reported for proteins other than those of egg white, and attributed to an increased exposure of carboxyl groups upon pressurization (Kurpiewska et al., 2018; Wang et al., 2019; Zhao et al., 2018). Data shown in Table 22 suggest pressurized storage to favor the formation of protein structures with reduced excluded volume and higher exposure of negatively charged groups, which are typically associated to a more efficient interaction with surrounding water molecules. These effects are in agreement with those

reported in the literature for proteins submitted to HHP (Harano et al., 2008). The latter would turn protein into moderately less compact structures with much larger water-accessible surface. According to this mechanistic interpretation, water would penetrate into the protein interior, leading to a swollen structure stabilized by water molecules with limited translational and rotational mobility (Harano et al., 2008). Reversely, translational restriction for water molecules outside the protein would be greatly reduced.

To understand whether the changes in egg white protein structure observed during hyperbaric storage could be associated to modifications in their techno-functional properties, samples were also analyzed for solubility and apparent viscosity, as well as for gelling and foaming properties (Table 23).

Table 23: Apparent viscosity, gel elastic modulus (G'), foaming capacity and foam stability of egg white stored for up to 28 days under refrigerated (0.1 MPa, 4.0 ± 0.5 °C) or hyperbaric conditions (200 MPa, 20 ± 2 °C).

Storage	Time (days)	Apparent η (Pa s)	G' (Pa · 1000)	Foaming capacity (%)	Foaming stability (%)
Fresh	0	0.078 ± 0.038	5.95 ± 0.63	63.3 ± 15.3[c]	93.5 ± 6.7[a]
Refrigerated	5	0.050 ± 0.023	7.20 ± 0.22	90.0 ± 10.0[bc]	96.5 ± 3.1[a]
	14	0.058 ± 0.032	N.D.	86.7 ± 14.1[bc]	91.2 ± 2.5[a]
	28	0.014 ± 0.002	6.57 ± 0.35	66.7 ± 15.3[c]	93.9 ± 5.9[a]
Hyperbaric	5	0.120 ± 0.071	5.80 ± 0.13	133.3 ± 11.5[a]	91.5 ± 4.0[a]
	14	0.421 ± 0.029	N.D.	113.3 ± 5.8[ab]	89.6 ± 5.4[a]
	28	0.318 ± 0.042	4.41 ± 0.32	100.0 ± 10.0[ab]	96.7 ± 2.8[a]

η Viscosity; [N.D.] Not determined; [a] Different letters in the same column indicate significantly different means (ANOVA; $p < 0.05$).

No changes in these properties were detected in egg white stored under refrigeration. Under HS, no change in egg white solubility was observed throughout the 28 days storage (~ 99 % w/w). By contrast, pressurized egg white presented a remarkable increase in apparent viscosity after 14 days storage. The higher viscosity of pressurized egg white is consistent with protein structural changes previously described (Table 22). Even if more compact, water swollen proteins with higher surface charge would better interact with the solvent, preventing free flowing of the aqueous media in a more efficient way

as compared to native ones. Actually, a good correlation ($r = 0.93$; $p < 0.05$) was found between particle size and apparent viscosity. Based on the better interaction with water, pressurized proteins would be less prone to interparticle interactions. To this regard, it is noteworthy that a slight decrease in gelling capacity of egg white was observed. In order to better investigate the mechanism at the basis of this change, specific information was obtained by DSC analysis. The thermograms relevant to egg white stored for increasing time under hyperbaric condition are shown as examples in Figure 14.

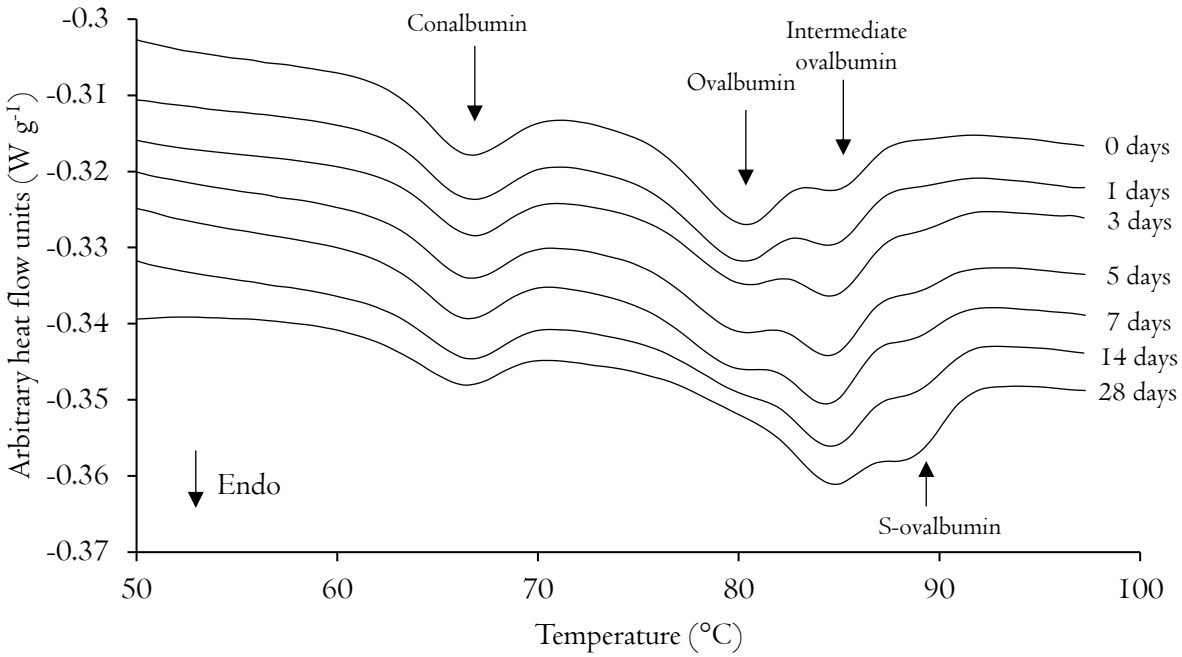

Figure 14: Differential scanning calorimetry thermograms of egg white stored for up to 28 days under hyperbaric conditions (200 MPa, 20 ± 2 °C).

Fresh egg white showed the presence of two phenomena, which were associated to the denaturation of the main protein fractions in egg white. In particular, the endothermal phenomenon between 62 and 70 °C was attributed to the denaturation of conalbumin (Singh & Ramaswamy, 2015). The latter is a highly pressure-sensitive protein that easily undergoes consistent tertiary structure loss upon high hydrostatic pressure (Rivalain et al., 2010; Singh & Ramaswamy, 2015; Van der Plancken et al., 2005). Accordingly, the intensity of this phenomenon progressively decreased during hyperbaric storage. A second complex transition in the temperature range 75-87 °C was attributed to ovalbumin, whose native form is characterized by a denaturation temperature of circa 80 °C. The ovalbumin double peak

shape revealed the presence of an intermediate ovalbumin form showing peak temperature at about 85 °C (de Groot & de Jongh, 2003). During hyperbaric storage, the thermal phenomena associated to the denaturation of ovalbumin native fraction progressively decreased with the increase of the intermediate form of ovalbumin and the appearance of a novel shoulder at temperatures above 89 °C. The latter was attributed to S-ovalbumin. Spontaneous ovalbumin conversion into S-ovalbumin is knowingly due to an irreversible multi-step process, involving L-D isomerization of Ser-164, Ser-236 and Ser-320, as well as distancing motion of 1A and 2A strands and burying of residues surrounding Phe-99 (Yamasaki et al., 2003). To get a quantitative information about the effect of storage conditions on the shift of ovalbumin to S-ovalbumin, enthalpy values of this thermal phenomenon were computed (Figure 15). Analogous data were also acquired for egg white stored under refrigerated conditions or maintained in shell at room temperature.

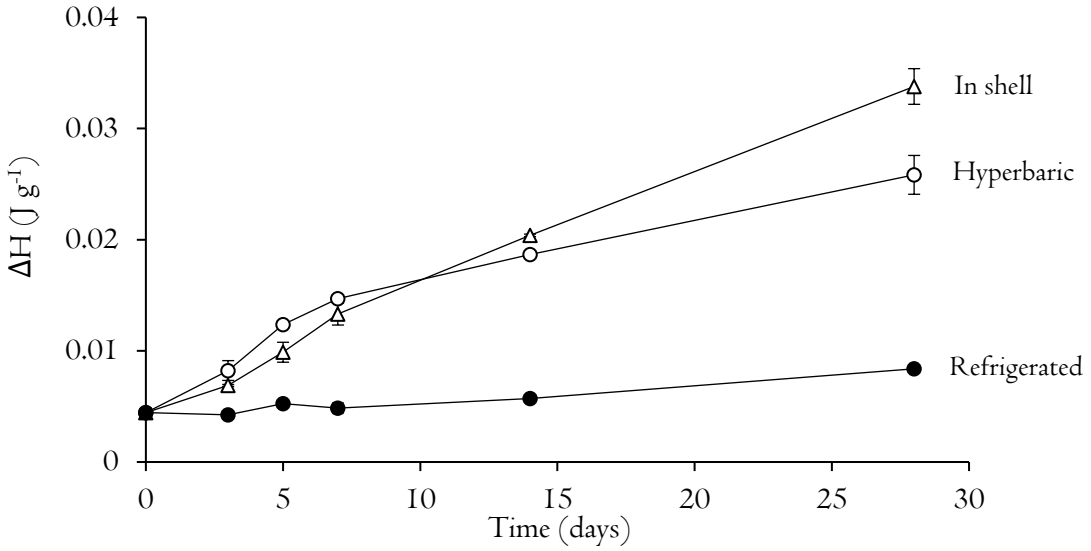

Figure 15: Transition enthalpy of S-ovalbumin in egg white stored for up to 28 days under refrigerated (0.1 MPa, 4.0 ± 0.5 °C) or hyperbaric conditions (200 MPa, 20 ± 2 °C). Egg white from shell egg stored at 0.1 MPa at 20 ± 2 °C is shown as additional control.

It can be noted that the increase in S-ovalbumin enthalpy was more pronounced in egg white stored under hyperbaric conditions as compared to refrigerated ones. This difference could further account for the lower gelling properties of pressurized egg white. In fact, the presence of even small amounts of ovalbumin forms undergoing denaturation at higher temperature has been reported to almost halve the

radius of the aggregates generated upon heat treatment. For this reason, S- and intermediate- ovalbumin are known to be characterized by impaired gel network formation as compared to native ovalbumin (de Groot & de Jongh, 2003). Nevertheless, data shown in Figure 15 clearly show that the intensity of conversion from native ovalbumin to thermally resistant ovalbumin forms in pressurized egg white was comparable to that observed in egg white maintained in shell at room temperature.

Despite the lower capacity of proteins to network, pressurized egg white presented a remarkable increase in foaming properties (Table 23). Being smaller and electrically more stable (Table 22), pressurized proteins would quickly set at the interface between water and gas phases, leading to more efficient air encapsulation. To this regard, it is noteworthy that changes in pH and ionic force are generally associated to better foaming capacity (Li, Wang et al., 2018). In addition, a good correlation ($r = 0.95$; $p < 0.05$) between foaming capacity and apparent viscosity was actually found, suggesting that the higher foaming capacity could also result from the lower mobility of protein particles in the aqueous interstices among air bubbles. This is also known to be associated to lower solvent drainage from the foams (Fameau & Salonen, 2014). The enhanced foaming capability of pressurized egg white could be of particular interest in the industrial context, in which the matrix is employed as a foaming agent in a wide spectrum of formulations (*e.g.*, baked goods) (Abeyrathne et al., 2013). Although hyperbarically-stored egg white was better foaming, the stability of the foams obtained from egg white subjected to HS resulted comparable to that of refrigerated samples. Egg white foam stability also depends on the capacity of proteins to network upon air contact at the gas-water interfaces. This property would be impaired by the lower networking capacity of pressurized proteins. In other words, the stability of pressurized egg white foams would be the result of two counterbalancing effects: an increase in viscosity, which stabilizes the foam, and a decrease in networking capacity, which has an opposite effect.

4.5 Egg yolk functionalization by hyperbaric storage

4.5.1 Validation of the antimicrobial efficacy of hyperbaric storage in egg yolk

Analogously to the case of egg white, preliminary microbiological tests were performed in the case of egg yolk to confirm the ability of 200 MPa-HS in inactivating inoculated *S. enterica* (3.35 logCFU g^{-1}) and *S. aureus* (2.78 logCFU g^{-1}). Inoculated samples stored at 0.1 MPa and 4 °C were kept as control. Results are shown in Table 24.

Table 24: *Salmonella enterica* and *Staphylococcus aureus* counts (logCFU g^{-1}) in egg yolk stored for up to 28 days under refrigerated (0.1 MPa, 4.0 ± 0.5 °C) or hyperbaric conditions (200 MPa, 20 ± 2 °C).

Time	*S. enterica*		*S. aureus*	
(hours)	Refrigerated	Hyperbaric	Refrigerated	Hyperbaric
0	3.35 ± 0.12	3.35 ± 0.12	2.78 ± 0.19	2.78 ± 0.19
1	N.D.	3.04 ± 0.10	N.D.	2.84 ± 0.04
3	N.D.	2.54 ± 0.04	N.D.	2.88 ± 0.02
6	N.D.	2.18 ± 0.04	N.D.	2.78 ± 0.02
24	3.40 ± 0.04	< L.o.D.	2.90 ± 0.06	2.00 ± 0.07
48	3.30 ± 0.05	< L.o.D.	2.84 ± 0.06	< L.o.D.
72	3.28 ± 0.01	< L.o.D.	2.98 ± 0.08	< L.o.D.

N.D. Not determined

L.o.D. = 1.7 logCFU g^{-1}

As expected, microbial counts did not change in control refrigerated samples, in accordance with the well-known bacteriostatic effect of low temperature storage. By contrast, in egg yolk stored under hyperbaric conditions, the concentration of *S. enterica* and *S. aureus* reached values below the detection limit after 24 and 48 h, respectively. Values below the detection limit were also recorded upon further storage for up to 72 h, confirming the complete inactivation of both microorganisms. Similar to what observed for egg white (Tables 19 and 20, Paragraph 4.4), *S. aureus* showed a slightly higher resistance to HS as compared to *S. enterica*, due to the higher barostability of Gram(+) bacteria (Wuytack et al., 2002). However, HS inactivation of these pathogens was much slower when they were inoculated in egg yolk. This was probably due to the high concentration of nutrients (*e.g.*, proteins, lipids, minerals)

in egg yolk as compared to egg white (Abeyrathne et al., 2013; Anton, 2013). In other words, the presence of readily available substrates might have boosted the viability of bacterial cells, increasing their resistance to physical stresses (*e.g.*, pressure) (Humphrey & Whitehead, 1993).

4.5.2 Effect of hyperbaric storage on egg yolk chemical stability

Given the capability of HS to guarantee the hygienic stability of egg yolk (Table 24), further analyses were performed to evaluate if this advantage was achieved to the detriment of the product oxidative status. The IR spectrum of fresh (*i.e.*, not stored) freeze-dried egg yolk displayed the presence of 12 well-defined bands that are ascribable to bonds of lipid compounds (Table 25).

Table 25: Absorbance (optical density) in IR spectrum at wavelengths relevant to specific chemical groups of lipids and relevant oxidation products in freeze-dried egg stored for up to 28 days under refrigerated (0.1 MPa, 4.0 ± 0.5 °C) or hyperbaric conditions (200 MPa, 20 ± 2 °C).

Wavelength (cm^{-1})	Assignment	Fresh	Refrigerated		Hyperbaric		
		0 days	14 days	28 days	5 days	14 days	28 days
720	*cis* C=C	0.583[a] (0.032)	0.589[a] (0.020)	0.581[a] (0.014)	0.592[a] (0.017)	0.588[a] (0.024)	0.588[a] (0.009)
1067	C-O-C	1.220[ab] (0.029)	1.158[b] (0.044)	1.187[ab] (0.039)	1.262[a] (0.059)	1.159[b] (0.063)	1.152[b] (0.017)
1087	P-O	1.236[ab] (0.031)	1.183[ab] (0.035)	1.199[ab] (0.030)	1.238[a] (0.042)	1.163[b] (0.058)	1.176[ab] (0.016)
1161	C-O-C	1.069[ab] (0.032)	1.090[a] (0.020)	1.038[bc] (0.025)	1.058[ac] (0.013)	1.016[c] (0.023)	1.028[bc] (0.008)
1234	P-O	1.030[ab] (0.025)	0.996[ab] (0.030)	0.999[ab] (0.026)	1.041[a] (0.022)	0.932[c] (0.055)	0.979[bc] (0.017)
1744	C=O	1.250[a] (0.033)	1.299[a] (0.032)	1.250[a] (0.043)	1.262[a] (0.036)	1.246[a] (0.027)	1.236[a] (0.011)
3008	*cis* C=C	0.423[a] (0.006)	0.404[a] (0.014)	0.408[a] (0.009)	0.417[a] (0.018)	0.406[a] (0.006)	0.418[a] (0.005)

[a] Different letters in the same row indicate significantly different means (ANOVA; $p < 0.05$).

The attention was focused on specific bands, which, according to the literature, can indicate the occurrence of lipid oxidation and lipolysis. In particular, a decrease in egg yolk absorbance at 720 and 3008 cm^{-1} in concomitance to an increase at 1744 cm^{-1} specifically indicates the simultaneous loss of acyl chain *cis* double bonds and formation of carbonylated oxidation products, respectively. Furthermore, a decrease in absorbance at 1067, 1087, 1161 and 1234 cm^{-1} was reported to indicate

disruption of ester and phosphodiester bonds due to triglyceride and phospholipid lipolysis (Araújo et al., 2011; Liu et al., 2002; Muik et al., 2007). Data reported in Table 25 indicate negligible changes in the absorbance of egg yolk samples at the specific wavelengths associated to oxidation. This result suggests that, similarly to refrigeration, storage under hyperbaric conditions for up to 28 days did not alter egg yolk oxidative status. The oxidative stability of egg yolk under hyperbaric conditions was further confirmed by the absence of changes in egg yolk peroxide value, which was always below the repeatability limit of the method (0.19 meqO_2 kg^{-1}) (data not shown). It is likely that the abundance of chain-breaking and oxygen-quenching antioxidants (*i.e.*, carotenoids) in egg yolk played a crucial role in withstanding the pro-oxidant effect of pressurization (Table 1), even when it is maintained for days/weeks as during HS (Nimalaratne & Wu, 2015). To this regard, 28 days of refrigeration (OD_{450} = 0.513 ± 0.006) promoted a slightly more intense degradation of fresh egg yolk carotenoids (OD_{450} = 0.607 ± 0.006) than 28 days of HS (OD_{450} = 0.540 ± 0.009). These results would suggest hyperbaric storage to guarantee egg yolk lipids stability while better preserving its nutritional value.

4.5.3 Effect of HS on egg yolk protein structure and techno-functionality

Despite the negligible effects on oxidation, HS was associated to a significant modification of egg yolk visual appearance.

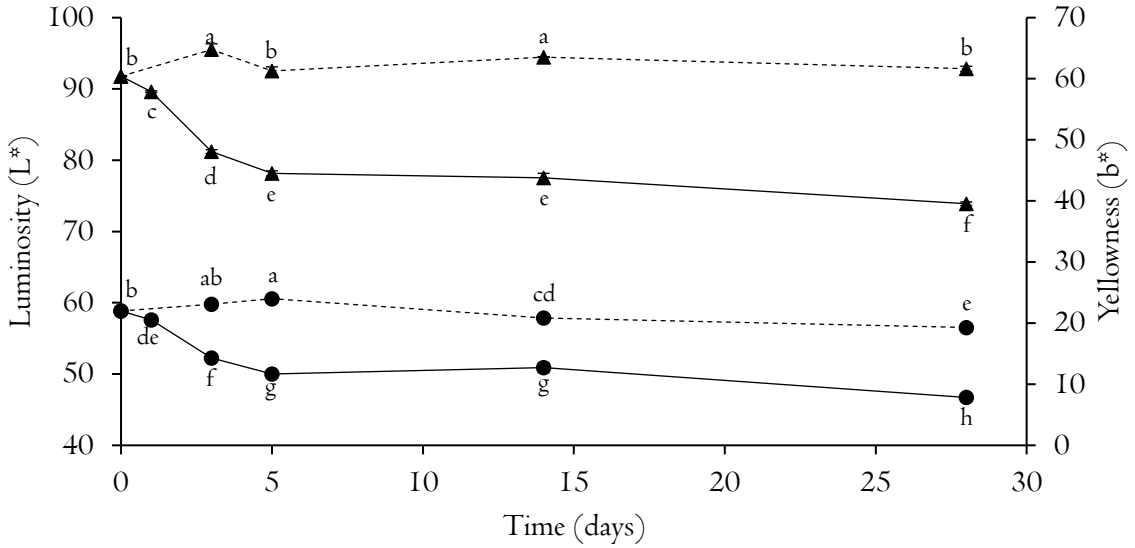

Figure 16: Luminosity (●) and yellowness (▲) of egg yolk stored for up to 28 days under refrigerated (----, 0.1 MPa, 4.0 ± 0.5 °C) or hyperbaric (—, 200 MPa, 20 ± 2 °C) conditions. [a] Different letters for the same color parameter indicate significantly different means (ANOVA; $p < 0.05$).

In particular, HS-stored samples appeared darker than refrigerated ones. Colorimetric analyses were thus performed (Figure 16), confirming that HS caused a remarkable decrease in egg yolk luminosity (L*) and yellowness (b*) within 5 days, with limited changes upon further storage for up to 28 days. Measurements of absorbance at 680 nm also revealed a significant increase in turbidity of pressurized samples (Table 26). In protein-rich food matrices such as egg yolk, these concomitant effects could be associated to protein denaturation and networking, which are known to modify light scattering properties (Manzocco et al., 2013a; Smith et al., 1996). Based on these considerations, even color fading can be mainly attributed to light scattering effects rather than carotenoid oxidation (Nys, 2018). As evident upon egg yolk removal from the HS autoclave, the most significant change induced by hyperbaric storage was a drastic thickening of the samples. To this regard, apparent viscosity of egg yolk was found to progressively increase with storage time, so that a gelled system was obtained after 28 days under pressure (Table 26). Gelling of this egg yolk sample was confirmed by a strong positive linear dependence ($R^2_{adj} > 0.976$) of elastic and viscous moduli logarithms on the logarithm of the oscillatory frequency (data not shown). It is noteworthy that brief HPP treatments (*i.e.*, 10 min) have been associated to changes in viscosity as intense as those reported in Table 26 only at much higher pressures (500 MPa) (Yan et al., 2010).

Table 26: Turbidity and apparent viscosity of egg yolk stored for up to 28 days under refrigerated (0.1 MPa, 4.0 ± 0.5 °C) or hyperbaric (200 MPa, 20 ± 2 °C) conditions.

Storage	Time (days)	Turbidity (optical density at 680 nm)	Apparent viscosity (Pa · s) · 10^{-1}
Fresh	0	0.204 ± 0.020^{e}	5.04 ± 0.01
Refrigerated	1	N.D.	3.11 ± 0.15
	3	N.D.	2.94 ± 0.02
	5	N.D.	3.76 ± 0.01
	7	0.244 ± 0.005^{cd}	4.75 ± 0.01
	14	0.258 ± 0.018^{bcd}	5.67 ± 0.60
	28	0.230 ± 0.011^{de}	6.14 ± 0.26
Hyperbaric	1	0.278 ± 0.004^{ac}	28.11 ± 0.20
	3	0.266 ± 0.002^{bc}	32.44 ± 3.80
	5	N.D.	29.39 ± 1.33
	7	N.D.	61.23 ± 4.91
	14	0.308 ± 0.015^{a}	101.98 ± 8.94
	28	0.289 ± 0.006^{ab}	Gelled

N.D. Not determined; [a] Different letters in the same column indicate significantly different means (ANOVA; $p < 0.05$).

This suggests that the capacity of egg yolk to form a network under pressure does not depend on pressure value solely but would be strongly time-dependent, becoming clearly evident on time scales typical of HS.

To understand the mechanism accounting for HS-induced modification of egg yolk physical properties, protein structure was firstly analyzed by differential scanning calorimetry.

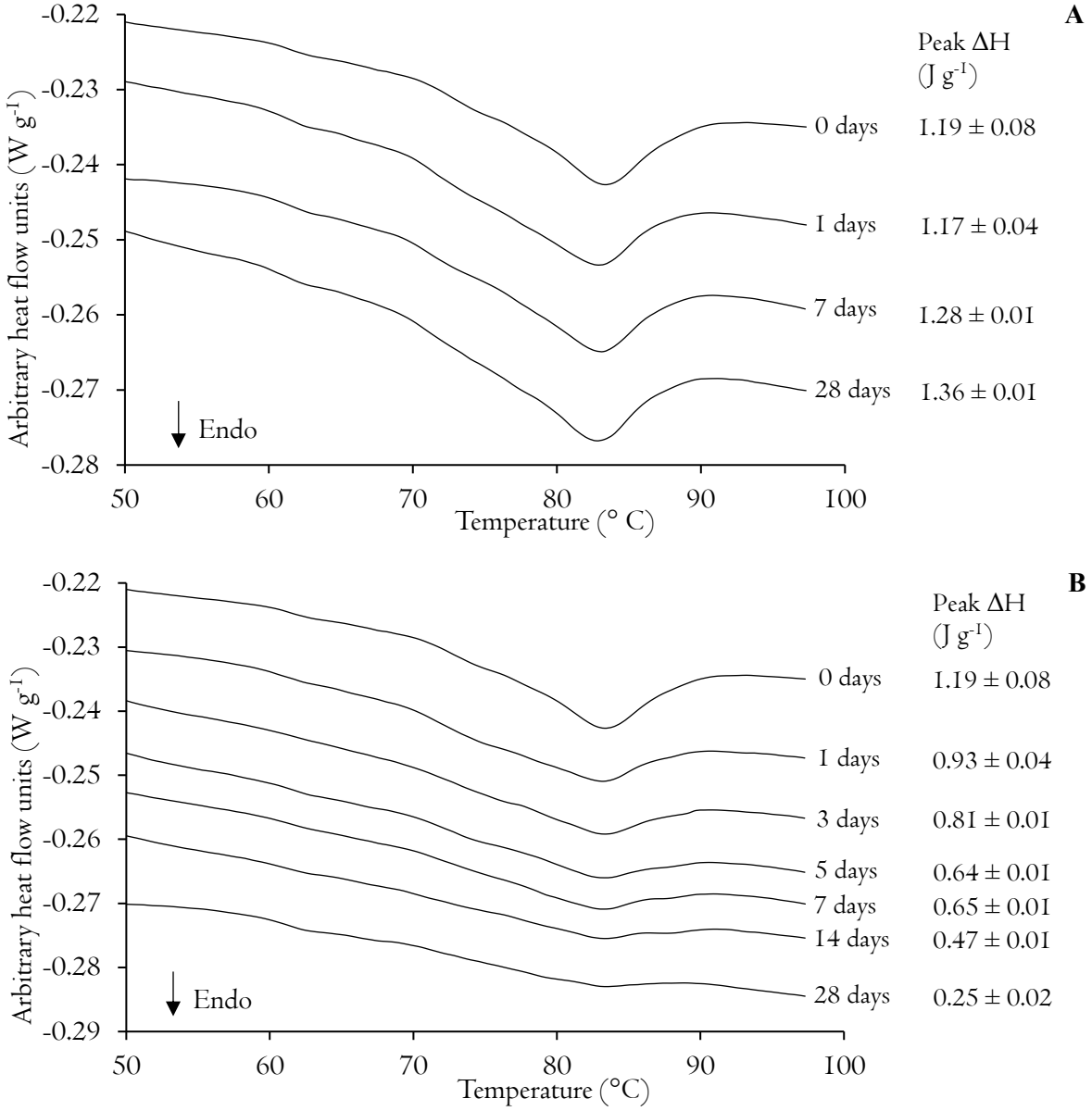

Figure 17: Differential scanning calorimetry thermograms of egg yolk stored for up to 28 days under refrigerated (A, 0.1 MPa, 4.0 ± 0.5 °C) or hyperbaric conditions (B, 200 MPa, 20 ± 2 °C). Enthalpy of protein denaturation peak (Peak ΔH) is also shown.

In all samples, calorimetric analyses revealed the presence of a broad endothermic peak at 83 °C (Figure 17), primarily ascribable to the thermal denaturation of low density-lipoproteins (LDL) and high density-lipoproteins (HDL) protein fractions (Yan et al., 2010). When egg yolk was stored under refrigerated conditions (Figure 17 A), a slight but progressive increase in this peak was detected throughout the 28 days storage. Such an increase could be associated to the rearrangement of protein structures towards a more ordered conformation, possibly indicating the presence of more abundant or more thermally stable molecular bonds (Arntfield & Murray, 1981; Li-Chan & Ma, 2002). By contrast, an opposite change in peak enthalpy was detected during HS, so that after 28 days it was about 20% of the one detected in the untreated sample (Figure 17 B). Such a different trend suggests that HS promoted extensive denaturation of egg yolk proteins by modifying their structure towards highly disordered random coil conformation (Seelig & Schönfeld, 2016). It is noteworthy that a strong negative correlation (r = -0.851) was found between protein denaturation enthalpy (Figure 17 B) and viscosity (Table 26) of pressurized egg yolk, further supporting the hypothesis that matrix thickening was mainly accounted for by protein structural changes (Lai et al., 2010; Yan et al., 2010).
To better understand the effects of HS on egg yolk proteins, samples were further analyzed for particles size, free SH groups and absorbance at 280 nm (Table 27).

Table 27: Particle size, free SH groups and absorbance at 280 nm of egg yolk stored for up to 28 days under refrigerated (0.1 MPa, 4.0 ± 0.5 °C) or hyperbaric (200 MPa, 20 ± 2 °C) conditions.

Storage	Time (days)	Particle size (nm)	Free SH groups ($\mu M\ g^{-1}$)	Absorbance at 280 nm
Fresh	0	134.38 ± 4.82^{d}	34.24 ± 1.18^{cd}	0.223 ± 0.006^{g}
Refrigerated	1	N.D.	28.73 ± 1.21^{e}	0.281 ± 0.002^{e}
	3	N.D.	33.05 ± 0.92^{de}	N.D.
	7	138.44 ± 6.22^{cd}	N.D.	N.D.
	14	133.34 ± 6.14^{cd}	38.75 ± 1.60^{cd}	0.264 ± 0.006^{f}
	28	157.96 ± 7.16^{ab}	48.79 ± 1.63^{a}	0.308 ± 0.001^{d}
Hyperbaric	1	N.D.	36.57 ± 1.18^{cd}	0.376 ± 0.003^{a}
	3	N.D.	42.10 ± 1.24^{b}	0.366 ± 0.005^{ab}
	7	148.16 ± 7.39^{bc}	N.D.	0.361 ± 0.006^{b}
	14	181.17 ± 5.52^{a}	48.25 ± 2.15^{a}	0.316 ± 0.005^{d}
	28	165.48 ± 5.90^{ab}	49.45 ± 1.85^{a}	0.345 ± 0.004^{c}

N.D. Not determined; [a] Different letters in the same column indicate significantly different means (ANOVA; p <0.05).

Before storage, egg yolk showed the presence of a single particle family with ~ 134 nm diameter, ascribable to LDL and HDL particles aggregates (Speroni et al., 2005). During storage under both pressurized and refrigerated conditions, size, SH groups exposure and absorbance at 280 nm of these particles progressively increased (Table 27), indicating that, regardless the applied conditions, egg yolk proteins swelled and exposed sulphurated and aromatic aminoacidic residues (Beveridge et al., 1974; Goldfarb et al., 1951). In the refrigerated samples, these changes might be associated to the activity of egg yolk endogenous proteases (*e.g.*, aspartic proteases, matrix metalloproteinase), which are known to modify protein structure during prolonged storage (*e.g.*, 20-40 days) (Gao et al., 2016). When samples were stored by HS, changes in free SH groups and absorbance at 280 nm occurred in shorter times. Such effect was probably due to the action of pressure on the highly barosensitive structure of egg yolk protein (Yan et al., 2010). In particular, absorbance at 280 nm of egg yolk increased by 70% after just 1 day and remained significantly higher ($p < 0.05$) than that of refrigerated samples for up to 28 days. These results indicate that HS promoted a higher exposure of hydrophobic aromatic aminoacids. In the light of this evidence, it is reasonable that egg yolk protein denaturation (Figure 17 B) occurred based on intense hydrophobic interaction between exposed aromatic aminoacids (Lai et al., 2010; Yan et al., 2010).

Based on the changes induced by hyperbaric storage on egg yolk physical properties and protein structure, further analyses were carried out to assess the effect of HS on the techno-functional properties of this matrix. In particular, solubility, foaming capacity, foam stability, thermal gelling capacity and emulsifying activity were considered. Results are shown in Table 28. No changes in solubility were observed under refrigerated storage for up to 28 days, whereas egg yolk was substantially less soluble after just 14 days under HS. Such trend has been frequently associated to protein unfolding and often observed in concomitance to thickening in pressurized egg yolk (Naderi et al., 2017). Independently on the application of pressure, an increase in foaming capacity was observed during both refrigeration and HS (Table 28), suggesting storage time to promote a more efficient displacement of proteins at solvent-air interfaces during storage of egg yolk. However, when HS was prolonged for up to 28 days, a decrease in this property was detected, indicating a slower positioning of proteins at the bubble interface, probably due to their entrapment in a gelled network (Table 26). Nevertheless, foam stability seemed not to be affected by storage conditions (Table 28). The thermal gelling capacity of egg yolk was observed to progressively decrease during both refrigerated and hyperbaric storage, but this effect faster occurred under pressure. This is likely due to the fact that pressurized proteins would be already

interconnected in a network (Table 26) and thus less prone to interconnect upon further heating (Kiosseoglou, 2003).

Table 28: Solubility, foaming capacity, foam stability, thermally-obtained gel elastic modulus (G') and emulsifying activity index (EAI) of egg yolk stored for up to 28 days under refrigerated (0.1 MPa, 4.0 ± 0.5 °C) or hyperbaric (200 MPa, 20 ± 2 °C) conditions.

Storage	Time (days)	Solubility (%)	Foaming capacity (%)	Foam stability (%)	G' (Pa · 1000)	EAI (m^2 g^{-1})
Fresh	0	95.7 ± 1.2[a]	113.3 ± 15.3[bc]	88.8 ± 6.0[ab]	33.95 ± 1.02	9.71 ± 0.43[ab]
Refrigerated	5	N.D.	N.D.	N.D.	29.92 ± 4.30	N.D.
	7	N.D.	140.0 ± 10.0[ac]	97.2 ± 2.5[a]	N.D.	9.58 ± 0.68[ab]
	14	92.0 ± 1.0[a]	156.7 ± 5.8[a]	92.3 ± 3.8[ab]	25.42 ± 1.20	7.95 ± 0.65[b]
	28	92.7 ± 1.5[a]	150.0 ± 10.0[a]	97.3 ± 2.4[a]	22.82 ± 2.51	9.54 ± 0.19[ab]
Hyperbaric	5	N.D.	N.D.	N.D.	25.31 ± 3.59	N.D.
	7	N.D.	146.7 ± 5.8[ab]	97.3 ± 2.3[a]	16.85 ± 0.57	11.07 ± 0.68[a]
	14	23.0 ± 4.5[c]	133.3 ± 15.3[ac]	95.7 ± 0.3[a]	15.54 ± 1.48	9.25 ± 0.87[ab]
	28	45.3 ± 0.6[b]	106.7 ± 20.8[c]	85.6 ± 3.9[b]	17.16 ± 0.56	9.88 ± 0.78[ab]

N.D. Not determined; [a] Different letters in the same column indicate significantly different means (ANOVA; $p < 0.05$).

The capacity of egg yolk to form stable emulsions (EAI) remained unaffected throughout pressurized storage and not different from that of the fresh sample (Table 28). This result indicates that even prolonged pressurization at 200 MPa did not significantly affect the capability of proteins to position at water-oil interfaces despite their extensive unfolding (Figure 17 B). It is however noteworthy that the maintenance of egg yolk emulsifying activity could be also due to the high concentration of amphiphilic phospholipids (Anton, 2013), which could have made negligible the effects of protein structural modifications.

The capability of HS to steer selected techno-functional properties of egg yolk might represent an interesting opportunity when referred to specific fields of application. For instance, HS-thickened egg yolk might be used to steer the rheological properties of emulsified dips and sauces (*e.g.*, mayonnaise) (Anton, 2013; Huang & Ahn, 2019). In this context, textural enhancement of these matrices could be obtained without affecting their physical stability (Table 28). Moreover, water-insoluble (*i.e.*, hydrophobic) egg yolk obtained by HS could find application to improve the oil-binding capacity of fat-rich spreads.

4.6 Conclusions

Hyperbaric storage was shown to modify protein structure and improve techno-functionality of raw skim milk, egg white and egg yolk. The effects of hyperbaric storage seem to be affected by protein native structure, as schematized in Figure 18.

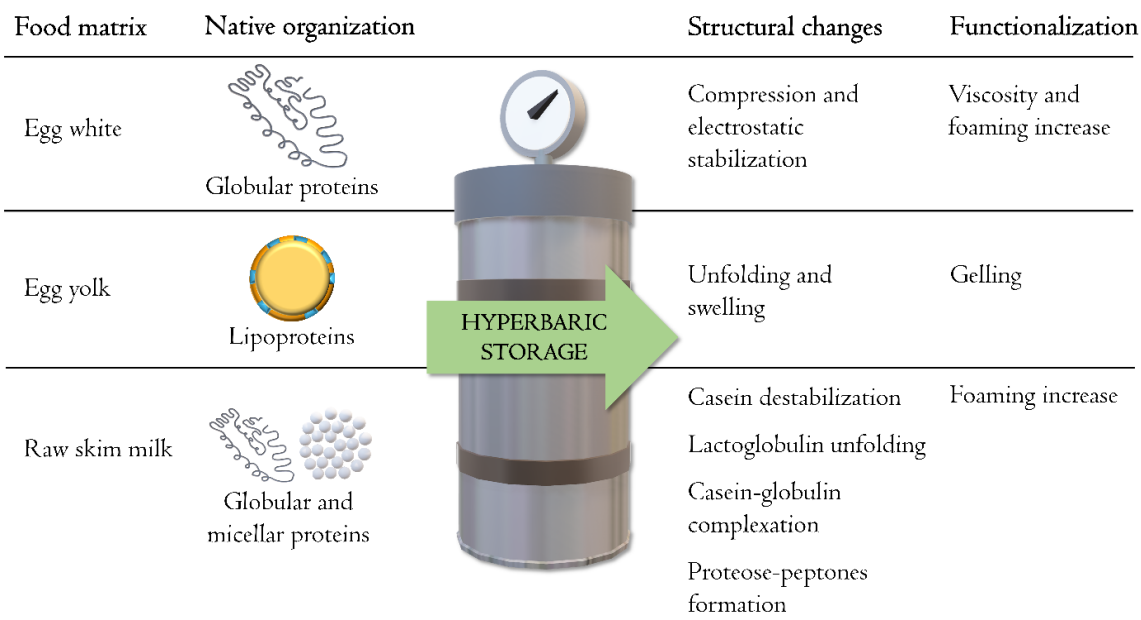

Figure 18: Schematization of the effect of hyperbaric storage on food matrices characterized by different protein native organization.

HS can induce slight modifications of particle size and electrostatic behavior of globular proteins as well as their severe unfolding (Figure 18). These structural modifications can result in changes in techno-functionality, as observed for the increase in foaming of egg white or milk. In the case of more complex proteins, such as micellar casein, HS can significantly induce destabilization, resulting in progressive coagulation (Paragraph 3.1). In addition, when different proteins are concomitantly present, HS is likely to promote their interaction. For instance, in the case of milk, destabilized micelles can serve as local aggregation points for unfolded β-lactoglobulin. In the case of even more complex protein-lipid structures, unfolding of membrane proteins could drive protein networking leading to the complete gelation of the system, as observed for egg yolk lipoproteins. Interestingly, HS-induced structural modification of proteins could make them more prone to enzymatic hydrolysis, suggesting

that the effect of HS on enzyme activity is not only directed towards the catalytic protein (Paragraph 3.2) but also towards its protein substrate.

It is reasonable to infer that functionalization of protein-rich foods by HS could be extended to matrices other than those here tested. However, considering the clear influence of protein native structure on the effect of HS, potentially unexpected outcomes might be obtained. This aspect should be taken into careful consideration in future research on HS. To this regard, plant-derived ingredients rich in proteins would be particularly worthy of investigation. The application of HS to these foods has never been attempted but could represent an innovative and sustainable way to enhance their poor techno-functionality, increasing their potentiality of being integrated in a number of food formulations.

Chapter 5: Industrial readiness of hyperbaric storage

Despite the demonstrated capability of HS of serving multiple purposes within the food production chain (*e.g.*, storage, pasteurization, blanching, protein functionalization), the scaling-up of the technology from research laboratories to industrial contexts has never been attempted (TRL = 2-3). This is due to the fact that many technical criticalities still need to be addressed before HS can be regarded as industrially viable. Besides the packaging issue, here addressed in Chapter 2, the most critical lack in the development of HS is represented by the design and construction of economically feasible working units and by the scarce techno-economical know-how. To the best of our knowledge, only one scientific publication has so far reported a rigorous environmental and techno-economical evaluation of the technology (Bermejo-Prada, et al., 2017). In this study, the cost and the carbon footprint of HS were compared to those of conventional refrigeration, considering strawberry juice as the reference product. By focusing the attention on this matrix, the Authors conceptualized a novel HS working unit, designed specifically for bulk liquid foods (Figure 2C, Chapter 1). The latter consisted of a single pressure intensifier, which would pump and pressurize (up to 25 MPa) liquid foods directly inside interchangeable cylindrical steel vessels. The pressurized vessels would then be stored in warehouses at room temperature for up to 15 days. After storage, the tanks would be depressurized, and the food would be pumped out, bottled, and shipped to retailers. Not needing any packaging material nor any dedicated pressurizing fluid, this equipment configuration allowed very low CO_2 emissions (*i.e.*, 0.0042 $kgCO_2 \cdot kg_{juice}^{-1} \cdot 15\ days^{-1}$), which were about 26 times lower than those of refrigeration. These data actually confirmed for the first time the capability of HS at room temperature to be significantly less environmentally impactful than cold storage. On the other hand, the cost of HS within the considered study boundaries was found to be high (*i.e.*, 0.291 € $\cdot kg_{juice}^{-1} \cdot 15\ days^{-1}$), being almost 4-fold that of refrigeration. This was obviously associated with the expensive amortization of the HS equipment (~ 40,000 € versus ~ 7,300 € for refrigeration) which, in its turn, was due to the high cost of pressure-holding vessels (35,000 € for 4 interchangeable tanks made of 15-5 PH steel) (Bermejo-Prada et al., 2017). Although the results of this analysis were not supportive of pressurized storage from an economic standpoint, it must be highlighted that several solutions could be readily adopted to overcome this issue. For instance, composite materials (*e.g.*, aramid, glass or carbon fibres) could be used instead

of specialized steel alloys for manufacturing the pressure-holding vessels. Besides allowing a drastic cost reduction, the use of composite HS tanks would offer several further upsides, such as weight reduction, and enhanced resistance to mechanical failure and wear (Bunsell & Thionnet, 2015). An advantage would be also provided by the fact that the technical know-how required to build composite HS vessels could be easily transferred from other industrial sectors (*e.g.*, gases production and containment), in which these elements are already widely employed (Bunsell & Thionnet, 2015).

The effort of implementing technical solutions to make HS economically viable would be strictly required if the technology was intended as a sustainable approach for food storage solely (Bermejo-Prada et al., 2017). Nevertheless, the results reported in this Thesis actually demonstrate that the scope of HS could be much wider. In particular, the technology showed potential as a novel, non-thermal approach to pasteurize, blanch, chemically stabilize (Chapter 3) and functionalize (Chapter 4) foods during their storage. Based on this evidence, it can be inferred that a proper assessment of the economic viability of HS should compare the technology not only to refrigeration, but also to conventional and non-conventional food treatment technologies. Although there is no evidence of such assessment in the literature, few studies have reported detailed cost analyses of food processing technologies, making possible a tentative comparison. For example, considering fruit juice pasteurization, the cost of thermal (0.015 € L^{-1}) and pulsed electric field (0.022 € L^{-1}) treatments is remarkably lower than that of juice storage by HS (Sampedro et al., 2013). This is primarily due to the fact that no pressure-holding vessel is required to apply heat or electric fields to foods, thus allowing for a significantly lower amortization as compared to HS. Coherently with these considerations, when pressure-based approaches like HHP and dense-phase carbon dioxide (DP-CO_2) are taken into account, the cost rises dramatically. In particular, juice pasteurization using HHP and DP-CO_2 are estimated to have a cost of 0.10-0.45 € kg^{-1} and 0.3 € kg^{-1}, respectively (Aganovic et al., 2017, 2020; Gallinaro et al., 2021, Sampedro et al., 2014). Based on the fact that these estimations match the one proposed by Bermejo-Prada et al. (2017) for pressurized storage of strawberry juice, it can be reasonably inferred that HS could be economically sustainable when considered in a food processing context. Although based on circumstantial evidence solely, this hypothesis is further corroborated by the fact that HHP and DP-CO_2 cost analyses were carried out within large production scale boundaries (*i.e.*, 200-3000 L h^{-1}), whereas HS was examined at pilot-plant scale solely (*i.e.*, 200 kg every 15 days). It is thus likely that, upon scaling-up, the processing cost of HS would become much more competitive, suggesting the possibility of its use as a low economic-intensive food processing technology. However, it must be reminded that this possibility

will be ascertained only upon the availability of sound cost analysis studies taking into account the economic viability of HS in its newly discovered fields of application.

Chapter 6: Conclusions and future perspectives

This Ph.D. Thesis demonstrates that HS represents not only a promising alternative to food refrigeration but also a multi-tasking technology concomitantly providing multiple advantages, including:

- non-thermal pasteurization of perishable foods;
- non-thermal inactivation of food enzymes;
- inhibition of the development of non-enzymatic browning;
- functionalization of protein-rich foods.

Based on these considerations, the results acquired suggest that HS has the potential to evolve from storage technology to non-conventional treatment to improve food quality in a number of different ways. For instance, moderate pressure treatments could be applied to improve food nutritional value. To this regard, pressure-induced enhancement of milk proteins surface activity is just an example of a potential approach to improve the rheological and nutritional properties of dairy products by integration of β-Lg in cheese curds or in the protein network of fermented milk. Similarly, HS could be applied to steer biotechnological processes based on protease activity (*e.g.*, ripening, curing, and development of fermentative processes) by controlling the structure of both the catalytic and the substrate proteins.

In this framework, a number of different scenarios requiring more in-depth investigations could be also envisaged. This could include functionalization of food biomolecules other than proteins, such as polysaccharides and lipids. For instance, HS could be applied to control fat crystallization allowing to steer their polymorphism, ultimately obtaining plastic fats with tailored mechanical properties and physical stability. The latter are completely unexplored, yet very promising, research topics.

It is noteworthy that the rational management of the effect of HS on food phenomena requires the predictive knowledge of their mechanisms and kinetics. The Thesis demonstrates the full applicability of traditional models, such as Bigelow, Eyring and Arrhenius ones to predict the development of phenomena occurring during HS. This result corroborates the hypothesis that HS could be efficaciously implemented in food processing lines, with easy prediction of processing outcomes. However, several development gaps need to be filled in order to make this technology viable for a food industry context. First of all, the technical development of HS equipment should be carefully considered, since current working units operate in lab-scale and for research purposes, solely. The

implementation of hyperbaric storage in food industries will strictly depend on the availability of working units viable for industrial application, easy to operate, and feasible from an economic perspective. An additional issue is represented by packaging since only petroleum-based plastic materials were found to be feasible for HS. An urgent research topic is represented by the identification of biodegradable or compostable packaging solutions withstanding HS conditions. Packaging-free working units for storage of bulk liquid foods would certainly represent an interesting opportunity to further improve the technology sustainability. Overcoming these gaps would allow to fully exploit the wide potential of hyperbaric storage.

Chapter 7: Impact of the Thesis

Although the possibility to store perishable foods using moderate hydrostatic pressure has been known since the '70s, the first literature evidence on food hyperbaric storage only appeared in 2012, along with the availability of the first lab-scale pilot plants (Figure 19). In the following years, two research groups (Prof. Otero, ICTAN-CSIC, Spain; Prof. Saraiva, University of Aveiro, Portugal), started to explore the potentiality of the technology. Hyperbaric storage is however still in its early steps, as shown by the limited number of papers published so far (Figure 19).

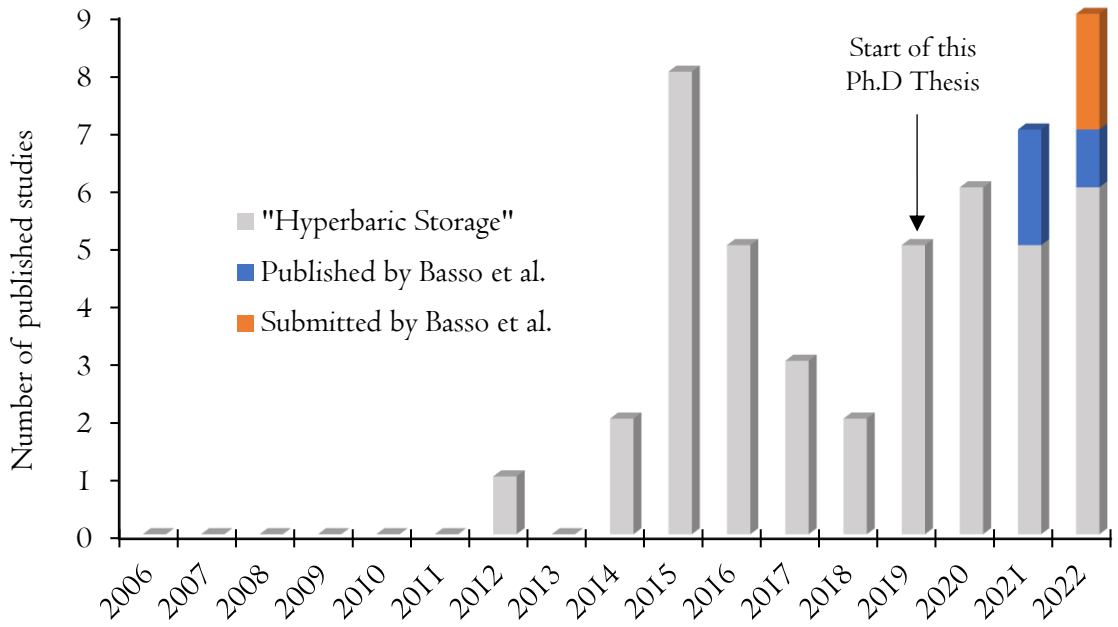

Figure 19: Number of papers available on "*FSTA® - the food science resource*" with "hyperbaric storage" as keyword (24/01/2023). Scientific contributions provided by this Ph.D Thesis are also shown.

In the last decade, the primary focus of the research on hyperbaric storage has been oriented towards the possibility of applying the technology at room temperature as a sustainable alternative to conventional refrigeration. In this framework, the contribution of the present Ph.D Thesis, which began in November 2019, has consisted of one review and two research papers (Table 29). The dissemination

of the results has thus already begun and will proceed over the next years. In fact, 2 more research papers are currently under review and 2 are under drafting. Out of the drafted papers, one is being prepared in collaboration with the research group led by Prof. Saraiva.
Dissemination is primarily oriented to researchers investigating pressure-based food technologies, but it could be expanded to the industrial sector. In particular, the work has been presented to the leading European company in the production of hyperbaric equipment, discussing its potential appeal as a technology worthy of future investments.

Further impact can be envisaged on Author's career as a researcher.
The work performed on hyperbaric storage in the context of this Ph.D has allowed me to learn and apply a sound scientific approach to research activity, from the planning and execution of laboratory work to the elaboration and visualization of gathered data, to critical interpretation and communication of results. Despite criticalities related to COVID-19, I had also the opportunity to improve my networking skills during the 6-month period of study and research at the University of Aveiro (Portugal) as well as by carrying out cooperative investigation with researchers from the University of Modena and Reggio Emilia. During the doctorate, I also had the chance to hold seminars on non-thermal food technologies for Food Science and Technology M.Sc. students, and to tutor 10 undergraduate students for the preparation of their Thesis projects.
Based on the work carried out during the Ph.D., I hope to have acquired the scientific and personal skills necessary to successfully apply for future research grants or job opportunities at both national and international level, hopefully in the growing sector of non-thermal food technologies. This would enable me to concretely transfer the acquired know-how into a significantly broad professional experience and to provide a substantial contribution to future developments in this field.

Table 29: List of scientific contributions of this Thesis.

Journal articles	Manzocco, L., Basso, F., & Nicoli, M. C. (2023). Effect of hyperbaric storage at room temperature on the activity of polyphenoloxidase in model systems and apple juice. *Food and Bioprocess Technology*.
	Basso, F., Innocente, N., Maifreni, M., Manzocco, L., & Nicoli, M. C. (2022). Raw milk preservation by hyperbaric storage: effect on microbial counts, protein structure and technological functionality. *Food Research International*, *156*, Article 111090.
	Basso, F., Manzocco, L., & Nicoli, M. C. (2022). Hyperbaric storage of food: applications, challenges and perspectives. *Food Engineering Reviews*, *14*, 20-30.
	Basso, F., Manzocco, L., Maifreni, M., & Nicoli, M. C. (2021). Hyperbaric storage of egg white at room temperature: effects on hygienic properties, protein structure and technological functionality. *Innovative Food Science and Emerging Technologies*, *74*, Article 102847.
	Manzocco, L., Basso, F., Plazzotta, S., & Calligaris, S. (2021). Study on the possibility of developing food-grade hydrophobic bio-aerogels by using an oleogel template approach. *Current Research in Food Science*, *4*, 115-120.
	Basso, F., Manzocco, L., Maifreni, M., Alongi, M., & Nicoli, M. C. (*under review*). Changes in microbial, chemical, physical and techno-functional properties of liquid egg yolk during hyperbaric storage. *LWT – Food Science and Technology*.
	Basso, F., Feroce, A., Manzocco, L., Licciardello, F., & Nicoli, M. C. (*under review*). Exploring the effects of hyperbaric storage on the structural, optical, mechanical and diffusional properties of food packaging materials. *Food Packaging and Shelf Life*.
	Basso, F., et al. (*paper drafting*). Effect of hyperbaric storage on the kinetics of the Maillard reaction in sugar-aminoacid model solutions at different pH.
Oral presentations	Basso, F. (2022). Hyperbaric storage: an innovative and sustainable technology to extend stability and improve functionality of food. *26th Workshop on the Developments in the Italian Ph.D. Research on Food Science Technology and Biotechnology*, Asti, Italy.
	Basso, F., Manzocco, L., & Nicoli, M. C. (2022). Steering the structural and functional properties of proteins in food by hyperbaric storage: the case studies of egg derivatives, raw skim milk and apple juice. *11th International Conference on High Pressure Bioscience and Biotechnology (HPBB 2022)*, Copenhagen, Denmark.

	Basso, F., Manzocco, L., & Nicoli, M. C. (2021). Exploring the potentiality of hyperbaric storage to steer hygienic and techno-functional properties of egg white. *6th International ISEKI-Food Conference (ISEKI-Food 2021)*, Online.
Poster presentations	Basso, F., Feroce, A., Manzocco, L., & Licciardello, F. (2022). Exploring the effects of hyperbaric storage on the structural, optical, mechanical and barrier properties of food packaging materials. *10th Shelf Life International Meeting (SLIM2022)*, Bogotà, Colombia. Basso, F. (2021). Hyperbaric storage: an innovative and sustainable preservation technology for fresh food ingredients. *Ist Virtual Workshop on the Developments in the Italian PhD Research on Food Science, Technology and Biotechnology*, Online. Basso, F., Manzocco, L., & Nicoli, M. C. (2021). DSC to reveal structural changes in egg white submitted to hyperbaric storage at room temperature. *XLII National Conference on Calorimetry, Thermal Analysis and Applied Thermodynamics*.
Awards	Best poster award of the *10th Shelf Life International Meeting (SLIM 2022)* Best oral presentation award of the *6th International ISEKI-Food Conference (ISEKI-Food 2021)*

Chapter 8: References

Abe, F. (2007). Exploration of the effects of high hydrostatic pressure on microbial growth, physiology and survival: perspectives from piezophysiology. *Bioscience, Biotechnology and Biochemistry*, *71*, 2347–2357.

Abe, F., & Iida, H. (2003). Pressure-induced differential regulation of the two tryptophan permeases Tat1 and Tat2 by ubiquitin ligase Rsp5 and its binding proteins, Bul1 and Bul2. *Molecular and Cellular Biology*, *23*, 7566–7584.

Abeyrathne, E. D. N. S., Lee, H. Y., & Ahn, D. U. (2013). Egg white proteins and their potential use in food processing or as nutraceutical and pharmaceutical agents-A review. *Poultry Science*, *92*, 3292–3299.

Aganovic, K., Hertel, C., Vogel, Rudi. F., Johne, R., Schlüter, O., Schwarzenbolz, U., Jäger, H., Holzhauser, T., Bergmair, J., Roth, A., Sevenich, R., Bandick, N., Kulling, S. E., Knorr, D., Engel, K.-H., & Heinz, V. (2020). Aspects of high hydrostatic pressure food processing: Perspectives on technology and food safety. *Comprehensive Reviews in Food Science and Food Safety*, *20*, 3225–3266.

Aganovic, K., Smetana, S., Grauwet, T., Toepfl, S., Mathys, A., Van Loey, A., & Heinz, V. (2017). Pilot scale thermal and alternative pasteurization of tomato and watermelon juice: An energy comparison and life cycle assessment. *Journal of Cleaner Production*, *141*, 514–525.

Ahromrit, A., Ledward, D. A., & Niranjan, K. (2007). Kinetics of high pressure facilitated starch gelatinisation in *Thai* glutinous rice. *Journal of Food Engineering*, *79*, 834–841.

Ajandouz, E. H., & Puigserver, A. (1999). Nonenzymatic browning reaction of essential amino acids: Effect of pH on caramelization and Maillard reaction kinetics. *Journal of Agricultural and Food Chemistry*, *47*, 1786–1793.

Alberini, F., Simmons, M. J. H., Parker, D. J., & Koutchma, T. (2015). Validation of hydrodynamic and microbial inactivation models for UV-C treatment of milk in a swirl-tube "SurePure TurbulatorTM." *Journal of Food Engineering*, *162*, 63–69.

Al-Ghamdi, S., Rasco, B., Tang, J., Barbosa-Cánovas, G. V., & Sablani, S. S. (2019). Role of package headspace on multilayer films subjected to high hydrostatic pressure. *Packaging Technology and Science*, *32*, 247–257.

Ami, D., Mereghetti, P., & Maria, S. (2013). *Multivariate analysis for Fourier transform infrared spectra of complex biological systems and processes*. L. Freitas, & A. P. B. R. De Freitas (Eds.). Intechopen.

Anema, S. G. (2008). Heat and/or high-pressure treatment of skim milk: Changes to the casein micelle size, whey proteins and the acid gelation properties of the milk. *International Journal of Dairy Technology*, *61*, 245–252.

Anema, S. G. (2012). Pressure-induced denaturation of β-lactoglobulin in skim milk: Effect of milk concentration. *Journal of Agricultural and Food Chemistry*, *60*, 6565–6570.

Anema, S. G., Lowe, E. K., & Stockmann, R. (2005). Particle size changes and casein solubilisation in high-pressure-treated skim milk. *Food Hydrocolloids*, *19*, 257–267.

Anema, S. G., Stockmann, R., & Lowe, E. K. (2005). Denaturation of β-lactoglobulin in pressure-treated skim milk. *Journal of Agricultural and Food Chemistry*, *53*, 7783–7791.

Anese, M., Nicoli, M. C., Dall'Aglio, G., & Lerici, C. R. (1994). Effect of high pressure treatments on peroxidase and polyphenoloxidase activities. *Journal of Food Biochemistry*, *18*, 285–293.

Anton, M. (2013). Egg yolk: Structures, functionalities and processes. *Journal of the Science of Food and Agriculture*, *93*, 2871–2880.

Anton, M., & Gandemer, G. (1997). Composition, solubility and emulsifying properties of granules and plasma of egg yolk. *Journal of Food Science*, *62*, 484–487.

AOAC. (1973). AOAC final action method 17.002, colour of eggs. *Journal of the Association of Official Analytical Chemists*, 56, 272.

Araújo, S. V., Rocha, B. S., Luna, F. M. T., Rola, E. M., Azevedo, D. C. S., & Cavalcante, C. L. (2011). FTIR assessment of the oxidation process of castor oil FAME submitted to PetroOXY and Rancimat methods. *Fuel Processing Technology*, *92*, 1152–1155.

Arntfield, S. D., & Murray, E. D. (1981). The influence of processing parameters on food protein functionality 1. Differential scanning calorimetry as an indicator of protein denaturation. *Canadian Institute of Food Science and Technology Journal*, *14*, 289–294.

Arrhenius, S. A. (1901). *Lärobok i teoretisk elektrokemi*. Quando&Handel.

Ashby, R. (1988). Migration from polyethylene terephthalate under all conditions of use. *Food Additives and Contaminants*, *5*, 485–492.

Ashoor, S. H., & Zent, J. B. (1984). Maillard browning of common amino acids and sugars. *Journal of Food Science*, 49, 1206–1207.

ASTM. (2001a). Standard test method for tensile properties of thin plastic sheeting (D882-12).

ASTM. (2001b). Standard test methods for water vapor transmission of materials (E96-00e1).

Aubourg, S. P., Tabilo-Munizaga, G., Reyes, J. E., Rodríguez, A., & Pérez-Won, M. (2010). Effect of high-pressure treatment on microbial activity and lipid oxidation in chilled coho salmon. *European Journal of Lipid Science and Technology*, *112*, 362–372.

Balny, C., & Masson, P. (1993). Effects of high pressure on proteins. *Food Reviews International*, *9*, 611–628.

Bartolomeoli, I., Maifreni, M., Frigo, F., Urli, G., & Marino, M. (2009). Occurrence and characterization of *Staphylococcus aureus* isolated from raw milk for cheesemaking. *International Journal of Dairy Technology*, *62*, 366–371.

Bermejo-Prada, A., Colmant, A., Otero, L., & Guignon, B. (2017). Industrial viability of the hyperbaric method to store perishable foods at room temperature. *Journal of Food Engineering*, *193*, 76–85.

Bermejo-Prada, A., & Otero, L. (2016). Effect of hyperbaric storage at room temperature on color degradation of strawberry juice. *Journal of Food Engineering*, *169*, 141–148.

Bermejo-Prada, A., Segovia-Bravo, K. A., Guignon, B., & Otero, L. (2015). Effect of hyperbaric storage at room temperature on pectin methylesterase activity and serum viscosity of strawberry juice. *Innovative Food Science and Emerging Technologies*, *30*, 170–176.

Bermejo-Prada, A., Vega, E., Pérez-Mateos, M., & Otero, L. (2015). Effect of hyperbaric storage at room temperature on the volatile profile of strawberry juice. *LWT – Food Science and Technology*, *62*, 906–914.

Beveridge, T., Toma, S. J., & Nakai, S. (1974). Determination of SH- and SS-groups in some food proteins using Ellman's reagent. *Journal of Food Science*, 39, 49–51.

Boonyaratanakornkit, B. B., Park, C. B., & Clark, D. S. (2002). Pressure effects on intra-and intermolecular interactions within proteins. *Biochimica et Biophysica Acta (BBA) – Protein Structure and Molecular Enzymology*, *1595*, 235–249.

Bravo, F. I., Felipe, X., López-Fandiño, R., & Molina, E. (2015). Skim milk protein distribution as a result of very high hydrostatic pressure. *Food Research International*, *72*, 74–79.

Bristow, M., & Isaacs, N. S. (1999). The effect of high pressure on the formation of volatile products in a model Maillard reaction. *Journal of the Chemical Society, Perkins transactions 2*, 2213–2218.

Buccioni, A., Minieri, S., & Rapaccini, S. (2013). Effect of total proteosepeptone content on the variability of bovine milk foaming property. *Italian Journal of Animal Science*, *12*, 72–76.

Bull, M. K., Steele, R. J., Kelly, M., Olivier, S. A., & Chapman, B. (2010). Packaging under pressure: Effects of high pressure, high temperature processing on the barrier properties of commonly available packaging materials. *Innovative Food Science and Emerging Technologies*, *11*, 533–537.

Bunsell, A. R., & Thionnet, A. (2015). The control of the residual lifetimes of carbon fibre-reinforced composite pressure vessels. In P. Beaumont, C. Soutis, & A. Hodzic (Eds.), *Structural Integrity and Durability of Advanced Composites: Innovative Modelling Methods and Intelligent Design* (pp. 309–423). Elsevier Ltd.

Campus, M. (2010). High pressure processing of meat, meat products and seafood. *Food Engineering Reviews*, *2*, 256–273.

Caner, C., Hernandez, R. J., & Harte, B. R. (2004). High-pressure processing effects on the mechanical, barrier and mass transfer properties of food packaging flexible structures: A critical review. *Packaging Technology and Science*, *17*, 23–29.

Caner, C., Hernandez, R. J., & Pascal, M. A. (2000). Effect of high-pressure processing on the permeance of selected high-barrier laminated films. *Packaging Technology and Science*, *13*, 183–195.

Caner, C., Hernandez, R. J., Pascall, M. A., & Riemer, J. (2003). The use of mechanical analyses, scanning electron microscopy and ultrasonic imaging to study the effects of high-pressure processing on multilayer films. *Journal of the Science of Food and Agriculture*, *83*, 1095–1103.

Chapleau, N., Mangavel, C., Compoint, J. P., & de Lamballerie-Anton, M. (2004). Effect of high-pressure processing on myofibrillar protein structure. *Journal of the Science of Food and Agriculture*, *84*, 66–74.

Charm, S. E., Longmaid, H. E., & Carver, J. (1977). A simple system for extending refrigerated, nonfrozen preservation of biological material using pressure. *Cryobiology*, *14*, 625–636.

Cheftel, J. C., & Culioli, J. (1997). Effects of high pressure on meat: A review. *Meat Science*, *46*, 211–236.

Cho, Y., Singh, H., & Creamer, L. K. (2003). Heat-induced interactions of β-lactoglobulin A and κ-casein B in a model system. *Journal of Dairy Research*, *70*, 61–71.

Choi, W. S., Son, N., Cho, J., Joo, I. S., Han, J. A., Kwak, H. S., Hong, J. H., & Suh, S. H. (2019). Predictive model of *Staphylococcus aureus* growth on egg products. *Food Science and Biotechnology*, *28*, 913–922.

de Groot, J., & de Jongh, H. H. J. (2003). The presence of heat-stable conformers of ovalbumin affects properties of thermally formed aggregates. *Protein Engineering*, *16*, 1035–1040.

de Kruif, C. G. (1999). Casein micelle interactions. *International Dairy Journal*, *9*, 183–188.

De Noni, I., Pellegrino, L., Cattaneo, S., & Resmini, P. (2007). HPLC of proteose peptones for evaluating ageing of packaged pasteurized milk. *International Dairy Journal*, *17*, 12–19.

Dewimille, B., Martin, J., & Jarrin, J. (1993). Behavior of thermoplastic polymers during explosive decompressions in a petroleum environment. *Journal De Physique*, *3*, C7/1559–C7/1564.

Dobiáš, J., Voldřich, M., Marek, M., & Chudáčková, K. (2004). Changes of properties of polymer packaging films during high pressure treatment. *Journal of Food Engineering*, *61*, 545–549.

EFSA. (2014). Scientific Opinion on the public health risks of table eggs due to deterioration and development of pathogens. *EFSA Journal*, *12*, 3782.

EFSA. (2015). Scientific Opinion on the public health risks related to the consumption of raw drinking milk. *EFSA Journal*, *13*, 3940.

Eisenmenger, M. J., & Reyes-De-Corcuera, J. I. (2009). High pressure enhancement of enzymes: A review. *Enzyme and Microbial Technology*, *45*, 331–347.

Ellman, G. L. (1959). Tissue sulhydryl groups. *Archives of Biochemistry and Biophysics*, *82*, 70–77.

Erijman, L., & Clegg, R. M. (1998). Reversible stalling of transcription elongation complexes by high pressure. *Biophysical Journal*, *75*, 453–462.

Erkmen, O., & Bozoglu, T. F. (2016). Enzymatic and nonenzymatic food spoilage. In O. Erkmen, & T. F. Bozoglu (Eds.), *Food Microbiology: Principles into Practice* (1st ed., Vol. 1, pp. 401–406). John Wiley & Sons, Ltd.

European Commission. (2011). Commission Regulation (EU) No 10/2011 of 14 January 2011 on plastic materials and articles intended to come in contact with food. *Official Journal of the European Union*, 12, 1–89.

Evans, M. G., & Polanyi, M. (1935). Some applications of the transition state method to the calculation of reaction velocities, especially in solution. *Transactions of the Faraday Society*, *31*, 875–894.

Eyring, H. (1935). The activated complex in chemical reactions. *The Journal of Chemical Physics*, *3*, 63–71.

Fameau, A. L., & Salonen, A. (2014). Effect of particles and aggregated structures on the foam stability and aging. *Comptes Rendus Physique*, *15*, 748–760.

Feigenbaum, A. E., Riquet, A. M., & Scholler, D. (2000). Fatty food simulants: Solvents to mimic the behavior of fats in contact with packaging plastics. In S. J. Risch (Ed.), *Food Packaging: Testing Methods and Applications, ACS Symposium Series* (Vol 753, pp. 71–81). American Chemical Society.

Fernandes, P. A. R., Moreira, S. A., Santos, M. D., Duarte, R. V., Santos, D. I., Inácio, R. S., Alves, S. P., Bessa, R. J. B., Delgadillo, I., & Saraiva, J. A. (2019). Hyperbaric storage at variable room temperature – a new preservation methodology for minced meat compared to refrigeration. *Journal of the Science of Food and Agriculture*, *99*, 3276–3282.

Fertsch, B., Müller, M., & Hinrichs, J. (2003). Firmness of pressure-induced casein and whey protein gels modulated by holding time and rate of pressure release. *Innovative Food Science and Emerging Technologies*, *4*, 143–150.

Fidalgo, L. G., Castro, R., Trigo, M., Aubourg, S. P., Delgadillo, I., & Saraiva, J. A. (2019). Quality of fresh Atlantic salmon (*Salmo salar*) under hyperbaric storage at low temperature by evaluation of microbial and physicochemical quality indicators. *Food and Bioprocess Technology*, *12*, 1895–1906.

Fidalgo, L. G., Delgadillo, I., & Saraiva, J. A. (2020). Autolytic changes involving proteolytic enzymes on Atlantic salmon (*Salmo salar*) preserved by hyperbaric storage. *LWT - Food Science and Technology*, *118*, Article 108755.

Fidalgo, L. G., Lemos, Á. T., Delgadillo, I., & Saraiva, J. A. (2018). Microbial and physicochemical evolution during hyperbaric storage at room temperature of fresh Atlantic salmon (*Salmo salar*). *Innovative Food Science and Emerging Technologies*, *45*, 264–272.

Fidalgo, L. G., Santos, M. D., Queirós, R. P., Inácio, R. S., Mota, M. J., Lopes, R. P., Gonçalves, M. S., Neto, R. F., & Saraiva, J. A. (2014). Hyperbaric storage at and above room temperature of a highly perishable food. *Food and Bioprocess Technology*, *7*, 2028–2037.

Fidalgo, L. G., Simões, M. M. Q., Casal, S., Lopes-da-Silva, J. A., Carta, A. M. S., Delgadillo, I., & Saraiva, J. A. (2020). Physicochemical parameters, lipids stability, and volatiles profile of vacuum-packaged fresh Atlantic salmon (*Salmo salar*) loins preserved by hyperbaric storage at 10 °C. *Food Research International*, *127*, Article 108740.

Fine, R. A., & Millero, F. J. (1973). Compressibility of water as a function of temperature and pressure. *The Journal of Chemical Physics*, *59*, 5529–5536.

Fleckenstein, B. S., Sterr, J., & Langowski, H. C. (2014). The effect of high pressure processing on the integrity of polymeric packaging – analysis and categorization of occurring defects. *Packaging and Technology and Science*, *27*, 83-103.

Fraldi, M., Cutolo, A., Esposito, L., Perrella, G., Pastore Carbone, M. G., Sansone, L., Scherillo, G., & Mensitieri, G. (2014). Delamination onset and design criteria of multilayer flexible packaging under high pressure treatments. *Innovative Food Science and Emerging Technologies*, *23*, 39–53.

Gallinaro, S., Zambon, A., Clavier, J. Y., Bertolini, M., Zulli, R., Greco, L., Benedito Fort, J. J., & Spilimbergo, S. (2021). Financial sustainability and profitability of supercritical CO_2 pasteurization of liquid products: A case study. *Chemical Engineering Transactions*, *87*, 349–354.

Galotto, M. J., Ulloa, P. A., Guarda, A., Gavara, R., & Miltz, J. (2009). Effect of high-pressure food processing on the physical properties of synthetic and biopolymer films. *Journal of Food Science*, *74*, E304-E311.

Galotto, M. J., Ulloa, P. A., Hernández, D., Fernández-Martín, F., Gavara, R., & Guarda, A. (2008). Mechanical and thermal behavior of flexible food packaging polymeric films materials under high pressure/temperature treatments. *Packaging Technology and Science*, *21*, 297–308.

Galotto, M. J., Ulloa, P., Escobar, R., Guarda, A., Gavara, R., & Miltz, J. (2010). Effect of high-pressure food processing on the mass transfer properties of selected packaging materials. *Packaging and Technology and Science*, *29*, 253-266.

Ganesan, A. R., Shanmugam, M., Ilansuriyan, P., Anandhakumar, R., & Balasubramanian, B. (2019). Composite film for edible oil packaging from carrageenan derivative and konjac glucomannan: Application and quality evaluation. *Polymer Testing*, 78, Article 105936.

Gänzle, M. G., Margosch, D., Buckow, R., Ehrmann, M. A., Heinz, V., & Vogel, R. F. (2007). Pressure and heat resistance of *Clostridium Botulinum* and other endospores. In C. J. Doona, & F. E. Feeherry (Eds.), *High Pressure Processing of Foods* (pp. 95–114). Blackwell Publishing.

Gao, D., Qiu, N., Liu, Y., & Ma, M. (2016). Comparative proteome analysis of egg yolk plasma proteins during storage. *Journal of the Science of Food and Agriculture*, *97*, 2392–2400.

Garcia, H. S., López-Hernandez, A., & Hill, C. G. (2017). Enzyme technology – Dairy industry applications. In M. Moo-Young (Ed.), *Comprehensive Biotechnology* (3rd ed., pp. 608–617). Elsevier B.V.

García-Risco, M. R., Olano, A., Ramos, M., & López-Fandiño, R. (2000). Micellar changes induced by high pressure. Influence in the proteolytic activity and organoleptic properties of milk. *Journal of Dairy Science*, *83*, 2184–2189.

Gaucheron, F., Famelart, M. H., Mariette, F., Raulot, K., Michela, F., & Le Graeta, Y. (1997). Combined effects of temperature and high-pressure treatments on physicochemical characteristics of skim milk. *Food Chemistry*, *59*, 439–447.

Gebhardt, R., Doster, W., Friedrich, J., & Kulozik, U. (2006). Size distribution of pressure-decomposed casein micelles studied by dynamic light scattering and AFM. *European Biophysics Journal*, *35*, 503–509.

Gekko, K., & Fukamizu, M. (1991). Effect of pressure on the sol-gel transition of agarose. *Agricultural and Biological Chemistry*, *55*, 2427–2428.

Gekko, K., & Kasuya, K. (1985). Effect of pressure on the sol-gel transition of carrageenans. *International Journal of Biological Macromolecules*, *7*, 299–306.

Goldfarb, R., Saidel, L. J., & Mosovich, E. (1951). The ultraviolet absorption spectra of proteins. *Journal of Biological Chemistry*, *193*, 397–404.

Gonzalez, M. E., & Barrett, D. M. (2010). Thermal, high pressure, and electric field processing effects on plant cell membrane integrity and relevance to fruit and vegetable quality. *Journal of Food Science*, *75*, R121-R130.

Götz, J., & Weisser, H. (2002). Permeation of aroma compounds through plastic films under high pressure: *In-situ* measuring method. *Innovative Food Science and Emerging Technologies*, *3*, 25–31.

Goyette, B., Charles, M. T., Vigneault, C., & Raghavan, V. G. S. (2007). Pressure treatment for increasing fruit and vegetable qualities. *Stewart Postharvest Review*, *3*, 1-6.

Goyette, B., Charles, M. T., Vigneault, C., & Raghavan, V. G. S. (2012). Effect of hyperbaric treatments on the quality attributes of tomato fruits. *Canadian Journal of Plant Science*, *92*, 541–551.

Grassia, L., Pastore Carbone, M. G., Mensitieri, G., & D'Amore, A. (2011). Modeling of density evolution of PLA under ultra-high pressure/temperature histories. *Polymer*, *52*, 4011–4020.

Greco, A., & Ferrari, F. (2021). Thermal behavior of PLA plasticized by commercial and cardanol-derived plasticizers and the effect on the mechanical properties. *Journal of Thermal Analysis and Calorimetry*, *146*, 131–141.

Griffiths, M. W., Phillips, J. D., & Muir, D. D. (1987). Effect of low-temperature storage on the bacteriological quality of raw milk. *Food Microbiology*, *4*, 285–291.

Gross, M., Auerbach, G., & Jaenicke, R. (1993). The catalytic activities of monomeric enzymes show complex pressure dependence. *FEBS Letters*, *321*, 256–260.

Gross, M., Lehle, K., Jaenicke, R., & Nierhaus, K. H. (1993). Pressure-induced dissociation of ribosomes and elongation cycle intermediates. Stabilizing conditions and identification of the most sensitive functional state. *European Journal of Biochemistry*, *218*, 463-468.

Guerrero-Beltrán, J. A., Barbosa-Cánovas, G. V., & Swanson, B. G. (2005). High hydrostatic pressure processing of fruit and vegetable products. *Food Reviews International*, *21*, 411–425.

Haghighi, H., Gullo, M., La China, S., Pfeifer, F., Siesler, H. W., Licciardello, F., & Pulvirenti, A. (2021). Characterization of bio-nanocomposite films based on gelatin/polyvinyl alcohol blend reinforced with bacterial cellulose nanowhiskers for food packaging applications. *Food Hydrocolloids*, *113,* Article 106454.

Harano, Y., Yoshidome, T., & Kinoshita, M. (2008). Molecular mechanism of pressure denaturation of proteins. *Journal of Chemical Physics*, *129*, Article 145103.

Hato, M. J., Motaung, T. E., Choi, H. J., Scriba, M., Khumalo, V. M., & Malwela, T. (2017). Effect of organoclay on the properties of maleic-anhydride grafted polypropylene and poly(methyl methacrylate) blend. *Polymer Composites*, *38*, 431–440.

Helm, V. J., & Miiller, B. W. (1991). Stability of the synthetic pentapeptide thymopentin in aqueous solution: Effect of pH and buffer on degradation. *International Journal of Pharmaceutics*, *70*, 29–34.

Henley, J. P., & Sadana, A. (1985). Categorization of enzyme deactivations using a series-type mechanism. *Enzyme and Microbial Technology*, *7*, 50-60.

Hill, V. M., Isaacs, N. S., Ledward, D. A., & Ames, J. M. (1999). Effect of high hydrostatic pressure on the volatile components of a glucose-lysine model system. *Journal of Agricultural and Food Chemistry*, *47*, 3675–3681.

Hill, V. M., Ledward, D. A., & Ames, J. M. (1996). Influence of high hydrostatic pressure and pH on the rate of Maillard browning in a glucose-lysine system. *Journal of Agricultural and Food Chemistry*, *44*, 594–598.

Hiramatsu, N., Inoue, T., Suzuki, M., & Sato, K. (1989). Pressure study on thermal transitions of oleic acid polymorphs by high-pressure differential thermal analysis. *Chemistry and Physics of Lipids*, *51*, 47–53.

Ho, T. M., Le, T. H. A., Yan, A., Bhandari, B. R., & Bansal, N. (2019). Foaming properties and foam structure of milk during storage. *Food Research International*, *116*, 379–386.

Hoque, M., McDonagh, C., Tiwari, B. K., Kerry, J. P., & Pathania, S. (2022). Effect of high-pressure processing on the packaging properties of biopolymer-based films: A review. *Polymers*, *14*, 1-30.

Huang, H. W., Lung, H. M., Yang, B. B., & Wang, C. Y. (2014). Responses of microorganisms to high hydrostatic pressure processing. *Food Control*, *40*, 250–259.

Huang, X., & Ahn, D. U. (2019). How can the value and use of egg yolk be increased?. *Journal of Food Science*, *84*, 205–212.

Huang, Y., Zhang, W., & Xiong, S. (2019). Modeling the effect of thermal combined with high-pressure treatment on intramuscular lipid oxidation in pork. *Journal of Food Process Engineering*, *42*, Article e13240.

Humphrey, T. J., & Whitehead, A. (1993). Egg age and the growth of *Salmonella enteritidis* PT4 in egg contents. *Epidemiology and Infection*, *111*, 209–219.

Huppertz, T., & de Kruif, C. G. (2007). Disruption and reassociation of casein micelles during high pressure treatment: Influence of whey proteins. *Journal of Dairy Research*, *74*, 194–197.

Huppertz, T., Fox, P. F., de Kruif, K. G., & Kelly, A. L. (2006). High pressure-induced changes in bovine milk proteins: A review. *Biochimica et Biophysica Acta (BBA) - Proteins and Proteomics*, *1764*, 593–598.

Huppertz, T., Fox, P. F., & Kelly, A. L. (2004). High pressure treatment of bovine milk: Effects on casein micelles and whey proteins. *Journal of Dairy Research*, *71*, 97–106.

Huppertz, T., Kelly, A. L., & de Kruif, C. G. (2006). Disruption and reassociation of casein micelles under high pressure. *Journal of Dairy Research*, *73*, 294–298.

Huppertz, T., Kelly, A. L., & Fox, P. F. (2002). Effects of high pressure on constituents and properties of milk. *International Dairy Journal*, *12*, 561–572.

Ichimori, H., Hata, T., Matsuki, H., & Kaneshina, S. (1998). Barotropic phase transitions and pressure-induced interdigitation on bilayer membranes of phospholipids with varying acyl chain lengths. *Biochimica et Biophysica Acta (BBA) - Biomembranes*, *1414*, 165–174.

Ikeuchi, Y., Suzuki, A., Oota, T., Hagiwara, K., Tatsumi, R., Ito, T., & Balny, C. (2002). Fluorescence study of the high pressure-induced denaturation of skeletal muscle actin. *European Journal of Biochemistry*, *269*, 364–371.

Illera, A. E., Chaple, S., Sanz, M. T., Ng, S., Lu, P., Jones, J., Carey, E., & Bourke, P. (2019). Effect of cold plasma on polyphenol oxidase inactivation in cloudy apple juice and on the quality parameters of the juice during storage. *Food Chemistry*: X, *3*, Article 100049.

Innocente, N., Biasutti, M., & Blecker, C. (2011). HPLC profile and dynamic surface properties of the proteose-peptone fraction from bovine milk and from whey protein concentrate. *International Dairy Journal*, *21*, 222–228.

International Olive Council IOC/T.20/Doc No 35/ Rev 1 (2017). Determination of peroxide value.

Isaacs, N. S., & Coulson, M. (1996). Effect of pressure on processes modelling the Maillard reaction. *Progress in Biotechnology*, *9*, 639–644.

James, S. J., & James, C. (2010). The food cold-chain and climate change. *Food Research International*, *43*, 1944–1956.

Jamshidian, M., Tehrany, E. A., Imran, M., Akhtar, M. J., Cleymand, F., & Desobry, S. (2012). Structural, mechanical and barrier properties of active PLA-antioxidant films. *Journal of Food Engineering*, *110*, 380–389.

Jarvis, K. L., Evans, P. J., Cooling, N. A., Vaughan, B., Habsuda, J., Belcher, W. J., Bilen, C., Griffiths, G., Dastoor, P. C., & Triani, G. (2017). Comparing three techniques to determine the water vapour transmission rates of polymers and barrier films. *Surfaces and Interfaces*, *9*, 182–188.

Jog, J. P. (1995). Crystallization of polyethyleneterephthalate. *Journal of Macromolecular Science, Part C*, *35*, 531–553.

Juliano, P., Koutchma, T., Sui, Q., Barbosa-Cánovas, G. V., & Sadler, G. (2010). Polymeric-based food packaging for high-pressure processing. *Food Engineering Reviews*, *2*, 274–297.

Kalichevsky, M. T., Knorr, D., & Lillford, P. J. (1995). Potential food applications of high-pressure effects on ice-water transitions. *Trends in Food Science and Technology*, *6*, 253–259.

Kamath, S., Huppertz, T., Houlihan, A. V, & Deeth, H. C. (2008). The influence of temperature on the foaming of milk. *International Dairy Journal*, *18*, 994–1002.

Kato, M., Hayashi, R., Tsuda, T., & Taniguchi, K. (2002). High pressure-induced changes of biological membrane: Study on the membrane-bound Na+/K+-ATPase as a model system. *European Journal of Biochemistry*, *269*, 110–118.

Katyal, A., & Morrison, R. D. (2007). Forensic applications of contaminant transport models in the subsurface. In B. L. Murphy & R. D. Morrison (Eds.), *Introduction to Environmental Forensics* (2nd Edition, pp. 513–575). Academic Press, Elsevier Inc.

Kiełczewska, K., Jankowska, A., Dąbrowska, A., Wachowska, M., & Ziajka, J. (2020). The effect of high pressure treatment on the dispersion of fat globules and the fatty acid profile of caprine milk. *International Dairy Journal*, *102*, Article 104607.

Kiosseoglou, V. (2003). Egg yolk protein gels and emulsions. *Current Opinion in Colloid and Interface Science*, *8*, 365–370.

Kirchkeszner, C., Petrovics, N., Tábi, T., Magyar, N., Kovács, J., Szabó, B. S., Nyiri, Z., & Eke, Z. (2022). Swelling as a promoter of migration of plastic additives in the interaction of fatty food simulants with polylactic acid- and polypropylene-based plastics. *Food Control*, *132*, Article 108354.

Knez, Ž., Markočič, E., Leitgeb, M., Primožič, M., Knez Hrnčič, M., & Škerget, M. (2014). Industrial applications of supercritical fluids: A review. *Energy*, *77*, 235–243.

Kong, W. S. E. (2005). Physical aging in epoxy matrices and composites. In K. Dušek (Ed.), *Epoxy Resins and Composites IV* (pp 125-171). Springer.

Kurpiewska, K., Biela, A., Loch, J. I., Świątek, S., Jachimska, B., & Lewiński, K. (2018). Investigation of high pressure effect on the structure and adsorption of β-lactoglobulin. *Colloids and Surfaces B: Biointerfaces*, *161*, 387–393.

Lacatus, E. E., & Rogers, C. E. (1986). The effect of fusion and physical aging on the toughness of poly(vinyl chloride). *Journal of Vinyl Technology*, *8*, 183–188.

Lai, K. M., Chuang, Y. S., Chou, Y. C., Hsu, Y. C., Cheng, Y. C., Shi, C. Y., Chi, H. Y., & Hsu, K. C. (2010). Changes in physicochemical properties of egg white and yolk proteins from duck shell eggs due to hydrostatic pressure treatment. *Poultry Science*, *89*, 729–737.

Laidler, K. J. (1951). The influence of pressure on the rates of biological reactions. *Archives of Biochemistry*, *30*, 226–236.

Laidler, K. J., & King, M. C. (1983). The development of Transition-State Theory. *Journal of Physical Chemistry*, 87, 2657–2664.

Lakshmanan, R., & Dalgaard, P. (2004). Effects of high-pressure processing on *Listeria monocytogenes*, spoilage microflora and multiple compound quality indices in chilled cold-smoked salmon. *Journal of Applied Microbiology*, *96*, 398–408.

Lambert, Y., Demazeau, G., Largeteau, A., Bouvier, J. M., Laborde-Croubit, S., & Cabannes, M. (2000a). New packaging solutions for high pressure treatments of food. *High Pressure Research*, *19*, 207–212.

Lambert, Y., Demazeau, G., Largeteau, A., Bouvier, J. M., Laborde-Croubit, S., & Cabannes, M. (2000b). Packaging for high-pressure treatments in the food industry. *Packaging Technology and Science*, *13*, 63–71.

Le Chatelier H. (1891). Sur les transformations moléculaires des métaux et leurs conductibilités électriques. *Journal de Physique Théorique et Appliquée*, *10*, 369–374.

Le Loir, Y., Baron, F., & Gautier, M. (2003). *Staphylococcus aureus* and food poisoning. *Genetics and Molecular Research*, *2*, 63–76.

Lemos, Á. T., Ribeiro, A. C., Delgadillo, I., & Saraiva, J. A. (2020). Preservation of raw watermelon juice up to one year by hyperbaric storage at room temperature. *LWT – Food Science and Technology*, *117*, Article 108695.

Lemos, Á. T., Ribeiro, A. C., Fidalgo, L. G., Delgadillo, I., & Saraiva, J. A. (2017). Extension of raw watermelon juice shelf-life up to 58 days by hyperbaric storage. *Food Chemistry*, *231*, 61–69.

Li, J., Wang, C., Li, X., Su, Y., Yang, Y., & Yu, X. (2018). Effects of pH and NaCl on the physicochemical and interfacial properties of egg white/yolk. *Food Bioscience*, *23*, 115–120.

Li, T. M., Hook, J. W., Drickamer, H. G., Weber, G. (1976). Effects of pressure upon the fluorescence of the riboflavin binding protein and its flavin mononucleotide complex. *Biochemistry*, *15*, 3205–3211.

Li, X., Mao, L., He, X., Ma, P., Gao, Y., & Yuan, F. (2018). Characterization of β-lactoglobulin gels induced by high pressure processing. *Innovative Food Science and Emerging Technologies*, *47*, 335–345.

Li-Chan, E. C. Y., & Ma, C. (2002). Thermal analysis of flaxseed (*Linum usitatissimum*) proteins by differential scanning calorimetry. *Food Chemistry*, *77*, 495–502.

Lin, Y., Bilotti, E., Bastiaansen, C. W. M., & Peijs, T. (2020). Transparent semi-crystalline polymeric materials and their nanocomposites: A review. *Polymer Engineering and Science*, *60*, 2351–2376.

Liu, H. S., & Cheng, Y. C. (2000). Stability enhancement of α-amylase by supercritical carbon dioxide pretreatment. *Bioseparation engineering*, *16*, 149–154.

Liu, K. Z., Shaw, R. A., Man, A., Dembinski, T. C., & Mantsch, H. H. (2002). Reagent-free, simultaneous determination of serum cholesterol in HDL and LDL by infrared spectroscopy. *Clinical Chemistry*, *48*, 499–506.

López-Rubio, A., Lagarón, J. M., Hernández-Muñoz, P., Almenar, E., Catalá, R., Gavara, R., & Pascall, M. A. (2005). Effect of high pressure treatments on the properties of EVOH-based food packaging materials. *Innovative Food Science and Emerging Technologies*, *6*, 51–58.

Lucey, J. A., Otter, D., & Horne, D. S. (2017). A 100-Year Review: Progress on the chemistry of milk and its components. *Journal of Dairy Science*, *100*, 9916–9932.

Lund, M. N., & Ray, C. A. (2017). Control of Maillard reactions in foods: Strategies and chemical mechanisms. *Journal of Agricultural and Food Chemistry*, *65*, 4537–4552.

Ma, H. J., Ledward, D. A., Zamri, A. I., Frazier, R. A., & Zhou, G. H. (2007). Effects of high pressure/thermal treatment on lipid oxidation in beef and chicken muscle. *Food Chemistry*, *104*, 1575–1579.

Macdonald, A. G. (1978). A dilatometric investigation of the effects of general anaesthetics, alcohols and hydrostatic pressure on the phase transition in smectic mesophases of dipalmitoyl phosphatidylcholine. *Biochimica et Biophysica Acta (BBA) - Biomembranes*, *507*, 26–37.

MacFarlane, J. J., & McKenzie, I. J. (1976). Pressure-induced solubilization of myofibrillar proteins. *Journal of Food Science*, *41*, 1442–1446.

Manzocco, L., Ignat, A., Valoppi, F., Burrafato, K. R., Lippe, G., Spilimbergo, S., & Nicoli, M. C. (2016). Inactivation of mushroom polyphenoloxidase in model systems exposed to high-pressure carbon dioxide. *Journal of Supercritical Fluids*, *107*, 669–675.

Manzocco, L., Panozzo, A., & Nicoli, M. C. (2013a). Effect of pulsed light on selected properties of egg white. *Innovative Food Science and Emerging Technologies*, *18*, 183–189.

Manzocco, L., Panozzo, A., & Nicoli, M. C. (2013b). Inactivation of polyphenoloxidase by pulsed light. *Journal of Food Science*, *78*, E1183–E1187.

Manzocco, L., Quarta, B., & Dri, A. (2009). Polyphenoloxidase inactivation by light exposure in model systems and apple derivatives. *Innovative Food Science and Emerging Technologies*, *10*, 506–511.

Marangoni Júnior, L., de Oliveira, L. M., Bócoli, P. F. J., Cristianini, M., Padula, M., & Anjos, C. A. R. (2020). Morphological, thermal and mechanical properties of polyamide and ethylene vinyl alcohol multilayer flexible packaging after high-pressure processing. *Journal of Food Engineering*, *276*, Article 109913.

Margosch, D., Ehrmann, M. A., Buckow, R., Heinz, V., Vogel, R. F., & Gänzle, M. G. (2006). High-pressure-mediated survival of *Clostridium botulinum* and *Bacillus amyloliquefaciens* endospores at high temperature. *Applied and Environmental Microbiology*, *72*, 3476–3481.

Margosch, D., Moravek, M., Gänzle, M. G., Märtlbauer, E., Vogel, R. F., & Ehrmann, M. A. (2005). Effect of high pressure and heat on bacterial toxins. *Food Technology and Biotechnology*, *43*, 211–217.

Marquis, R. E. (1976). High-pressure microbial physiology. *Advances in Microbial Physiology*, *14*, 159–241.

Martinez-Monteagudo, S. I., & Saldaña, M. D. A. (2014). Chemical reactions in food systems at high hydrostatic pressure. *Food Engineering Reviews*, *6*, 105–127.

Martino, V. P., Jiménez, A., & Ruseckaite, R. A. (2009). Processing and characterization of poly(lactic acid) films plasticized with commercial adipates. *Journal of Applied Polymer Science*, *112*, 2010–2018.

Martins, S. I. F. S., & van Boekel, M. A. J. S. (2005). Kinetics of the glucose/glycine Maillard reaction pathways: Influences of pH and reactant initial concentrations. *Food Chemistry*, *92*, 437–448.

Martins, S. I. F. S., Jongen, W., van Boekel, M. A. J. S. (2000). A review of Maillard reaction in food and implications to kinetic modelling. *Trends in Food Science and Technology*, *11*, 364–373.

Masuda, M., Saito, Y., Iwanami, T., & Hirai, Y. (1992). Effect of hydrostatic pressure on packaging materials for food. In C. Balny, R. Hayashi, K. Heremans, & P. Masson (Eds.), *High Pressure and Biotechnology* (pp. 545–547). Colloque INSERM/John Libbery.

Matak, K. E., Churey, J. J., Worobo, R. W., Sumner, S. S., Hovingh, E., Hackney, C. R., & Pierson, M. D. (2005). Efficacy of UV light for the reduction of *Listeria monocytogenes* in goat's milk. *Journal of Food Protection*, *68*, 2212–2216.

Mazri, C., Sánchez, L., Ramos, S. J., Calvo, M., & Pérez, M. D. (2012). Effect of high-pressure treatment on denaturation of bovine lactoferrin and lactoperoxidase. *Journal of Dairy Science*, *95*, 549–557.

Medina-Meza, I. G., Barnaba, C., & Barbosa-Cánovas, G. V. (2014). Effects of high pressure processing on lipid oxidation: A review. *Innovative Food Science and Emerging Technologies*, *22*, 1–10.

Meganathan, R., & Marquis, R. E. (1973). Loss of bacterial motility under pressure. *Nature*, 246, 525–527.

Melchior, S., Calligaris, S., Bisson, G., & Manzocco, L. (2020). Understanding the impact of moderate-intensity pulsed electric fields (MIPEF) on structural and functional characteristics of pea, rice and gluten concentrates. *Food and Bioprocess Technology*, *13*, 2145–2155.

Mensitieri, G., Scherillo, G., & Iannace, S. (2013). Flexible packaging structures for high pressure treatments. *Innovative Food Science and Emerging Technologies*, *17*, 12–21.

Mininni, R. M., Moore, R. S., Flick, J. R., & Petrie, S. E. B. (1973). The effect of excess volume on molecular mobility and on the mode of failure of glassy poly(ethylene terephthalate). *Journal of Macromolecular Science, Part B*, *8*, 343–359.

Minton, A. P. (2005). Models for excluded volume interaction between an unfolded protein and rigid macromolecular cosolutes: Macromolecular crowding and protein stability revisited. *Biophysical Journal*, *88*, 971–985.

Mitsuda, H., Kawai, F., & Yamamoto, A. (1972). Underwater and underground storage of cereal grains. *Food Technology*, *26*, 50–56.

Mochizuki, M. (2009). Synthesis, properties and structure of polylactic acid fibres. In S. J. Eichhorn, J. W. S. Hearle, M. Jaffe, & T. Kikutani (Eds.), *Handbook of Textile Fibre Structure* (Vol. 1, pp. 257–275). Woodhead Publishing Ltd.

Montserrat, S., & Cortés, P. (1995). Physical ageing studies in semicrystalline poly(ethylene terephthalate). *Journal of material science*, *30*, 1790-1793.

Mozhaev, V. V., Lange, R., Kudryashova, E. V., & Balny, C. (1996). Application of high hydrostatic pressure for increasing activity and stability of enzymes. *Biotechnology and Bioengineering*, *52*, 320–331.

Muik, B., Lendl, B., Molina-Diaz, A., Valcarcel, M., & Ayora-Cañada, M. J. (2007). Two-dimensional correlation spectroscopy and multivariate curve resolution for the study of lipid oxidation in edible oils monitored by FTIR and FT-Raman spectroscopy. *Analytica Chimica Acta*, *593*, 54–67.

Muller, J., González-Martínez, C., & Chiralt, A. (2017). Combination of poly(lactic) acid and starch for biodegradable food packaging. *Materials*, *10*, 1-22.

Munier, C., Gaillard-Devaux, E., Tcharkhtchi, A., & Verdu, J. (2002). Durability of cross-linked polyethylene pipes under pressure. *Journal of Materials Science*, *37*, 4159–4163.

Mussa, D. M., & Ramaswamy, H. S. (1997). Ultra-high pressure pasteurization of milk: Kinetics of microbial destruction and changes in physico-chemical characteristics. *LWT - Food Science and Technology*, *30*, 551–557.

Naderi, N., House, J. D., Pouliot, Y., & Doyen, A. (2017). Effects of high hydrostatic pressure processing on hen egg compounds and egg products. *Comprehensive Reviews in Food Science and Food Safety*, *16*, 707–720.

Nasiri, A., Peyron, S., Gastaldi, E., & Gontard, N. (2016). Effect of nanoclay on the transfer properties of immanent additives in food packages. *Journal of Materials Science*, *51*, 9732–9748.

Needs, E. C., Capellas, M., Bland, A. P., Manoj, P., MacDougal, D., & Paul, G. (2000). Comparison of heat and pressure treatments of skim milk, fortified with whey protein concentrate, for set yogurt preparation: Effects on milk proteins and gel structure. *Journal of Dairy Research*, *67*, 329–348.

Needs, E. C., Stenning, R. A., Gill, A. L., Ferragut, V., & Rich, G. T. (2000). High-pressure treatment of milk: Effects on casein micelle structure and on enzymic coagulation. *Journal of Dairy Research*, *67*, 31–42.

Neuman, R. C., Kauzmann, W., & Zipp, A. (1973). Pressure dependence of weak acid ionization in aqueous buffers. *Journal of Physical Chemistry*, *77*, 2687–2691.

Ngarize, S., Herman, H., Adams, A., & Howell, N. (2004). Comparison of changes in the secondary structure of unheated, heated, and high-pressure-treated β-lactoglobulin and ovalbumin proteins using Fourier transform Raman spectroscopy and self-deconvolution. *Journal of Agricultural and Food Chemistry*, *52*, 6470–6477.

Nicoli, M. C., Elizande, B. E., Pitotti, A., & Lerici, C. R. (1991). Effect of sugars and Maillard reaction products on polyphenol oxidase and peroxidase activity in food. *Journal of Food Biochemistry*, *15*, 169–184.

Nimalaratne, C., & Wu, J. (2015). Hen egg as an antioxidant food commodity: A review. *Nutrients*, *7*, 8274–8293.

Nys, Y. (2018). Dietary carotenoids and egg yolk coloration - A review. *European Poultry Science*, *64*, 45–54.

Oh, J. H., & Swanson, B. G. (2006). Polymorphic transitions of cocoa butter affected by high hydrostatic pressure and sucrose polyesters. *Journal of the American Oil Chemists' Society*, *83*, 1007–1014.

Ohba, R., Teramoto, Y., & Ueda, S. (1993). Clarification of spray-dried egg yolk suspensions and solubilization of proteins from lipoproteins. *Journal of Food Science*, *58*, 307–309.

Otero, L. (2019). Hyperbaric storage at room temperature for fruit juice preservation. *Beverages*, *5*, 49.

Otero, L., & Pérez-Mateos, M. (2021). Hyperbaric storage of Atlantic razor clams: effect of the storage conditions. *Food and Bioprocess Technology*, *14*, 530–541.

Otero, L., Pérez-Mateos, M., Holgado, F., Márquez-Ruiz, G., & López-Caballero, M. E. (2019). Hyperbaric cold storage: Pressure as an effective tool for extending the shelf-life of refrigerated mackerel (*Scomber scombrus, L.*). *Innovative Food Science and Emerging Technologies*, *51*, 41–50.

Otero, L., Pérez-Mateos, M., & López-Caballero, M. E. (2017). Hyperbaric cold storage versus conventional refrigeration for extending the shelf-life of hake loins. *Innovative Food Science and Emerging Technologies*, *41*, 19–25.

Palmeri, R., Parafati, L., Trippa, D., Siracusa, L., Arena, E., Restuccia, C., & Fallico, B. (2019). Addition of olive leaf extract (OLE) for producing fortified fresh pasteurized milk with an extended shelf life. *Antioxidants*, *8*, 1-14.

Panowicz, R., Konarzewski, M., Durejko, T., Szala, M., Łazińska, M., Czerwińska, M., & Prasuła, P. (2021). Properties of polyethylene terephthalate (PET) after thermo-oxidative aging. *Materials*, *14*, 1-16.

Paredes-Sabja, D., Gonzalez, M., Sarker, M. R., & Torres, J. A. (2007). Combined effects of hydrostatic pressure, temperature, and pH on the inactivation of spores of *Clostridium perfringens* type A and *Clostridium sporogenes* in buffer solutions. *Journal of Food Science*, *72*, M202-M206.

Patazca, E., Koutchma, T., & Balasubramaniam, V. M. (2007). Quasi-adiabatic temperature increase during high pressure processing of selected foods. *Journal of Food Engineering*, *80*, 199-205.

Patel, H. A., & Huppertz, T. (2014). Effects of high-pressure processing on structure and interactions of milk proteins. In H. Singh, M. Boland, & A. Thompson (Eds.), *Milk Proteins* (2nd ed., pp. 243–267). Elsevier Inc.

Pinto, C. A., Martins, A. P., Santos, M. D., Fidalgo, L. G., Delgadillo, I., & Saraiva, J. A. (2019). Growth inhibition and inactivation of *Alicyclobacillus acidoterrestris* endospores in apple juice

by hyperbaric storage at ambient temperature. *Innovative Food Science and Emerging Technologies*, *52*, 232–236.

Pinto, C. A., Moreira, S. A., Fidalgo, L. G., Santos, M. D., Delgadillo, I., & Saraiva, J. A. (2016). Shelf-life extension of watermelon juice preserved by hyperbaric storage at room temperature compared to refrigeration. *LWT - Food Science and Technology*, *72*, 78–80.

Pinto, C. A., Moreira, S. A., Fidalgo, L. G., Santos, M. D., Vidal, M., Delgadillo, I., & Saraiva, J. A. (2017). Impact of different hyperbaric storage conditions on microbial, physicochemical and enzymatic parameters of watermelon juice. *Food Research International*, *99*, 123–132.

Pinto, C. A., Santos, M. D., Fidalgo, L. G., Delgadillo, I., & Saraiva, J. A. (2018). Enhanced control of *Bacillus subtilis* endospores development by hyperbaric storage at variable/uncontrolled room temperature compared to refrigeration. *Food Microbiology*, *74*, 125–131.

Piskulich, Z. A., Mesele, O. O., & Thompson, W. H. (2019). Activation energies and beyond. *Journal of Physical Chemistry A*, *123*, 7185–7194.

Rabinovitch, E. B., & Summers, J. W. (1992). The effect of physical aging on properties of rigid polyvinyl chloride. *Journal of Vinyl Technology*, 14, 126–130.

Read, A. J. (1982). Ionization constants of aqueous ammonia from 25 to 250°C and to 2000 bar. *Journal of Solution Chemistry*, *11*, 649–664.

Reyes, F. G. R., & Wrolstad, R. E. (1982). Maillard browning reaction of sugar-glycine model systems: changes in sugar concentration, color and appearance. *Journal of Food Science*, *47*, 1376–1377.

Ribeiro, D. S., Henrique, S. M. B., Oliveira, L. S., Macedo, G. A., & Fleuri, L. F. (2010). Enzymes in juice processing: A review. *International Journal of Food Science and Technology*, *45*, 635–641.

Richter, T., Sterr, J., Jost, V., & Langowski, H. C. (2010). High pressure-induced structural effects in plastic packaging. *High Pressure Research*, *30*, 555–566.

Rivalain, N., Roquain, J., & Demazeau, G. (2010). Development of high hydrostatic pressure in biosciences: Pressure effect on biological structures and potential applications in biotechnologies. *Biotechnology Advances*, *28*, 659–672.

Roche, J., & Royer, C. A. (2018). Lessons from pressure denaturation of proteins. *Journal of the Royal Society Interface*, *15*, 1-21.

Rosenthal, A., Ledward, D., Defaye, A., Gilmour, S., & Trinca, L. (2002). Effect of pressure, temperature, time and storage on peroxidase and polyphenol oxidase from pineapple. *Trends in High Pressure Bioscience and Biotechnology*, *19*, 525–532.

Ruiz-Espinosa, H., Amador-Espejo, G. G., Barcenas-Pozos, M. E., Angulo-Guerrero, J. O., Garcia, H. S., & Welti-Chanes, J. (2013). Multiple-pass high-pressure homogenization of milk for the development of pasteurization-like processing conditions. *Letters in Applied Microbiology*, *56*, 142–148.

Sadana, A. (1988). Enzyme deactivation. *Biotechnology Advances*, *6*, 349–446.

Saini, R. K., Nile, S. H., & Park, S. W. (2015). Carotenoids from fruits and vegetables: Chemistry, analysis, occurrence, bioavailability and biological activities. *Food Research International*, *76*, 735–750.

Sampedro, F., McAloon, A., Yee, W., Fan, X., & Geveke, D. J. (2014). Cost analysis and environmental impact of pulsed electric fields and high pressure processing in comparison with thermal pasteurization. *Food and Bioprocess Technology*, *7*, 1928–1937.

Sampedro, F., McAloon, A., Yee, W., Fan, X., Zhang, H. Q., & Geveke, D. J. (2013). Cost analysis of commercial pasteurization of orange juice by pulsed electric fields. *Innovative Food Science and Emerging Technologies*, *17*, 72–78.

San Martín, M. F., Barbosa-Cánovas, G. V., & Swanson, B. G. (2002). Food processing by high hydrostatic pressure. *Critical Reviews in Food Science and Nutrition*, *42*, 627–645.

Santos, M. D., Castro, R., Delgadillo, I., & Saraiva, J. A. (2020). Improvement of the refrigerated preservation technology by hyperbaric storage for raw fresh meat. *Journal of the Science of Food and Agriculture*, *100*, 969–977.

Santos, M. D., Delgadillo, I., & Saraiva, J. A. (2020). Extended preservation of raw beef and pork meat by hyperbaric storage at room temperature. *International Journal of Food Science and Technology*, *55*, 1171–1179.

Santos, M. D., Fidalgo, L. G., Pinto, C. A., Duarte, R. V, Lemos, Á. T., Delgadillo, I., & Saraiva, J. A. (2021). Hyperbaric storage at room like temperatures as a possible alternative to refrigeration: Evolution and recent advances. *Critical Reviews in Food Science and Nutrition*, *61*, 2078–2089.

Santos, M. D., Matos, G., Casal, S., Delgadillo, I., & Saraiva, J. A. (2021). Quality evolution of raw meat under hyperbaric storage – Fatty acids, volatile organic compounds and lipid oxidation profiles. *Food Bioscience*, *42*, Article 101108.

Schmerder, A., Richter, T., Langowski, H. C., & Ludwig, H. (2005). Effect of high hydrostatic pressure on the barrier properties of polyamide-6 films. *Brazilian Journal of Medical and Biological Research*, *38*, 1279–1283.

Seelig, J., & Schönfeld, H. J. (2016). Thermal protein unfolding by differential scanning calorimetry and circular dichroism spectroscopy. Two-state model *versus* sequential unfolding. *Quarterly Reviews of Biophysics*, *49*, 1–24.

Segat, A., Misra, N. N., Cullen, P. J., & Innocente, N. (2015). Atmospheric pressure cold plasma (ACP) treatment of whey protein isolate model solution. *Innovative Food Science and Emerging Technologies*, *29*, 247–254.

Segovia-Bravo, K. A., Guignon, B., Bermejo-Prada, A., Sanz, P. D., & Otero, L. (2012). Hyperbaric storage at room temperature for food preservation: A study in strawberry juice. *Innovative Food Science and Emerging Technologies*, *15*, 14–22.

Serment-Moreno, V., Barbosa-Cánovas, G. V., Torres, J. A., & Welti-Chanes, J. (2014). High-pressure processing: Kinetic models for microbial and enzyme inactivation. *Food Engineering Reviews*, *6*, 56–88.

Shiga, K., Horiike, K., Nishina, Y., Otani, S., Watari, H., & Yamano, T. (1979). A study of flavin-protein and flavoprotein-ligand interactions: Binding aspects and spectral properties of D-amino acid oxidase and riboflavin binding protein. *Journal of Biochemistry*, *85*, 931–941.

Sila, D. N., Smout, C., Satara, Y., Truong, V., Van Loey, A., & Hendrickx, M. (2007). Combined thermal and high pressure effect on carrot pectinmethylesterase stability and catalytic activity. *Journal of Food Engineering*, *78*, 755–764.

Silva, S., Espiga, A., Niranjan, K., Livings, S., Gumy, J. C., & Sher, A. (2008). Formation and stability of milk foams. In G. M. Campbell, M. G. Scanlon, & D. L. Pyle (Eds.), *Bubbles in Food 2: Novelty, Health and Luxury* (pp. 153–161). Elsevier Inc.

Singh, A., & Ramaswamy, H. (2013). Effect of high pressure processing on color and textural properties of eggs. *Journal of Food Research*, *2*, 11-24.

Singh, A., & Ramaswamy, H. S. (2015). High pressure modification of egg components: Exploration of calorimetric, structural and functional characteristics. *Innovative Food Science and Emerging Technologies*, *32*, 45–55.

Sisak, C., Csanádi, Z., Rónay, E., & Szajáni, B. (2006). Elimination of glucose in egg white using immobilized glucose oxidase. *Enzyme and Microbial Technology*, *39*, 1002-1007.

Smith, L. J., Fiebig, K. M., Schwalbe, H., & Dobson, C. M. (1996). The concept of a random coil : Residual structure in peptides and denatured proteins. *Folding and Design*, *1*, R95–R106.

Sousa, A. F., Patrício, R., Terzopoulou, Z., Bikiaris, D. N., Stern, T., Wenger, J., Loos, K., Lotti, N., Siracusa, V., Szymczyk, A., Paszkiewicz, S., Triantafyllidis, K. S., Zamboulis, A., Nikolic, M. S., Spasojevic, P., Thiyagarajan, S., van Es, D. S., & Guigo, N. (2021). Recommendations for replacing PET on packaging, fiber, and film materials with biobased counterparts. *Green Chemistry*, *23*, 8795–8820.

Speroni, F., Puppo, M. C., Chapleau, N., de Lamballerie, M., Castellani, O., Añón, M. C., & Anton, M. (2005). High-pressure induced physicochemical and functional modifications of low-density lipoproteins from hen egg yolk. *Journal of Agricultural and Food Chemistry*, *53*, 5719–5725.

Stetsiv, Y. A., Yatsyshyn, M. M., Nykypanchuk, D., Korniy, S. A., Saldan, I., Reshetnyak, O. V., & Bednarchuk, T. J. (2021). Characterization of polyaniline thin films prepared on polyethylene terephthalate substrate. *Polymer Bulletin*, *78*, 6251–6265.

Stratakos, A. C., Inguglia, E. S., Linton, M., Tollerton, J., Murphy, L., Corcionivoschi, N., Koidis, A., & Tiwari, B. K. (2019). Effect of high pressure processing on the safety, shelf life and quality of raw milk. *Innovative Food Science and Emerging Technologies*, *52*, 325–333.

Struik, L. C. E. (1981). Physical aging and thermal history effects in PVC, both above and below T_g. *Pure and Applied Chemistry*, *53*, 467–469.

Swain, M. J., Evans, J. A., & James, S. J. (2005). Energy consumption in the UK food chill chain – primary chilling. *Food Manufacturing Efficiency*, *2*, 25–33.

Syed, Q. A., Hassan, A., Sharif, S., Ishaq, A., Saeed, F., Afzaal, M., Hussain, M., & Anjum, F. M. (2021). Structural and functional properties of milk proteins as affected by heating, high pressure, Gamma and ultraviolet irradiation: a review. *International Journal of Food Properties*, *24*, 871–884.

Tamaoka, T., Itoh, N., & Hayashi, R. (1991). High pressure effect on Maillard reaction. *Agricultural and Biological Chemistry*, *55*, 2071–2074.

Tang, Z., Fan, F., Fan, C., Jiang, K., & Qin, Y. (2020). The performance changes and migration behavior of PLA/Nano-TiO_2 composite film by high-pressure treatment in ethanol solution. *Polymers*, *12*, 1-14.

Tant, M. R., & Wilkes, G. L. (1981). An overview of the nonequilibrium behavior of polymer glasses. *Polymer Engineering and Science*, *21*, 874–895.

Tomasula, P. M., Renye, J. A., Van Hekken, D. L., Tunick, M. H., Kwoczak, R., Toht, M., Leggett, L. N., Luchansky, J. B., Porto-Fett, A. C. S., & Phillips, J. G. (2014). Effect of high-pressure

processing on reduction of *Listeria monocytogenes* in packaged Queso Fresco I. *Journal of Dairy Science*, *97*, 1281–1295.

Uygun-Sarıbay, M., Ergun, E., Kalaycı, Y., & Köseoğlu, T. (2017). The secondary structure of proteins in liquid, frozen, and dried egg-white samples: Effect of gamma irradiation treatment. *International Journal of Food Properties*, *20*, 1195–1203.

Van Boekel, M. A. J. S. (2001). Kinetic aspects of the Maillard reaction: A critical review. *Nahrung - Food*, *45*, 150–159.

Van Boekel, M. A. J. S. (2008). Kinetic modeling of food quality: A critical review. *Comprehensive Reviews in Food Science and Food Safety*, *7*, 144–158.

Van den Berg, B., Ellis, R. J., & Dobson, C. M. (1999). Effects of macromolecular crowding on protein folding and aggregation. *The EMBO Journal*, *18*, 6927-3933.

Van der Plancken, I., Van Loey, A., & Hendrickx, M. (2005). Combined effect of high pressure and temperature on selected properties of egg white proteins. *Innovative Food Science and Emerging Technologies*, *6*, 11–20.

Van der Plancken, I., Van Loey, A., & Hendrickx, M. (2007). Kinetic study on the combined effect of high pressure and temperature on the physico-chemical properties of egg white proteins. *Journal of Food Engineering*, *78*, 206–216.

Van Laack, R. L. J. M. (1999). The role of proteins in water-holding capacity of meat. In Y. L. Xiong, H. Chi-Tang, & F. Shahidi (Eds.), *Quality Attributes of Muscle Foods* (pp. 309–318). Springer.

Vasavada, P. C. (1988). Pathogenic bacteria in milk - A review. *Journal of Dairy Science*, *71*, 2809–2816.

Verbeyst, L., Van Crombruggen, K., Van der Plancken, I., Hendrickx, M., & Van Loey, A. (2011). Anthocyanin degradation kinetics during thermal and high pressure treatments of raspberries. *Journal of Food Engineering*, *105*, 513–521.

Verbeyst, L., Oey, I., Van der Plancken, I., Hendrickx, M., & Van Loey, A. (2010). Kinetic study on the thermal and pressure degradation of anthocyanins in strawberries. *Food Chemistry*, *123*, 269–274.

Verlent, I., Smout, C., Duvetter, T., Hendrickx, M., & Van Loey, A. (2005). Effect of temperature and pressure on the activity of purified tomato polygalacturonase in the presence of pectins with

different patterns of methyl esterification. *Innovative Food Science and Emerging Technologies*, *6*, 293–303.

Wang, C. Y., Huang, H. W., Hsu, C. P., & Yang, B. B. (2016). Recent advances in food processing using high hydrostatic pressure technology. *Critical Reviews in Food Science and Nutrition*, *56*, 527–540.

Wang, Y., Wang, Z., & Shan, Y. (2019). Assessment of the relationship between ovomucin and albumen quality of shell eggs during storage. *Poultry Science*, *98*, 473–479.

Weemaes, C., Ludikhuyze, L., Van den Broeck, I., & Hendrickx, M. (1998). High pressure inactivation of polyphenoloxidases. *Journal of Food Science*, *63*, 873-877.

Wuytack, E. Y., Diels, A. M. J., & Michiels, C. W. (2002). Bacterial inactivation by high-pressure homogenisation and high hydrostatic pressure. *International Journal of Food Microbiology*, *77*, 205–212.

Yamasaki, M., Takahashi, N., & Hirose, M. (2003). Crystal structure of S-ovalbumin as a non-loop-inserted thermostabilized serpin form. *Journal of Biological Chemistry*, *278*, 35524–35530.

Yan, W., Qiao, L., Gu, X., Li, J., Xu, R., Wang, M., Reuhs, B., & Yang, Y. (2010). Effect of high pressure treatment on the physicochemical and functional properties of egg yolk. *European Food Research and Technology*, *231*, 371–377.

Yayanos, A. A., & Pollard, E. C. (1969). A study of the effects of hydrostatic pressure on macromolecular synthesis in *Escherichia coli*. *Biophysical Journal*, *9*, 1464–1482.

Yoo, S., Lee, J., Holloman, C., & Pascall, M. A. (2009). The effect of high pressure processing on the morphology of polyethylene films tested by differential scanning calorimetry and X-ray diffraction and its influence on the permeability of the polymer. *Journal of Applied Polymer Science*, *112*, 107–113.

Yoruk, R., & Marshall, M. R. (2003). Physicochemical properties and function of plant polyphenol oxidase: A review. *Journal of Food Biochemistry*, *27*, 361–422.

Zaks, A., & Russell, A. J. (1988). Enzymes in organic solvents: properties and applications. *Journal of Biotechnology*, *8*, 259-269.

Zamora, W. R. M., Leyva, N., Chero, M. J. S., Timaná-Alvarez, M., More, L. A. V., Vera, P. E. L., & Taboada, M. M. M. (2021). Analysis of the activation volume and the pressure resistance for handling kinetic of processing food. In Russo, D., Ahram, T., Karwowski, W., Di Bucchianico,

& G., Taiar, R. (Eds.), *Intelligent Human Systems Integration 2021*. IHSI 2021. *Advances in Intelligent Systems and Computing*, Vol 1322. Springer.

Zhao, Z. K., Mu, T. H., Zhang, M., & Richel, A. (2018). Chemical forces, structure, and gelation properties of sweet potato protein as affected by pH and high hydrostatic pressure. *Food and Bioprocess Technology*, *11*, 1719–1732.

Acknowledgements

The completion of this Thesis would not have been possible without the support of my supervisors, Professor Lara Manzocco and Professor Maria Cristina Nicoli. I would like to thank them for the opportunity to conduct this Ph.D, and for their patience and teachings, which allowed me to grow both professionally and personally. I want to extend my sincere thanks to Professor Monica Anese and to Professor Sonia Calligaris, for the help and support they provided me during these years. Many thanks also to Professor Nadia Innocente and Dr. Michela Maifreni, who I had the pleasure to work with.

I am very grateful to Professor Jorge M. A. Saraiva, for allowing me to work in his lab in Aveiro during my 5-month stay, which has been a great experience not only from a professional point of view.

Thanks also to Professor Fabio Licciardello and to Andrea Feroce, for the fruitful research collaboration focused on food packaging materials.

Heartfelt thanks to the amazing people that are my colleagues, but first of all friends, in Udine: Sofia, Marilisa, Stella, Giulia R. and Giulia D. F., Martina, Niccolò, Francesco, Lorenzo B. and Lorenzo D. B., Marco, Umberto, Luca, Angelo. I learned something from all of you, and you made this journey a lot more worthy.

I'm extremely grateful to my fiancée, Chiara, for always having my back, and for being by my side no matter what. The same goes to my amazing family: my mother Michela, my father Ezio, and my brother Francesco. Thank you for always being there for me.

Thanks should also go to my dearest, long-time friends, Matteo, Riccardo, Andrea, Fabrizio, Matjaž, Tomas, Daniel, Silvia, Danut and Stefano, for the support, but especially for the many shared moments worth to be remembered.

Last, but certainly not least, *muito obrigado* to all my amazing Portuguese friends, Carlos, Jessica, Ricardo, Gabriella, Renata, Ana, Vasco, Rodolfo, Álvaro, Diogo, Natacha and Rafaela, and to my favourite Brazilian scientist, Paulo. You filled my stay in Portugal with unforgettable moments, and I can't wait to see you all soon!